5-2022

Strategies for Protection of the Blood Brain Barrier in Rodent Models of Intracerebral Hemorrhage

Derek Sunil Nowrangi

LOMA LINDA UNIVERSITY
School of Medicine
In conjunction with the
Faculty of Graduate Studies

Strategies for Protection of the Blood Brain Barrier in Rodent Models of Intracerebral Hemorrhage

by

Derek Sunil Nowrangi

A Dissertation submitted in partial satisfaction of the requirements for the degree
Doctor of Philosophy in Physiology

May 2022

Each person whose signature appears below certifies that this dissertation in his/her opinion is adequate, in scope and quality, as a dissertation for the degree Doctor of Philosophy.

Chairperson

John H. Zhang, Professor of Anesthesiology, Neurosurgery, Neurology, and Physiology

Richard Hartman, Professor of Psychology

Lei Huang, Associate Research Professor of Neurosurgery

Kerby Oberg, Professor of Pathology and Human Anatomy

Jiping Tang, Professor of Physiology and Pharmacology

ACKNOWLEDGEMENTS

I would like to express my deepest gratitude to Dr. John H. Zhang and Dr. Jiping Tang for being excellent mentors and examples of the work ethic needed to be a successful scientist. They have provided me many opportunities during to publish, review articles, write grants, and be a leader in the laboratory. I truly thank the both of you for all you have done for me with your time, money, energy, passion, guidance, and sacrifices that you have invested in me. The thanks I have for both of you is so tremendous is difficult to put into words. I hope that you can be proud of the scientist and medical doctor that you have helped to develop after all these years.

I would also like to thank my other committee members Dr. Oberg, Dr. Hartman, and Dr. Huang for their advice and direction. Dr. Hartman, thank you so much for taking the time to meet with me and give ideas about my presentations as well as providing your expertise to our lab. Dr. Huang, your help with developing my project and working in the lab was indispensable. Dr. Oberg, I really do appreciate you taking your time to help to mentor me throughout my education. To the rest of those in the Zhang Neuroscience Laboratory and Center for Stroke Research with whom I have had the opportunity and pleasure of collaborating with, thank you for your time, support, and efforts. Without your help throughout these years, achieving everything I have would have been beyond difficult. I want to give special thanks to members in the ICH and GMH groups that I have worked with throughout the years. I would like to especially thank Brandon Dixon, Jerry Flores, and Anatol Manaenko.

DEDICATION

I would like to dedicate this dissertation to my immediate family, specifically my father and mother Dr. Sunil Nowrangi and Dr. Pushpa Nowrangi. Thank you for providing an abundance of examples of dedicating your life to the service of others, education, family, and God. You both have always believed in me and have provided me the continued support needed to make it through difficult times. Your wisdom and selfless actions have continued to provide me with the courage I needed to make it through all my life. To my brother Kevin Nowrangi, you have always pushed me to go further and aim for ideals beyond my scope of vision. To all of you, thank you all! This portion of my journey through life would have been impossible if it wasn't for you, your prayers, and God.

CONTENTS

FIGURES

Figures Page

ABBREVIATIONS

ICH	Intracerebral Hemorrhage
BBB	Blood-Brain Barrier
GCS	Glasgow Coma Scale
IGF	Insulin-Like Growth Factor
rhIGF-1	Recombinant Human Insulin-Like Growth Factor-1
IGF-1R	Insulin-Like Growth Factor 1 Receptor
PI3K	Phosphoinositide 3-Kinase
GSK3	Glycogen Synthase Kinase 3 Beta
MMP	Matrix Metalloproteinases
ROS	Reactive Oxygen Species
MAPK	Mitogen Activated Protein
MEK	Mitogen Activated Kinase
MEKK1	Mitogen Activated Kinase Kinase
JNK	c-Jun N-Terminal Kinase
GMH	Germinal Matrix Hemorrhage
SAH	Subarachnoid Hemorrhage
EPO	Erythropoietin
MCAO	Middle Cerebral Artery Occlusion
S.C.	Subcutaneous
I.V.	Intravenous
I.C.V.	Intracerebroventricular
I.P.	Intraperitoneal

I.N.	Intranasal
siRNA	Small Interfering Ribonucleic Acid
scRNA	Scramble Ribonucleic Acid
IgG	Immunoglobulin G
PBS	Phosphate-Buffered Saline
TCA	Trichloroacetic Acid
IQR	Interquartile Range
CNS	Central Nervous System
WW	Wet Weight
DW	Dry Weight
RIPA	Radioimmunoprecipitation Assay Buffer
PDGF	Platelet-Derived Growth Factor
PDGFR	Platelet-Derived Growth Factor Receptor
DMSO	Dimethyl Sulfoxide
EB	Evan's Blue
SDS-PAGE	Sodium Dodecyl Sulfate-Polyacrylamide Gel Electrophoresis
ANOVA	Analysis of Variance

ABSTRACT OF THE DISSERTATION

STRATEGIES FOR PROTECTION OF THE BLOOD BRAIN BARRIER IN RODENT MODELS OF INTRACEREBRAL HEMORRHAGE

by

Derek Sunil Nowrangi

Doctor of Philosophy, Graduate Program in Physiology
Loma Linda University, May 2022
Dr. John Zhang, Chairperson

Intracerebral Hemorrhage (ICH) is a devastating disease that causes a cascade of both mechanical and molecular injury to the central nervous system. It is a debilitating disease that has no well-established treatments, thus leaving an important area to study the pathophysiology of the disease so that new clinically translatable treatments can be found. In the development of translational treatments in experimental ICH, several challenges exist including the designing of studies, method to deliver drugs, proper dosages, and development of models. In our exploration to establish new therapies for ICH, we studied several methods and models that may help to develop treatments. We studied the treatment efficacy of insulin-like growth factor-1 (IGF-1) and Adropin, and inhibition of platelet-derived growth factor receptor-β (PDGFR-β) in protecting against blood-brain barrier injury and improving hematoma resolution following ICH. Our work showed that intranasal administration of IGF-1 and Adropin was able to reduce brain edema, improve neurological behavior, and reduce permeability of the BBB after ICH. We also found that inhibition of PDGFR-β was able to reduce stress fiber formation and reduce BBB permeability following ICH. Additionally, we have also reviewed and discussed the current literature on the pathophysiology, potential intervention regions, and future directions concerning ICH.

CHAPTER 1

INTRODUCTION

Intracerebral Hemorrhage

Within the medical care practices, stroke is a common but debilitating disease in which there are approximately 7.6 million incidences in the US per year and is increasing over time. Intracerebral Hemorrhage (ICH) is debilitating form of stroke that has a greater morbidity and mortality when compared with ischemic stroke but accounts for only 10-15% of stroke incidences [1]. Though stroke is now the fifth leading cause of death in the US, the incidence rates continue to increase along with health care costs to now be approximately $38.6 billion annually [2]. ICH incidences remain the least treatable form of stroke and leaves a mortality rate of about 40-50% in the first six months after the initial incidence [3]. Of the patients that survive the incident 80% are unable to live independently in the first year. In the clinical setting, the disease is treated using emergency interventions to regulate blood pressure or to surgically relieve intracranial pressure. However, with such a high mortality rate even after emergency treatments, the disease is in dire need of new methods for treating the patients. Surgical methods are not recommended as they may worsen the outcomes through the trauma that surgery itself brings and a high post operation hemorrhage rate [4]. Though elderly and hypertensive patients are displayed as having the highest incidence rates, no effective screening criteria and preventative treatments have been developed for the disease because no underlying malformations or coagulopathy have been found.

Non-traumatic ICH can be considered either primary or secondary. Primary ICH is a spontaneous incident that has no known underlying malformations while secondary ICH can be associated with underlying conditions such as arteriovenous malformations, aneurysm, neoplasia, or coagulopathies [5, 6]. The primary disease is caused when small blood vessels in the brain parenchyma are ruptured causing blood to fill the extracellular space in the brain. The resulting accumulation of blood results in physical damage by 1) dissection of the brain tissue severing white matter tracts and 2) the formation of a mass effect in the brain space, which causes mechanical stretching of the tissue which can also produce a compressive ischemia in nearby tissue and increase intracranial pressure. The mechanical destruction of cells releases several cellular factors into the extracellular space, which along with the products in the blood cause the symptoms of the secondary brain injury characteristic of the disease including blood-brain barrier (BBB) disruption, inflammation, excitotoxicity, and apoptosis (Figure 1).

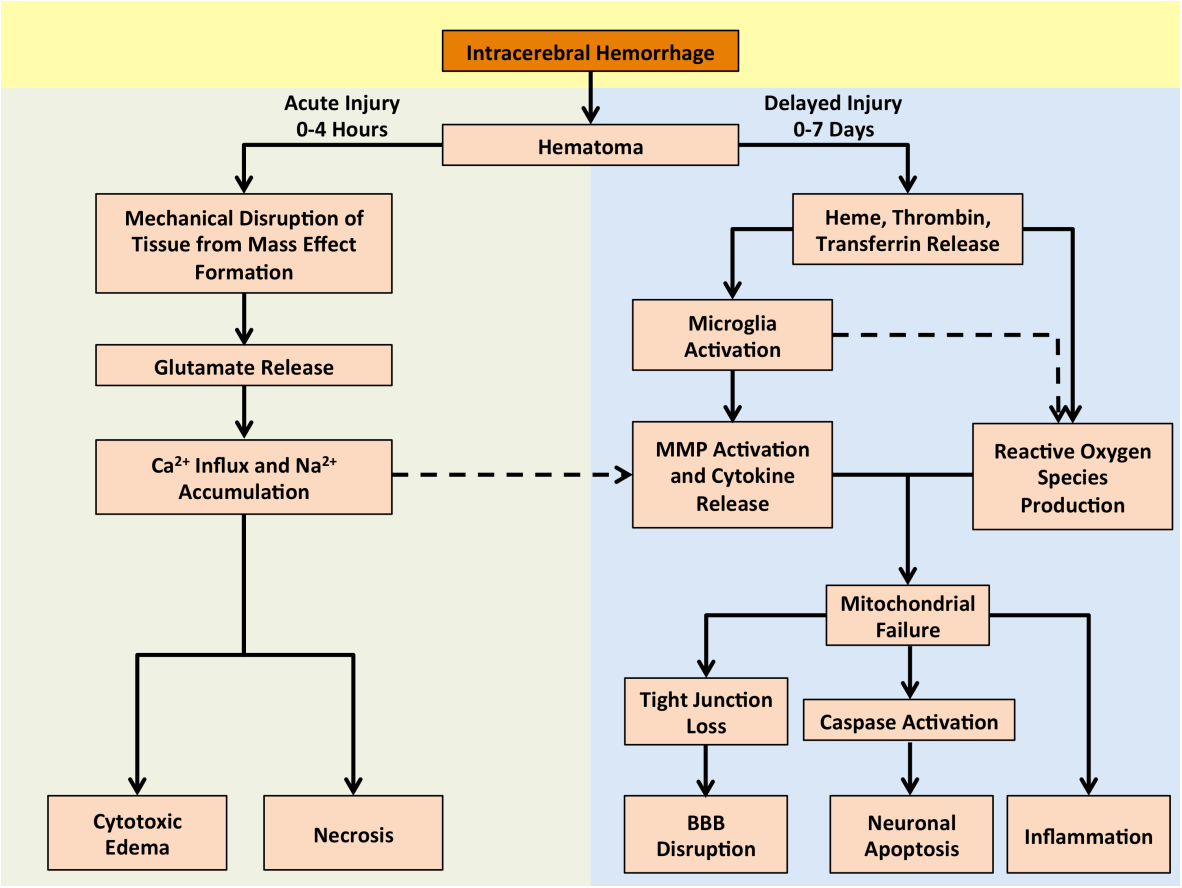

Figure 1. Pathophysiology of ICH showing the difference between the Acute and Delayed phases of injury. Outcomes after the hematoma formation include cytotoxic edema, necrosis, BBB disruption, neuronal apoptosis, and inflammation.

Preclinical and Clinical Features

Though an underlying mechanism is currently unknown as to what causes the disease, risk factors such as hypertension, diabetes, and low serum cholesterol are known to increase the risk with increasing evidence of ICH secondary to anti-coagulation therapies [1, 7, 8]. In the primary form of ICH, hypertensive arteriosclerosis and amyloid angiopathy account for 78-88% of incidences [9]. Chronic hypertension produces a stage of vascular remodeling that causes smooth muscle cell proliferation followed by death of these cells [10]. During this stage, the elastic tissue of the vascular wall is lost and collagen is laid down in a reactive manner [11]. Because of the brittle nature of collagen, these vessels become primed to break thus resulting in the hemorrhage. Alternatively, if too much collagen is placed, this may also lead to an occlusion of the vessel. In amyloid angiopathy associated ICH, there is an increased deposition of β-amyloid protein within the brain. Normally, this protein is eliminated from the brain through bulk flow along perivascular pathways, but an egress failure can cause an accumulation within the vessels [12]. This causes the vessels to become less compliant and more susceptible to rupture.

ICH generally occurs in small arteriolar vessels less than 600 μm and therefore has a slower bleed than in a rupture of larger vessels [13, 14]. Early sealing of these leaks can help explain the occurrence of asymptomatic hemorrhages. Additionally, this accounts for the clinical deterioration of the disease being on a scale of hours rather than minutes [15]. Studies have shown that most of the hematoma growth occurs within the first six hours following the

symptom onset and has a rate of 36-38% during the first three hours of the therapeutic window [16, 17]. Hematoma expansion into the ICH occurs in 18-38% of patients within three hours of the onset but in only 11% of patients after suggesting that there is an acute mechanism [16, 17]. There is some debate as to occurrence of aneurysmal bleeding in ICH. Due to the small size of the vessels affected and the method of vessel wall thinning from hypertension, the presence of Charcot-Bouchard aneurysms has been suggested as an underlying structure. However, there is some debate on the existence of these aneurysms in the disease or at all [18, 19]. These aneurysms are considered fusiform aneurysms that occur in vessels smaller than 300 μm [20] compared to a saccular aneurysm that is found in subarachnoid hemorrhage [21].

The clinical symptoms of ICH can range from fatal to asymptomatic (hemorrhage found during autopsy). The outcome severity of ICH is graded on the volume of the clot and the level of consciousness of the patient measured by the Glasgow Coma Scale (GCS). A higher volume of blood with a low GCS score can be a predictor of higher mortality rates [22]. Other predictors of poor outcomes following the disease include age, heart disease, diabetes mellitus, and hyperglycemia [23, 24]. The location of a hemorrhage to classify as ICH remains a major determinant of its etiology. ICH hemorrhages can occur in the ganglionic (deep gray matter of thalamus or basal ganglia) and lobar (gray and white matter of frontal, temporal, parietal, or occipital lobes) tissues [24-27]. Additionally, the widespread changes to the brain caused by the disease may produce a recurrent hemorrhage which will likely occur in the same general

location of the first bleed, but can also produce a satellite hemorrhage in another area with damaged vessels [28].

Preclinical Surgery Models

Preclinical ICH research has seen the development of several surgical models to mimic the disease. However, due to their ease of use and reproducibility, two models of surgery are most commonly utilized to demonstrate the clinical outcomes after ICH: autologous blood injection and collagenase-induced hemorrhage [29, 30]. The “blood” model is defined by the injection of blood into the region of interest in the brain, whereas the “collagenase” model is defined by the infusion of collagenase in order to produce the hematoma. Both of these experimental models of mimicking the ICH injury are utilized the region of the basal ganglia and as such are considered to be models of a ganglionic hemorrhage. The procedure for both the autologous blood injection and collagenase models utilizes a stereotactically guided needle that is inserted into a specific region of the brain of an anesthetized animal. In order to produce a consistent hemorrhage, a precise volume of autologous whole blood or collagenase is infused over a particular time. Both models are commonly used due to their ease of use and reproducibility. However, each model has fundamental strengths and weaknesses that are inherent in their use.

The autologous blood injection model has been utilized on rodents since the mid-1980s but has also been adapted to several other species. Whereas issues of blood reflux along the needle track were considered issues when the

model was first developed, this has since been mostly resolved since the introduction of the “double-injection” of autologous whole blood technique developed by Deissberger et al. [31, 32]. The blood injection model is able to simulate the mechanistic effects of the injury in relation to the presence of blood. However, because it uses a direct injection of blood, it does not simulate the small vessel rupture that is considered to be found in the vast majority of spontaneous ICH cases in humans. Due to this, the model is not useful in evaluating rebleeding or the effect of vascular breakdown.

The collagenase injection model was introduced by Rosenberg et al. in the early 1990s to simulate the spontaneous rupture of the small vessels in the brain and has since been adapted to several species [29]. The collagenase degrades the collagen of the basal lamina and extracellular matrix around the cerebral capillaries to cause damage to the BBB and produce a spontaneous hematoma [33]. Unlike the autologous blood injection model, the collagenase model is able to mimic the rebleeding and small vascular breakdown effects. However, the collagenase model is unsuitable to study the inflammatory response of ICH due to the collagenase itself producing an inflammatory effect unrelated to the hematoma [34].

Blood-Brain Barrier

Inflammatory, excitotoxic, and apoptotic pathways are commonly known to be implicated in the pathology of the disease. However, the major concern in regard to the progression and maintenance of the disease is found from the

damage to the blood-brain barrier (BBB). When the BBB is disturbed, one of the major results is the formation of edema in the brain. With the elevation of edema, the swelling of the tissues further increases the mechanical stretch and elevates the intracranial pressure, both of which can contribute towards cellular damage [35]. It is therefore our belief that reducing damage to the BBB after ICH will result in improved outcomes for those with the disease.

The BBB is a unique vascular structure only located in the regions of the central nervous system where the capillary exchange of substances occurs. Physiologically, it is considered to be a mechanism of controlling substances that can enter the brain to protect the delicate structure inside. The basic structure of the BBB is composed of vascular endothelial cells creating the brain capillary system, which are surrounded by pericytes, astrocytes, and neuron foot processes [36, 37].

Endothelial cells act as the major component of the barrier in which substances must first encounter and as such are commonly referred to as the BBB itself. The endothelial cells of the brain differ in comparison to those of the systemic system due to two primary reasons [37-40]. First, no detectable transendothelial pathways have been recognized in the BBB that utilize intracellular vesicles. Second, there exists a continuous network of tight junctions between the brain endothelial cells to prevent the paracellular transport of materials. These tight junctions located between endothelial cells are responsible for the function of the BBB, limiting the diffusion of molecules across by both size and polar properties. The tight junction proteins play an integral part

in preventing unwanted materials from entering the brain space by preventing transcellular transportation between endothelial cells of the brain capillary system [41]. These proteins act as barriers anchoring adjacent endothelial cells together reducing the space available for materials to pass.

In the pathology of ICH, reactive oxygen species, inflammatory cytokines, and other mediators released from cellular damage signal endothelial breakdown of these tight junction proteins [41]. With decreased tight junction interactions between endothelial cells and mechanical stress due to the mass effect, gaps between the endothelial cells are created and the BBB is disrupted. With the barrier function damaged, blood products are able to enter the brain space resulting in the primary concern of ICH: cerebral edema.

Cerebral Edema

Edema is characterized as an irregular accumulation of water in either extracellular or intracellular spaces. In most traditional literature, edema is categorized into two divisions: cytotoxic and vasogenic. Cytotoxic edema is a process in which water is moved into the intracellular space from the extracellular space to produce cellular swelling without disrupting the blood-brain barrier. On the other hand, vasogenic edema is characterized as the movement of water from a damaged BBB, where water travels from the blood to parenchyma [35, 42].

Within the pathology of ICH, though both types of edema are known to be present, vasogenic edema is considered the primary issue due to its role on gap

junction protein damage [31, 40]. The initial mechanical stretch of the injury along with the toxic breakdown elements of the blood, damage cells in the immediate vicinity which release materials such as reactive oxygen species and cytokines into the extracellular space. These materials spread to regions beyond the injury site stimulating the breakdown of junction proteins that stitch together the endothelial cells of the brain capillaries. When these junction proteins are damaged, gaps in the endothelial layer are produced giving way for paracellular transport of blood materials into the brain space [36]. Though water is normally able to freely cross the BBB into the brain, the solute movement from the blood into the brain shifts the osmotic gradient driving water into the brain thus producing vasogenic edema. As a consequence of the vasogenic edema, the cellular swelling produces further mechanical stretch with continued tissue damage.

Cytotoxic edema is a consequence of changes in the extracellular osmolarity or in conditions where there is ion redistribution between the intracellular and extracellular brain compartments. This results in the activation of transcapillary ion channels that cause water fluxes primarily into astrocytes and neurons resulting in what is known as cytotoxic edema [43]. This type of edema has been observed in several pathologies including head trauma, ischemia, brain tumors, multiple sclerosis, and other vascular diseases. Cytotoxic edema does not always occur with the disruption of the BBB tight junctions either physically or functionally. However, if the barrier is affected, this can result in

cellular, fluid, and protein leakage into the brain parenchyma resulting in vasogenic edema.

Insulin-like Growth Factor-1 Signaling in the Brain

Insulin-like growth factor (IGF) is a family of proteins that are ubiquitously expressed in most organisms, including humans and rodents. The name given to this family of proteins is a consequence of their structural similarity to the insulin family. The IGF system is composed of two ligands (IGF-1 and IGF-2), two receptors (IGF-1R and IGF-2R), and six binding proteins (IGFBP-1 through IGFBP-6) that collectively function in a variety of physiologic mechanisms such as metabolism, cell growth, and cell proliferation [44, 45]. IGF-1 is the most abundant of the ligands in circulation and has been confirmed to play a pivotal role in several physiological functions [46]. IGF-1 is able to bind to both IGF-1R and IGF-2R as well as insulin receptor, but has an extremely high affinity for the IGF-1R only binding to the other receptors when concentrations of their appropriate ligands are severely depleted.

IGF-1/IGF-1R is generally found to signal through the PI3K/AKT pathway to exert its effects. This pathway has been previously studied to inhibit GSK3β and thus provide its protective functions [46]. GSK3β is an intracellular protein that has a variety of effects in a cell, but after ICH has a particularly strong effect in aiding in BBB disruption [47]. GSK3β inhibits the activity of β-catenin through phosphorylation thus reducing production of tight junction proteins [48, 49].

Additionally, GSK3β works in conjunction with c-Jun/JNK inflammatory pathways to produce MMP9 [50, 51]. In its active form, GSK3β acts by physically binding to and phosphorylating mitogen activated kinase (MEK) kinase 1 (MEKK1) an important regulator of MEK [52]. MEK phosphorylates and activates c-Jun N-terminal Kinase (JNK) which activates activated which degrades collagen IV found in the basal lamina. Degradation of the basal lamina produces porous entries for materials that pass the tight junction barrier to enter the brain.

The role of IGF-1 in Neuroprotection and Neurogenesis

The receptor has previously been found to be located in the human brain in several regions including the hippocampus, amygdala, parahippocampal gyrus, cerebellum, cerebral cortex, caudate nucleus, substantia nigra, red nucleus, white matter, and cerebral pedunculus [53]. In the adult brain, the majority of neurogenesis has been terminated besides a select few areas such as subventricular zone and dentate gyrus of the hippocampus. Interestingly, the progenitor cells in this area have demonstrated increased proliferation in response to introduction of IGF-1 in both in vitro and in vivo models [54, 55].

Stress, depression, and aging have both been implicated in reduced IGF-1 levels and a decline in serum IGF-1 has been associated with age-related cognitive decline in the elderly population [54, 56]. However, it has been observed that brain injury stimulates an increase in neurogenesis and an increase of IGF-1 in the brain. It has been noted that in the acute stages of

stroke, serum IGF-1 levels are greater and that it is found in lower quantities in the older population suggesting it is found higher in the rehabilitation phase of stroke [54, 56, 57]. Further studies have observed that ischemic stroke patients with high endogenous serum IGF-1 levels showed greater neurological symptom improvement than those with low IGF-1 levels [58].

Most studies of IGF-1 regarding the central nervous system (CNS) are related to its effects on neuroplasticity and neuronal survival, but a few have also described its effect on the BBB. In animal models, it has been shown to reduce ischemic size in ischemic stroke animal models [59, 60]. Given together with EPO, it was also shown that there were improved outcomes in an MCAO model as well [61]. In a model examining the neurotoxic effects of nanoparticles, it was found that pretreatment with IGF-1 was able to reduce BBB breakdown and edema formation [62].

Conclusion

ICH is a disease that has several mechanisms involved to exert its deleterious effects. The acute severity of the injury makes treatment modalities difficult to develop. Research shows that treating for BBB injury and edema formation are primary focuses due to the swelling of the brain being the primary factor in determining the severity of the disease progression. The role of IGF-1 in stroke is a promising area of study as it has been observed in other neurological disorders to be dysregulated. Its ability to promote synaptic plasticity and its effects as a neurotrophic and BBB injury sparing peptide suggest that its role in

the recovery phase of stroke is an important modulator. However, its use must be carefully monitored as well due to its role as a tumor promotor [56]. Though it may provide a useful target for treatments of neurological diseases including stroke, consideration on the dosage and route of administration must be carefully elucidated. In our study, we will examine if the BBB can be preserved with administration of exogenous IGF-1. We will also discuss other methods that we have utilized to show how BBB injury can be reduced including the administration of Adropin and inhibition of PDGFR-β.

References

1. Virani, S.S., et al., *Heart Disease and Stroke Statistics-2021 Update: A Report From the American Heart Association.* Circulation, 2021. 143(8): p. e254-e743.

2. Go, A.S., et al., *Heart disease and stroke statistics--2013 update: a report from the American Heart Association.* Circulation, 2013. 127(1): p. e6-e245.

3. McGurgan, I.J., et al., *Acute intracerebral haemorrhage: diagnosis and management.* Practical Neurology, 2021. 21(2): p. 128.

4. Batjer, H.H., et al., *Failure of surgery to improve outcome in hypertensive putaminal hemorrhage. A prospective randomized trial.* Arch Neurol, 1990. 47(10): p. 1103-6.

5. Gomes, J.A. and E. Manno, *New developments in the treatment of intracerebral hemorrhage.* Neurol Clin, 2013. 31(3): p. 721-35.

6. Qureshi, A.I., A.D. Mendelow, and D.F. Hanley, *Intracerebral haemorrhage.* Lancet, 2009. 373(9675): p. 1632-44.

7. Qureshi, A.I., et al., *Isolated and borderline isolated systolic hypertension relative to long-term risk and type of stroke: a 20-year follow-up of the national health and nutrition survey.* Stroke, 2002. 33(12): p. 2781-8.

8. Ariesen, M.J., et al., *Risk factors for intracerebral hemorrhage in the general population: a systematic review.* Stroke, 2003. 34(8): p. 2060-5.

9. Rasool, A.H., et al., *Blood pressure in acute intracerebral haemorrhage.* J Hum Hypertens, 2004. 18(3): p. 187-92.

10. Diez, J., et al., *Altered regulation of smooth muscle cell proliferation and apoptosis in small arteries of spontaneously hypertensive rats.* Eur Heart J, 1998. 19 Suppl G: p. G29-33.

11. Campbell, G.J. and M.R. Roach, *Fenestrations in the internal elastic lamina at bifurcations of human cerebral arteries.* Stroke, 1981. 12(4): p. 489-96.

12. Nicoll, J.A., et al., *Cerebral amyloid angiopathy plays a direct role in the pathogenesis of Alzheimer's disease. Pro-CAA position statement.* Neurobiol Aging, 2004. 25(5): p. 589-97; discussion 603-4.

13. Fisher, C.M., *Pathological observations in hypertensive cerebral hemorrhage.* J Neuropathol Exp Neurol, 1971. 30(3): p. 536-50.

14. Sutherland, G.R. and R.N. Auer, *Primary intracerebral hemorrhage.* J Clin Neurosci, 2006. 13(5): p. 511-7.

15. Mayer, S.A., et al., *Neurologic deterioration in noncomatose patients with supratentorial intracerebral hemorrhage.* Neurology, 1994. 44(8): p. 1379-84.

16. Brott, T., et al., *Early hemorrhage growth in patients with intracerebral hemorrhage.* Stroke, 1997. 28(1): p. 1-5.

17. Kazui, S., et al., *Enlargement of spontaneous intracerebral hemorrhage. Incidence and time course.* Stroke, 1996. 27(10): p. 1783-7.

18. Cole, F.M. and P. Yates, *Intracerebral microaneurysms and small cerebrovascular lesions.* Brain, 1967. 90(4): p. 759-68.

19. Challa, V.R., D.M. Moody, and M.A. Bell, *The Charcot-Bouchard aneurysm controversy: impact of a new histologic technique.* J Neuropathol Exp Neurol, 1992. 51(3): p. 264-71.

20. Charcot, J.M. and C. Bouchard, *Nouvelles recherches sur la pathogenie de l'hemorrhagie cerebrale.* Arch Physiol Norm Pathol, 1868. 1(1): p. 110-127.

21. Nikolic, S., I. Banjanin, and A. Stanojevic, *[Subarachnoidal hemorrhage from saccular aneurysms as a cause of natural death].* Srp Arh Celok Lek, 2004. 132(7-8): p. 236-9.

22. Broderick, J.P., et al., *Volume of intracerebral hemorrhage. A powerful and easy-to-use predictor of 30-day mortality.* Stroke, 1993. 24(7): p. 987-93.

23. Nilsson, O.G., et al., *Prediction of death in patients with primary intracerebral hemorrhage: a prospective study of a defined population.* J Neurosurg, 2002. 97(3): p. 531-6.

24. Passero, S., G. Ciacci, and M. Ulivelli, *The influence of diabetes and hyperglycemia on clinical course after intracerebral hemorrhage.* Neurology, 2003. 61(10): p. 1351-6.

25. Labovitz, D.L. and R.L. Sacco, *Intracerebral hemorrhage: update.* Curr Opin Neurol, 2001. 14(1): p. 103-8.

26. Kumral, E., et al., *Thalamic hemorrhage. A prospective study of 100 patients.* Stroke, 1995. 26(6): p. 964-70.

27. Gilbert, J.J. and H.V. Vinters, *Cerebral amyloid angiopathy: incidence and complications in the aging brain. I. Cerebral hemorrhage.* Stroke, 1983. 14(6): p. 915-23.

28. Neau, J.P., et al., *Recurrent intracerebral hemorrhage.* Neurology, 1997. 49(1): p. 106-13.

29. Rosenberg, G.A., et al., *Autoradiographic patterns of brain interstitial fluid flow after collagenase-induced haemorrhage in rat.* Acta Neurochir Suppl (Wien), 1990. 51: p. 280-2.

30. James, M.L., D.S. Warner, and D.T. Laskowitz, *Preclinical models of intracerebral hemorrhage: a translational perspective.* Neurocrit Care, 2008. 9(1): p. 139-52.

31. Yang, G.Y., et al., *Experimental intracerebral hemorrhage: relationship between brain edema, blood flow, and blood-brain barrier permeability in rats.* J Neurosurg, 1994. 81(1): p. 93-102.

32. Deinsberger, W., et al., *Local fibrinolysis and aspiration of intracerebral hematomas in rats. An experimental study using MR monitoring.* Neurol Res, 1998. 20(4): p. 349-52.

33. Harris, E.D., Jr. and S.M. Krane, *Collagenases (first of three parts).* N Engl J Med, 1974. 291(11): p. 557-63.

34. Enzmann, D.R., et al., *Natural history of experimental intracerebral hemorrhage: sonography, computed tomography and neuropathology.* AJNR Am J Neuroradiol, 1981. 2(6): p. 517-26.

35. Xi, G., R.F. Keep, and J.T. Hoff, *Mechanisms of brain injury after intracerebral haemorrhage.* Lancet Neurol, 2006. 5(1): p. 53-63.

36. Neuwelt, E.A., *Mechanisms of disease: the blood-brain barrier.* Neurosurgery, 2004. 54(1): p. 131-40; discussion 141-2.

37. Rieckmann, P. and B. Engelhardt, *Building up the blood-brain barrier.* Nat Med, 2003. 9(7): p. 828-9.

38. Keep, R.F., et al., *Vascular disruption and blood-brain barrier dysfunction in intracerebral hemorrhage.* Fluids Barriers CNS, 2014. 11: p. 18.

39. Lee, K.R., et al., *Mechanisms of edema formation after intracerebral hemorrhage: effects of thrombin on cerebral blood flow, blood-brain barrier permeability, and cell survival in a rat model.* J Neurosurg, 1997. 86(2): p. 272-8.

40. Ballabh, P., A. Braun, and M. Nedergaard, *The blood-brain barrier: an overview: structure, regulation, and clinical implications.* Neurobiol Dis, 2004. 16(1): p. 1-13.

41. Liu, W.Y., et al., *Tight junction in blood-brain barrier: an overview of structure, regulation, and regulator substances.* CNS Neurosci Ther, 2012. 18(8): p. 609-15.

42. Fewel, M.E., B.G. Thompson, Jr., and J.T. Hoff, *Spontaneous intracerebral hemorrhage: a review.* Neurosurg Focus, 2003. 15(4): p. E1.

43. Unterberg, A.W., et al., *Edema and brain trauma.* Neuroscience, 2004. 129(4): p. 1021-9.

44. Bayes-Genis, A., C.A. Conover, and R.S. Schwartz, *The insulin-like growth factor axis: A review of atherosclerosis and restenosis.* Circ Res, 2000. 86(2): p. 125-30.

45. Baxter, R.C., *Insulin-like growth factor binding protein-3 (IGFBP-3): Novel ligands mediate unexpected functions.* J Cell Commun Signal, 2013. 7(3): p. 179-89.

46. Bondy, C.A. and C.M. Cheng, *Signaling by insulin-like growth factor 1 in brain.* Eur J Pharmacol, 2004. 490(1-3): p. 25-31.

47. Ramirez, S.H., et al., *Inhibition of glycogen synthase kinase 3beta promotes tight junction stability in brain endothelial cells by half-life extension of occludin and claudin-5.* PLoS One, 2013. 8(2): p. e55972.

48. Mishra, R., et al., *Glycogen synthase kinase-3beta induces neuronal cell death via direct phosphorylation of mixed lineage kinase 3.* J Biol Chem, 2007. 282(42): p. 30393-405.

49. Cortes-Vieyra, R., et al., *Role of glycogen synthase kinase-3 beta in the inflammatory response caused by bacterial pathogens.* J Inflamm (Lond), 2012. 9(1): p. 23.

50. Carrozzino, F., et al., *Inhibition of basal p38 or JNK activity enhances epithelial barrier function through differential modulation of claudin expression.* Am J Physiol Cell Physiol, 2009. 297(3): p. C775-87.

51. Yatsushige, H., et al., *Role of c-Jun N-terminal kinase in early brain injury after subarachnoid hemorrhage.* J Neurosci Res, 2007. 85(7): p. 1436-48.

52. Kim, J.W., et al., *Glycogen synthase kinase 3 beta is a natural activator of mitogen-activated protein kinase/extracellular signal-regulated kinase kinase kinase 1 (MEKK1).* J Biol Chem, 2003. 278(16): p. 13995-4001.

53. Adem, A., et al., *Insulin-like growth factor 1 (IGF-1) receptors in the human brain: quantitative autoradiographic localization.* Brain Res, 1989. 503(2): p. 299-303.

54. Anderson, M.F., et al., *Insulin-like growth factor-I and neurogenesis in the adult mammalian brain.* Brain Res Dev Brain Res, 2002. 134(1-2): p. 115-22.

55. Brooker, G.J., et al., *Endogenous IGF-1 regulates the neuronal differentiation of adult stem cells.* J Neurosci Res, 2000. 59(3): p. 332-41.

56. Aleman, A. and I. Torres-Aleman, *Circulating insulin-like growth factor I and cognitive function: neuromodulation throughout the lifespan.* Prog Neurobiol, 2009. 89(3): p. 256-65.

57. Aberg, D., et al., *Serum IGF-I levels correlate to improvement of functional outcome after ischemic stroke.* J Clin Endocrinol Metab, 2011. 96(7): p. E1055-64.

58. De Smedt, A., et al., *Insulin-like growth factor I serum levels influence ischemic stroke outcome.* Stroke, 2011. 42(8): p. 2180-5.

59. Beilharz, E.J., et al., *Co-ordinated and cellular specific induction of the components of the IGF/IGFBP axis in the rat brain following hypoxic-ischemic injury.* Brain Res Mol Brain Res, 1998. 59(2): p. 119-34.

60. De Geyter, D., et al., *Neuroprotective efficacy of subcutaneous insulin-like growth factor-I administration in normotensive and hypertensive rats with an ischemic stroke.* Neuroscience, 2013. 250C: p. 253-262.

61. Fletcher, L., et al., *Intranasal delivery of erythropoietin plus insulin-like growth factor-I for acute neuroprotection in stroke. Laboratory investigation.* J Neurosurg, 2009. 111(1): p. 164-70.

62. Sharma, H.S., et al., *Neuroprotective effects of insulin like growth factor-1 on engineered metal nanoparticles Ag, Cu and Al induced blood-brain barrier breakdown, edema formation, oxidative stress, upregulation of neuronal nitric oxide synthase and brain pathology.* Prog Brain Res, 2021. 266: p. 97-121.

CHAPTER TWO

RHIGF-1 REDUCES THE PERMEABILITY OF THE BLOOD-BRAIN BARRIER FOLLOWING INTRACEREBRAL HEMORRHAGE IN MICE

Derek Sunil Nowrangi[1], Devin McBride[1], Anatol Manaenko[1], Brandon Dixon[1], Jiping Tang[1], John H. Zhang[1,2]

[1] Department of Physiology, [2]Department of Neurosurgery, Loma Linda University School of Medicine, Loma Linda, CA, USA

Corresponding Author: John H. Zhang, M.D./PhD

Department of Physiology & Pharmacology

Loma Linda University School of Medicine Risley Hall, Room 223

Loma Linda, CA 92354, USA

Phone: 909-558-4723

Fax: 909-558-0119

Email: johnzhang3910@yahoo.com

The work presented in this chapter has been published.

Exp Neurol. 2019 Feb;312:72-81.

Abstract

Disruption of the blood-brain barrier results in the formation of edema and contributes to the loss of neurological function following intracerebral hemorrhage (ICH). This study examined insulin-like growth factor-1 (IGF-1) as a treatment and its mechanism of action for protecting the blood-brain barrier after ICH in mice. 171 Male CD-1 mice were subjected to ICH via collagenase or autologous blood. A dose study for recombinant human IGF-1 (rhIGF-1) was performed. Brain water content and behavioral deficits were evaluated at 24 and 72 hours after the surgery, and Evans blue extravasation and hemoglobin assay were conducted at 24 hours. Western blotting was performed for the mechanism study and interventions were used targeting the IGF-1R/GSK3β/MEKK1 pathway. rhIGF-1 reduced edema and blood-brain barrier permeability, and improved neurobehavior outcomes. Western blots showed that rhIGF-1 reduced p-GSK3β and MEKK1 expression, thereby increasing occludin and claudin-5 expression. Inhibition and knockdown of IGF-1R reversed the therapeutic benefits of rhIGF-1. The findings within suggest that stimulation of the IGF-1R is a therapeutic target for ICH which may lead to improved neurofunctional and blood-brain barrier protection.

Introduction

Intracerebral hemorrhage (ICH) is one of the most dangerous forms of stroke that currently has no effective treatments. Among the several pathological sequelae of ICH, the hematoma-induced breakdown of the blood-brain barrier (BBB) is one of the major concerns which plays a critical role in the pathophysiology of the disease [1, 2]. Loss of endothelial tight junction proteins contribute to increased permeability of the BBB leading to the formation of vasogenic edema and a deterioration of neurological functions [3, 4]. Previous studies have demonstrated that the protection and recovery of tight junction proteins decreases the severity of the ICH injury with improved neurological outcomes [5].

Insulin-like growth factor 1 (IGF-1) is highly selective for the IGF-1 receptor (IGF-1R), which is expressed on several cell types in the brain including neurons, astrocytes, and endothelial cells [6-8]. Canonically, stimulation of the IGF-1R causes of the phosphatidylinositol 3-kinase (PI3K)-Akt pathway thus attenuating glycogen synthase kinase-3β (GSK3β) activation [9, 10]. Previously, our lab demonstrated that preventing activation of glycogen synthase kinase-3β (GSK3β) reduces edema and damage to the BBB following injury through protecting tight junction proteins [5]. GSK3β physically binds to and activates mitogen-activated protein kinase (MAPK) kinase (MEK) kinase 1 (MEKK1), an important stimulator of the c-Jun/JNK pathway, which has been shown to increase MMP9 production [11, 12]. GSK3β has also been shown to reduce

expression of the tight junction proteins occludin and claudin-5, indicating an increase in the permeability of the barrier [13].

IGF-1 has been previously described to have protective effects in ischemic brain injury models, however the role of this growth factor remains unexplored in ICH. In addition, the role and mechanism by which IGF-1 and IGF-1R protects the BBB is not completely understood. We hypothesize that IGF-1 will decrease the permeability of the BBB and reduce edema in an ICH mouse model via IGF-1R stimulation, reducing GSK3β/MEKK1 activation, to prevent the loss of tight junction protein expression.

Materials and Methods

Animal Care

All procedures were done in accordance to institutionally approved protocols and the NIH Guide for Critical Care and Use of Laboratory Animals. Male CD-1 mice from Charles River, Wilmington, WA were housed in a light and temperature controlled room with access to water and food.

Intracerebral Hemorrhage Surgery

Intracerebral hemorrhage was induced either by sterile collagenase type VII infusion or a double injection of autologous blood both which we have previously utilized [5, 14]. Mice were anesthetized using an intraperitoneal (i.p.) co-injection of ketamine (100 mg/kg) and xylazine (10 mg/kg). An incision on the scalp was made to reveal the location of bregma and the mouse then positioned

on a stereotactic head frame (Stoelting Company, Wood Dale, IL). A small burr hole was created (coordinates from bregma: 0.2 mm anterior, 2.2 mm right lateral) for the insertion of a 27-gauge Hamilton needle (Hamilton Company, Reno, NV). A 10 µl or 250 µl Hamilton needle was filled with collagenase or autologous whole blood respectively and lowered into the burr hole. For the collagenase injection model, 0.075 U (dissolved in 0.5 µl of PBS) of collagenase was infused into the right hemispheric basal ganglia at a rate of 0.1667 µl/min and a depth of 3.5 mm. For the autologous blood injection model, 5 µl of blood was first injected at a rate of 2 µl/min and depth of 3.0 mm. The needle was then lowered to 3.7 mm where following a 5-minute wait, 25 µl was injected at a rate of 2 µl/min. All infusions were controlled with a micro perfusion pump (Harvard Apparatus, Holliston, MA). Following the infusions, the needle was left in place for 5 minutes before being retracted at a rate of 1 mm/min. Sham operated animals were only subjected to the needle insertion. Following the retraction of the needle, the burr hole was sealed using bone wax and the scalp sutured. All animals received subcutaneous (s.c.) injections of 0.2 ml of saline into each flank (0.4 ml total) while the mice were placed on a warm heating pad for recovery and observation. During the surgery, all animals were temperature regulated using a heating pad with a rectal probe.

siRNA Intracerebroventricular Injection

Two different IGF-1R siRNAs (Cell Signaling and Santa Cruz Biotechnology) were mixed and administered via intracerebroventricular (i.c.v.)

injection [15]. Briefly, both siRNAs were prepared following the manufacturer's instructions by dissolving in sterile RNase-free water. Mice were anesthetized with ketamine (100mg/kg) and xylazine (10mg/kg) i.p. co-injection. The IGF-1R siRNA mixture and scramble siRNA (100 pmol) was administered via i.c.v. 24 hours before ICH induction as previously described [16, 17]. A small burr hole was created at 1.0 mm left lateral from bregma) and a 27-gauge Hamilton needle lowered to 2.3 mm deep and infused at 0.67 µl/min. The needle was left to rest for 5 minutes and then retracted at a rate of 1 mm/min. Following the retraction, the burr hole was sealed with bone wax and scalp sutured.

Experimental Groups and Pharmacological Interventions

A total of N=171 (Experimental N=168; Exclusions N=3) animals were used in this study with 3 animals excluded due to mortality during the surgery procedure (1 Vehicle, 1 rhIGF-1 + AG1024, 1 rhIGF-1 + scramble siRNA). Experimental groups consisted of mice subjected to either sham surgery (N=30), collagenase-induced ICH (n=126), or autologous whole blood-induced ICH (N=12). Animals were randomly selected for treatments following the ICH surgery. Recombinant human IGF-1 (rhIGF-1; Cell Signaling) was prepared in concentrations of 10 µg (N=12) or 50 µg (N=66) in 12 µl of PBS and given through intranasal (i.n.) administration 3 hours after the surgery [18, 19]. Alternatively, a daily dose of 50 µg rhIGF-1 (N=6) was given starting 3 hours after the surgery up to 72 hours after the surgery. AG1024 (Santa Cruz Biotechnology), a specific inhibitor of the IGF-1R, was given in 40 µg/100 µl

through i.p. injections 1 hour after the surgery [20, 21]. Preparation of scramble siRNA and IGF-1R siRNA was previously discussed. 50 μg rhIGF-1 was given alone or in combination with AG1024 (N=12), scramble siRNA (N=12), or mixed IGF-1R siRNA (N=12). Temperature and heart rate were monitored for variations throughout the surgery as well as before neurological testing and animal sacrifice.

Neurobehavioral Assessment

A blinded investigator performed all neurological testing. The modified Garcia Neuroscore, corner turn evaluation, and forelimb placement exam were utilized to examine sensorimotor deficits in mice at 24 and 72 hours after the surgery [22]. The modified Garcia Neuroscore evaluates the animals sensorimotor abilities using 7 tests including 1) spontaneous activity, 2) side stroking, 3) vibrissae proprioception, 4) limb symmetry, 5) lateral turning, 6) forelimb walking, and 7) climbing [23]. Performance for each individual test was graded on a scale of 0 (worst performance) to 3 (best performance) with the sum of the scores (max = 21) providing the overall performance of the animal. For the corner turn exam, animals advanced into a 30° corner and the direction rotated to exit the corner was recorded (10 or 20 total trials). A turn was counted when the animal completes its rotation by lifting its forepaws to the sidewall and then returning to the ground in a direction opposite of the corner. The overall performance was evaluated as the number of left turns/total turns x 100 (%). The forelimb placement exam evaluates the reflex motor capabilities of the animal.

The animal is lightly restrained, and vibrissae-stimulation provided to both ipsilateral (10 trials) and contralateral sides (10 trials). The overall performance was recorded as the number of times the forelimb elicited a reaching response/number of trials x 100 (%). Mice that were sacrificed at 72 hours were tested for neurobehavior at both 24 and 72 hours following the surgery.

Measuring Brain Water Content

Brain water content was evaluated at 24 and 72 hours after the ICH surgery using the wet/dry method [15]. Briefly, mice were anesthetized with isofluorane and decapitated. The brains were quickly removed, and a coronal brain section of 4 mm centered on the needle tract was separated into ipsilateral and contralateral cortex and basal ganglia regions as well as the cerebellum for individual analysis. All sections were weighed on an analytical microbalance immediately to produce a wet weight and after 24 hours (100°C) to get a dry weight. To calculate the brain water content, the formula used was: (wet weight-dry weight)/wet weight x 100.

Evans Blue Extravasation

Blood-brain barrier permeability was examined 24 hours after the ICH surgery through evans blue extravasation as described before [24]. Briefly, an I.P. injection of 2% evans blue dye was given to the mice 3 hours before a transcardial perfusion with 100 ml PBS. The brain was separated into right and left hemisphere, frozen with liquid nitrogen, and stored at -80°C. 1000 µl of PBS

was added to the right hemisphere tissue, which was homogenized and sonicated. The mixture was then centrifuged for 30 minutes at 14000 rpm and 4°C. A mixture comprised of 500 µl of supernatant and 500 µl of 50% Trichloroacetic acid (TCA) was created and left to incubate at 4°C overnight before centrifuging again. The resulting mixture was then transferred to the spectrophotometer for analysis. A standard curve was created to analyze the data. The data is represented as µg of Evans Blue Dye/g of tissue.

Hemoglobin Assay

For hematoma evaluation, the blood volume in the brain was examined using a hemoglobin assay [24]. Briefly, 200 µl of the supernatant collected from the Evans Blue method described above was mixed with 800 µl of Drabkins's reagent (Sigma Aldrich) and left to incubate for 15 minutes at room temperature. The resulting mixture was then transferred to the spectrophotometer for analysis. A standard curve was created to analyze the data. Values are represented as µl of hemoglobin/hemisphere.

Western Blotting

Animals were euthanized at 0, 3, 6, 12, 24, and 72 hours for western blot analysis. At each time, animals were heavily sedated using isofluorane and euthanized through transcardial perfusions using 100 µl of PBS. The brain was divided into hemispheres and then frozen in liquid nitrogen and stored at -80°C. The right and left hemispheres were removed from -80°C storage and weighed

before being homogenized in lysis buffer. After resting for 30 min, the samples were centrifuged for 20 minutes at 14000 rpm and 4°C. The supernatant was collected, and the protein concentration was analyzed using a spectrophotometer. Western blots were done using the following primary antibodies. Anti-β-actin (1:2000), anti-p-GSK3β (Y216; 1:500), anti-GSK3β (1:500), anti-MEKK1 (1:500), anti-Occludin (1:1000), and anti-Claudin 5 (1:1000) were purchased from Abcam Inc. (Cambridge, MA). Anti-IGF-1 and anti-IGF-1R were purchased from Santa Cruz Biotechnology. (Santa Cruz, CA). The optical bands were visualized using ECL Plus (GE Healthcare Life Sciences) and analyzed with Image J Software (National Institute of Health).

Statistical Evaluations

Data was expressed as mean ± Standard Deviation (SD) for brain water content, corner turn, forelimb placement, Evans blue, hemoglobin assay, and western blots. Significance analysis between groups was calculated using a One-Way Analysis of Variance with a Tukey post-hoc. Data for Modified Garcia neuroscore was expressed as median ± Interquartile Range (IQR). Significance analysis between groups was calculated using a Kruskal-Wallis One-Way Analysis on Ranks with Dunn's post-hoc test. Significance was indicated with a P value of <0.05, unless otherwise noted. Statistical power was calculated for determining sample size using previously published data for brain water content in the ICH models before starting the study. Analysis was done using $\beta=0.80$, $\alpha=0.05$, and a SD of 0.75. 6 mice were allocated to each group in the brain water

content experiments with a minimal detectable difference in the means of 1.35. All statistics were generated using SigmaPlot version 11.0 (Systat Software).

Results

High Dose of rhIGF-1 Reduces Brain Edema and Improves Neurobehavior at 24 Hours after Collagenase Induced ICH

Brain water content (N=6/group) and neurofunctional deficits (N=12-18/group) were examined at 24 hours following the surgery in the collagenase injection model. No animals were excluded from this experiment and no mortalities were found in any groups. All groups were compared to sham (* = $P<0.05$) and vehicle (# = $P<0.05$) groups. For brain water content, groups in tissue regions were compared independently. Mice subjected to ICH with vehicle, low dose (10 μg) of rhIGF-1, high dose (50 μg) of rhIGF-1, AG1024 with high dose of rhIGF-1, or IGF-1R siRNA with high dose of rhIGF-1 displayed significantly elevated brain water content compared with sham-operated animals in the ipsilateral basal ganglia (*$p<0.05$; Figure 2A). However, the high dose of rhIGF-1 and scramble siRNA with high dose of rhIGF-1 groups showed significantly decreased brain water content in the ipsilateral basal ganglia compared to vehicle (#$p<0.05$, Figure 2A). No significance was found with the scramble siRNA with rhIGF-1 group compared to sham ($p>0.05$). No significant differences were calculated between groups for the ipsilateral cortex, contralateral cortex and basal ganglia, and the cerebellum ($p>0.05$).

Mice subjected to ICH with vehicle (N=18) showed significant neurobehavior deficits as compared to the sham (N=18) operated animals ($p<0.05$; Figure 2B-D). The low dose of rhIGF-1 (N=12) was unable to improve behavior scores in any test. However, the high dose of rhIGF-1 (N=18) displayed an improvement to behavior scores as compared to the vehicle animals in all tests ($p<0.05$; Figure 2B-D), but remained significantly different from the sham group in the Corner Turn and Forelimb Placement tests ($p<0.05$; Figure 2C and 1D). The AG1024 (N=12) and IGF-1R siRNA (N=12) groups with the high dose of rhIGF-1 failed to demonstrate improved neurobehavior scores in all three tests ($p>0.05$). The scramble siRNA (N=12) group with the high dose of rhIGF-1 showed improved scores for all tests compared with vehicle ($p<0.05$: Figure 2B-D), but remained statistical significance different from the sham group in the Corner Turn Test ($p<0.05$; Figure 2C).

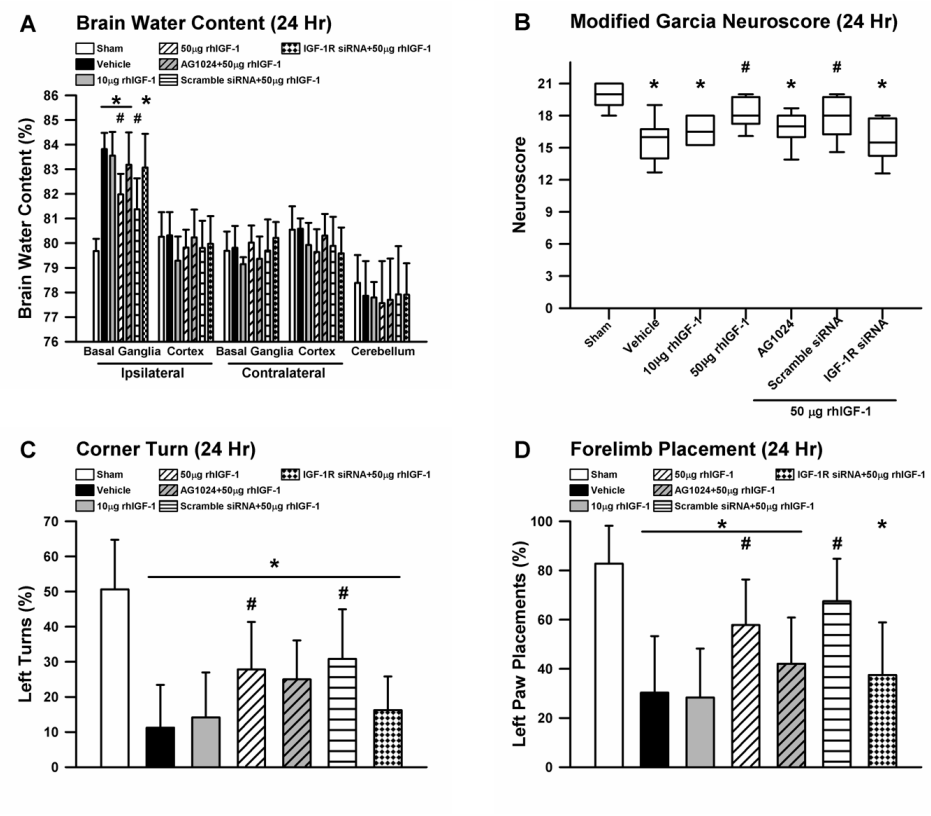

Figure 2. Collagenase injection ICH model at 24 hours. (A) Brain water content at 24 hours (N=6 per group). (B) Modified Garcia neuroscore. (C) Corner turn test. (D) Forelimb placement test. (B, C, D: N=18 for Sham, Vehicle, and 50 μg rhIGF-1 groups; N=12 for 10 μg rhIGF-1, AG1024 + 50 μg rhIGF-1, Scramble siRNA + 50 μg rhIGF-1, and IGF-1R siRNA + 50 μg rhIGF-1 groups). A, C, D: Values are expressed as mean±SD. B: Values expressed as median±IQR. *P<0.05 compared with sham, #P<0.05 compared with vehicle.

Daily Administration of 50 μg rhIGF-1 Reduces Brain Edema and Improves Neurobehavior at 72 Hours After Collagenase Induced ICH

Brain water content (N=6/group) and neurofunctional deficits (N=6/group) were examined at 72 hours following the surgery in the collagenase injection model. In this experiment, 1 mouse under the "ICH + Vehicle" group was omitted due to mortality during the surgery procedure. All groups displayed statistically significant elevated brain edema compared with sham-operated animals in the ipsilateral basal ganglia ($p<0.05$; Figure 3A). The high dose of rhIGF-1 given daily showed significantly decreased brain water content in the ipsilateral basal ganglia compared to vehicle ($p<0.05$). No statistical differences were observed between groups for the ipsilateral cortex, contralateral cortex, basal ganglia, and cerebellum ($p>0.05$). Within the ipsilateral cortex, 10 μg of rhIGF-1 displayed a slight elevation to edema compared to sham but did not reach significant differences ($p=0.059$).

Mice subjected to ICH with vehicle, low dose of rhIGF-1, and high dose of rhIGF-1 showed significant neurobehavior deficits as compared to the sham operated animals ($p<0.05$; Figure 3B-D). However, the high dose of rhIGF-1 (50 μg) given daily displayed improved scores in the Modified Garcia Neuroscore and Corner Turn tests as compared to the vehicle animals ($p<0.05$; Figure 3B and 3C). The daily dose of rhIGF-1 group was not significant to sham or vehicle groups in the Forelilmb Placement test ($p>0.05$; Figure 3D).

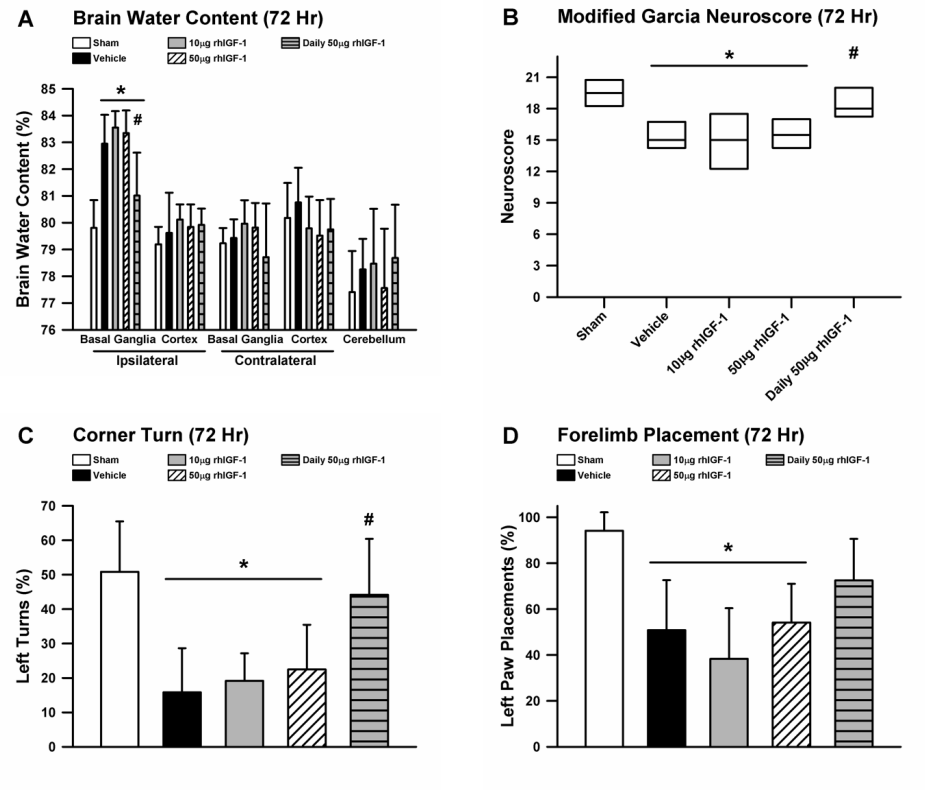

Figure 3. Collagenase injection ICH model at 72 hours. (A) Brain water content at 72 hours (N=6 per group). (B) Modified Garcia neuroscore (N=6 per group). (C) Corner turn test (N=6 per group). (D) Forelimb placement test (N=6 per group). A, C, D: Values are expressed as mean±SD. B: Values expressed as median±IQR. *P<0.05 compared with shame, #P<0.05 compared with vehicle.

High Dose of rhIGF-1 Reduces Brain Edema and Improves Neurobehavior at 24 Hours after Autologous Blood Induced ICH

Brain water content (N=6/group) and neurofunctional deficits (N=6/group) were examined at 24 hours following the surgery in the autologous blood injection model. No animals were excluded from this experiment and no mortalities were found in any groups. Mice subjected to ICH with vehicle displayed significantly elevated brain water content compared to sham-operated animals ($p<0.05$; Figure 4A). A mild improvement was found in the high dose of rhIGF-1 treatment group compared to the vehicle operated group ($p=0.048$). Additionally, the rhIGF-1 remained significantly different to the sham group ($p<0.05$). No statistically significant differences were calculated between groups for the ipsilateral cortex, contralateral cortex and basal ganglia, and the cerebellum ($p>0.05$).

Mice subjected to ICH with vehicle showed significant neurobehavior deficits as compared to the sham-operated animals in all exams ($p<0.05$; Figure 4B-D). The high dose of rhIGF-1 displayed improved neurobehavior scores compared to vehicle in the Modified Garcia Neuroscore and Forelimb placement exam ($p<0.05$; Figure 4B, D). The high dose of rhIGF-1 failed to significantly improve scores for the Corner Turn test ($p>0.05$; Figure 4C).

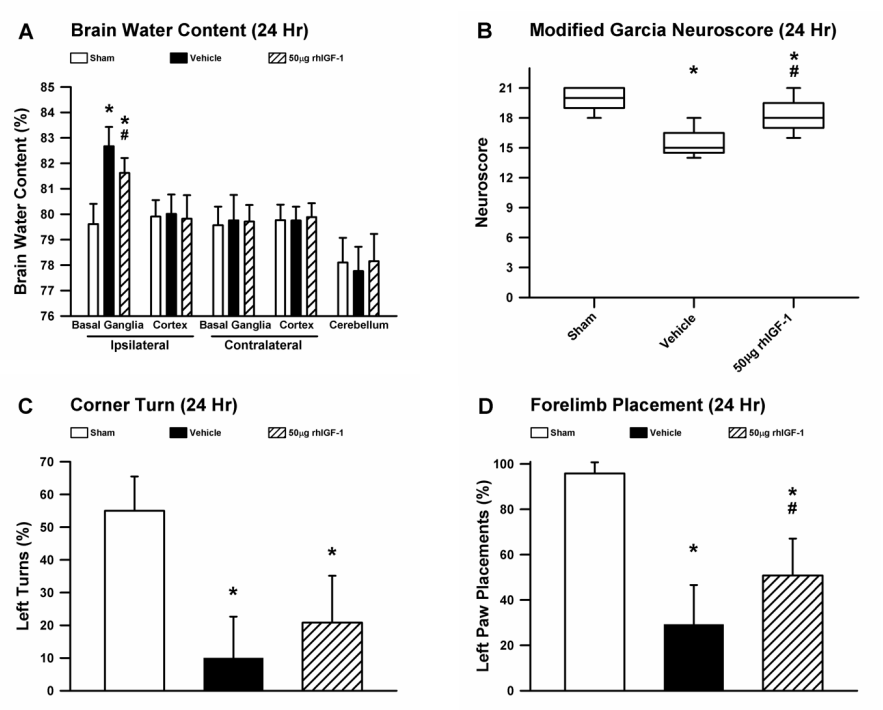

Figure 4. Blood injection ICH model at 24 hours. (A) Brain water content at 24 hours (N=6 per group). (B) Modified Garcia neuroscore (N=6 per group). (C) Corner turn test (N=6 per group). (D) Forelimb placement test (N=6 per group). A, C, D: Values are expressed as mean±SD. B: Values expressed as median±IQR. *P<0.05 compared with sham, #P<0.05 compared with vehicle.

rhIGF-1 Decreases Blood-Brain Barrier Permeability but Does Not Change Hematoma Volume at 24 hours after ICH

Based on the results from the previous experiments measuring brain edema and neuroscores, the high dose of rhIGF-1 (50 μg) was used for the following studies. No animals were excluded from this experiment and no mortalities were found in any groups. Figure 5A displays representative images of the hematoma formed in the collagenase induced ICH model at 24 and 72 hours following the surgery and the autologous-blood induced ICH model at 24 hours after the surgery. Animals from sham, vehicle, and rhIGF-1 treatment groups were tested for blood-brain barrier functionality at 24 hours following the collagenase induced ICH surgery using Evans Blue Extravasation assays (N=6/group). The ICH with vehicle group and rhIGF-1 group exhibited a statistically significant increase in Evans Blue content compared with sham animals in the ipsilateral hemispheric tissue ($p<0.05$; Figure 5B). However, rhIGF-1 significantly reduced the amount of Evans Blue present in the brain as compared to the vehicle group, thus suggesting a preserved BBB integrity ($p<0.05$).

Hemoglobin assays were used to determine if changes to edema and BBB integrity outcomes were a result of a change in hematoma size (N=6/group). ICH with vehicle animals showed a significantly greater amount of hemoglobin content as compared to the sham animals ($p<0.05$, Figure 5C). rhIGF-1 also showed significantly higher hemoglobin content than sham animals ($p<0.05$), but failed to demonstrate a significant change as compared to vehicle ($p>0.05$).

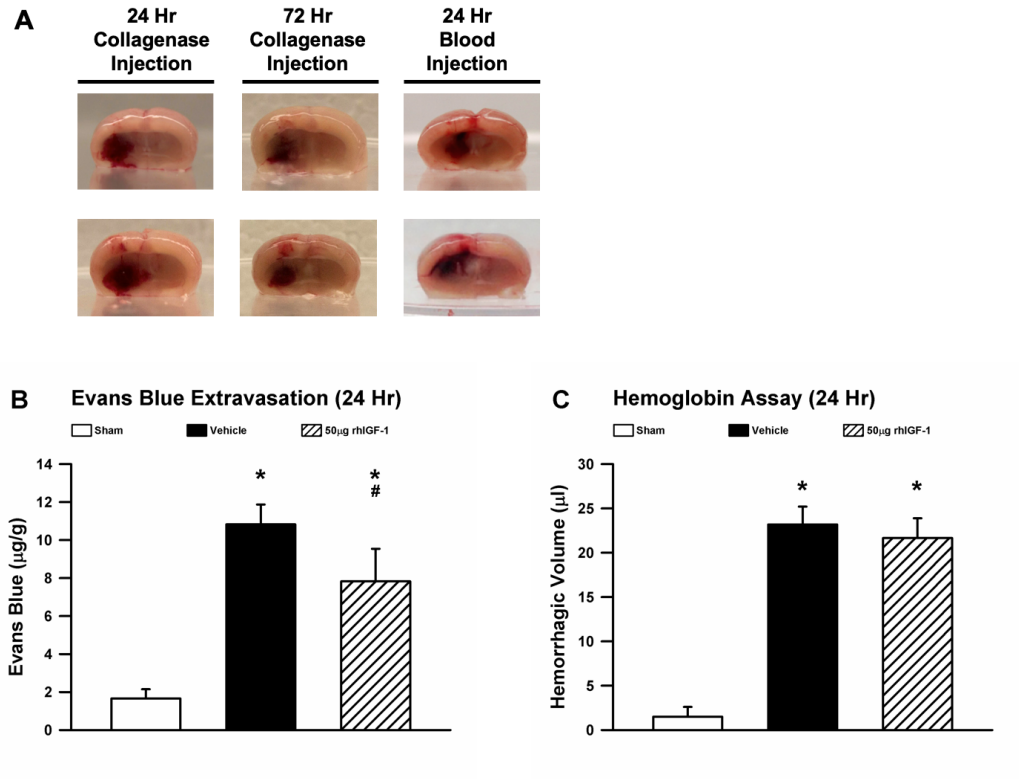

Figure 5. (A) Representative images of hemorrhage location and size at 24 and 72 hours for both collagenase injections and blood injections. (B) Evans blue extravasation at 24 hours after collagenase injection (N=6 per group). (C) Hemoglobin assay at 24 hours after collagenase injection (N=6 per group). Evans blue and Hemoglobin assay completed on ipsilateral hemisphere. Values are expressed as mean±SD. *P<0.05 compared with sham, #P<0.05 compared with vehicle.

Endogenous IGF-1 but not IGF-1R expression is decreased following ICH

Western Blot analyses of endogenous levels of IGF-1 and IGF-1R were examined in the ipsilateral brain tissue at 3, 6, 12, 24, and 72 hours after the collagenase induced ICH surgery and compared to sham-operated tissue collected 24 hours after the surgery (N=6/group). No animals were excluded from this experiment and no mortalities were found in any groups. Changes in the expression of IGF-1 were found to exhibit an increase from 12 hours to 72 hours after the injury compared to sham results ($p<0.05$; Figure 6A). IGF-1R protein expression did not exhibit any significant changes at any time point compared to sham ($p>0.05$; Figure 6B).

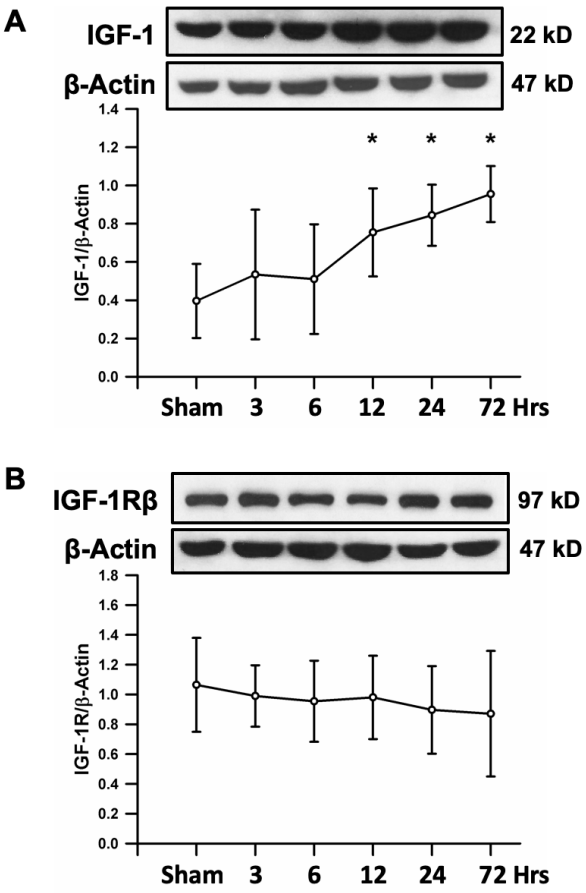

Figure 6. Western blot analysis of (A) IGF-1 and (B) IGF-1Rβ. N=6 per time point. Values are expressed as mean±SD, normalized to sham. *P<0.05 vs sham.

rhIGF-1 reduces p-GSK3β and p-MEKK1 expression and increases Occludin and Claudin 5 expression

Western Blot analyses of the ipsilateral brain hemisphere were conducted at 24 hours following the collagenase induced ICH surgery (N=6/group). In this experiment, 1 mouse under the "ICH + rhIGF-1 + scramble siRNA" group and 1 from the "ICH + rhIGF-1 + AG1024" group were omitted due to mortality during the surgery procedure. Sham and vehicle samples were shared from the previous experiment. Changes in the protein expression of p-GSK3β, MEKK1, Occludin, and Claudin 5 were quantified between groups (Figure 7A-D). p-GSK3β was decreased in the rhIGF-1 and rhIGF-1+scramble siRNA groups compared to the vehicle group ($p<0.05$; Figure 7A). AG1024 and IGF-1R siRNA increased expression of p-GSK3β compared to the sham group ($p<0.05$). MEKK1 expression was decreased in the rhIGF-1, AG1024, and scramble siRNA groups compared to the vehicle group ($p<0.05$; Figure 7B). IGF-1R siRNA elevated MEKK1 expression so it was no longer significant compared to the vehicle group ($p>0.05$). Occludin and Claudin 5 expression was decreased in the vehicle, AG1024, and IGF-1R siRNA groups compared to the sham group ($p<0.05$, Figure 7C+D), whereas expression was elevated in the rhIGF-1 and rhIGF-1+scramble siRNA groups so that it was no longer significant to sham ($p>0.05$).

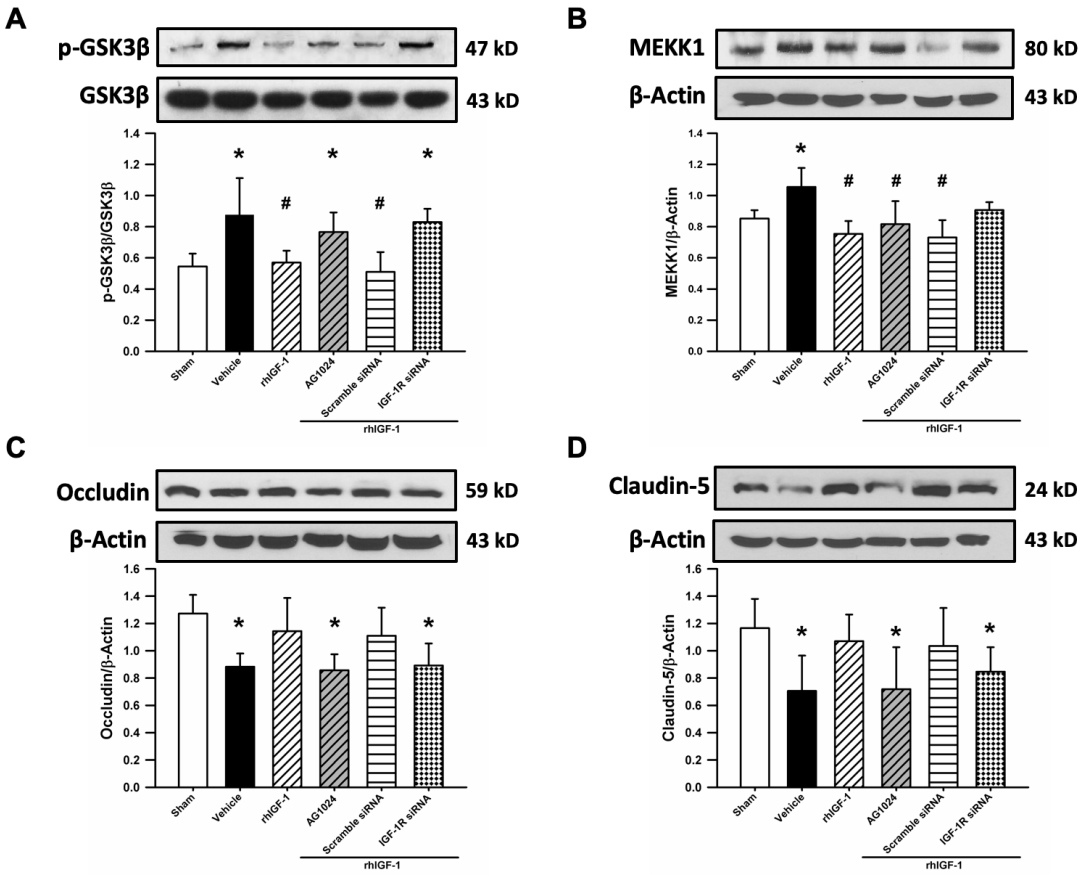

Figure 7. Western blot analysis of (A) p-GSK3β, (B) MEKK1, (C) Occludin, and (D) Claudin 5. Values are expressed as mean±SD, normalized to sham. *P<0.05 compared with sham, #P<0.05 compared with vehicle. N=6 per group.

Discussion

The first aim of this study was to investigate if IGF-1R agonist rhIGF-1 could ameliorate brain edema and behavioral deficits after experimental ICH in mice. It is well known that basal ganglia hemorrhages lead to debilitating neurofunctional deficits in humans [25]. The high dose of rhIGF-1 (50 μg) significantly improved edema and neurobehavior outcomes in the Garcia, corner turn, and forelimb placement test at 24 hours after surgery (compared to vehicle) in the collagenase injection model while showing improvements in edema and Garcia and forelimb placement tests in the blood injection model. Interestingly, both doses of rhIGF-1 were unable to improve edema or neurobehavior at 72 hours in the collagenase injection model. However, giving a daily dose of 50 μg of rhIGF-1 did show improvements 72 hours after ICH. The half-life of rhIGF-1 has been previously reported to be 10-12 hours and may suggest that the continued injury of ICH can overpower a single dose beyond the initial 24 hours [26]. This may help to explain our observations and this data suggests that a continued treatment regimen may be needed for long-term studies on the use of rhIGF-1 on neuroprotection.

Our second objective was to determine if rhIGF-1 stimulation would decrease MEKK1/GSK3β activation thus decreasing BBB injury. Few experimental studies have evaluated the effects of IGF-1 treatment after ischemic stroke, but little information is given to its effect after a hemorrhagic stroke [18, 19, 27-29]. Additionally, the role of IGF-1 in BBB preservation is not well documented, but few studies suggest a protective effect [6, 30, 31]. The

improvement to edema by rhIGF-1 provides the initial evidence in this study to suggest that rhIGF-1 is able to stimulate the protection of the BBB. To further add support, we found that rhIGF-1 was also able to decrease permeability of the BBB through Evans blue extravasation (Figure 5). Indeed, a previous study of ours showed that rhIGF-1 decreased BBB permeability in a germinal matrix hemorrhage model [32]. rhIGF-1 treatments did not, however, have any effect on the hematoma volume. This suggests that the injury model is stable, and the amount of bleeding is not affected by the treatment. Since the bleeding remains consistent between the groups, this indicates that the decrease in edema and Evans blue amount is a result of BBB permeability changes and not a result due to the amount of blood or severity of the injury.

The IGF-1R is located ubiquitously in several cell types including BBB forming endothelial cells [33, 34]. Stimulation of the IGF-1R has been shown to activate PI3K-Akt signaling [35]. Additionally, Akt has been reported to reduce MEKK1 and GSK3β activation [36, 37]. GSK3β activation (phosphorylation at Tyr216) has been correlated to loss of tight junction expression including occludin and claudin-5 [5, 38]. In connection with this theory, we found that there was greater p-GSK3β and MEKK1 expression and decreased occludin and claudin-5 expression in the brains of ICH animals, but that rhIGF-1 administration reversed these levels.

In order to ensure stimulation of the IGF-1R produced beneficial effects through this pathway, we administered AG1024 (a pharmaceutical competitive inhibitor of the receptor) and IGF-1R siRNA (to decrease the availability of the

receptor) to try preventing the effects of the rhIGF-1 treatments [39, 40]. Both interventions reversed the beneficial effects on edema and neurobehavior by rhIGF-1 at 24 hours in the collagenase injection model. Additionally, both also inhibited the effects of rhIGF-1 on protein expression levels of p-GSK3β, occludin, and claudin 5. However, AG1024 was unable to reverse the effect on MEKK1. Several reasons may explain why AG1024 was unable to change the levels of MEKK1 significantly. First, it could be that MEKK1 is not a major signaling molecule in the pathway we initially hypothesized. MEKK1 is a protein that is part of a signaling pathway activated by p-GSK3β and is involved in the activation of JNK and NFκB pathways [41, 42]. However, GSK3β has been demonstrated to signal several other downstream pathways that may have led to the change in occludin and claudin proteins [38, 43-46]. However, because IGF-1R siRNA was able to change the levels of MEKK1, this suggests there is a relationship with IGF-1R stimulation and MEKK1. Another possibility is that the toxic environment from the hemorrhage produced may prevent AG1024 from fully being able to produce its effect. IGF-1R siRNA was given 24 hours before the induction of the hemorrhage to decrease the available receptors that signaling can occur through, while AG1024 was given after the hemorrhage has been induced. Further studies are needed to determine the pathway that rhIGF-1 may confer its protective effects.

Interestingly, though we demonstrated that the high dose of rhIGF-1 improves edema and neurofunctional outcomes at 24 hours in the collagenase injection model, the protein expression of MEKK1 and occludin were only mildly

improved. Additionally, there was only a mild improvement of edema and behavior in the blood injection model. Several factors can contribute to these results. First, rhIGF-1 may also effect cytotoxic edema [47]. We utilized both brain water content and Evans blue extravasation to evaluate BBB integrity. While brain water content can account for both cytotoxic and vasogenic brain edema, the Evans blue assay only observes BBB permeability through means of vasogenic brain edema [48, 49]. It is generally accepted that both forms of brain edema are present 24 hours after ICH [50]. Second, the pathophysiological mechanisms of edema formation may be different between the collagenase and blood injection models. The collagenases infused are proteolytic enzymes that may have a greater effect on the BBB than the autologous blood [51]. In addition, the edema formed from the blood injection model may also be more associated from the clot retraction causing serum extrusion [52, 53]. As the mechanism of IGF-1 protection in this study is more appropriate to treating vasogenic edema, this may account for the milder improvements observed in the blood injection model. Third, treatments with rhIGF-1 may also improve outcomes through mechanisms of anti-inflammation and anti-apoptosis, which were not evaluated in this study [19, 54-56]. Finally, this may be a result of a difference in the sample sizes. Though the N values were consistent between the brain water content experiments, the changes in the sample size varied in the neurobehavioral outcomes as more experiments were done using the collagenase model.

Previous ischemic studies have shown that IGF-1 treatments can reduce the injury development promoting its use as a potential clinical treatment [19, 21]. However, some debate exists if IGF-1 will cross the blood-brain barrier effectively to exert its role on the cerebral tissues. Previous studies have therefore utilized the intranasal administration route to effectively deliver the drug to the brain [18]. Utilizing this method, it was shown to effectively cross-the blood-brain barrier and protect against neuronal apoptosis. Though our study aims to study the blood-brain barrier and we would have no need to directly bypass it, we also applied the intranasal administration method to provide the maximum effectiveness to the cerebral tissues. We decided to use 50 μg of rhIGF-1 due to previous studies in neuroprotection showing positive effects using this dose [19]. Being wary of the tumorigenic properties that high levels of IGF-1 can stimulate, we decided to observe if a lower dose (10 μg) can also stimulate the neuroprotective qualities as lower doses have shown positive effects in other models of brain injury [18]. Our recording of physiological parameters did not show significant variations to temperature and heart rate with administration of rhIGF-1, AG1024, scramble siRNA, or IGF-1R siRNA (data not shown).

Some limitations exist for this study that suggest a need for further studies. Though we were able to show that 50 μg of rhIGF-1 was able to show a certain level of neuroprotection, it still showed statistical significance in comparison to sham in several of the experiments including brain water content, neurobehavioral assessments, and Evans blue extravasation. Though Evans blue extravasation is a marker for blood-brain barrier permeability, it examines

permeability based on the size of the openings that allow for the dye to infiltrate the brain [57]. Newer techniques such as albumin extravasation and histological analysis using fluorescent markers may provide more insight [58]. Other histological studies are needed to determine if there was a neuroprotection of the other cell populations by rhIGF-1. Furthermore, this study only viewed rhIGF-1 treatments given up to 3 days daily. Though an improvement in edema and neurobehavior can be seen up through that time, it is uncertain if continued treatments beyond this period of time will continue to show benefits to edema or for other potential protective effects from conditions of apoptosis or inflammation.

In summary, IGF-1R agonist rhIGF-1 reversed ICH-produced edema and neurobehavior deficits in both collagenase and blood injection models of ICH. In addition, these outcomes were paralleled by improved BBB integrity and molecular elevation of occludin and claudin-5 expression. However, IGF-1R antagonism by AG1024 and IGF-1R siRNA reversed the treatment effects on edema, behavior, and molecular expression. Based on these findings, we conclude that IGF-1R induced activation of the PI3K-Akt pathway resulted in the inhibition of p-GSK3β and MEKK1, thereby increasing occludin and claudin-5 expression and preserving the BBB.

References

1. Selim, M. and K.N. Sheth, *Perihematoma edema: a potential translational target in intracerebral hemorrhage?* Transl Stroke Res, 2015. 6(2): p. 104-6.

2. Xi, G., et al., *Brain edema after intracerebral hemorrhage: the effects of systemic complement depletion.* Acta Neurochir Suppl, 2002. 81: p. 253-6.

3. Liu, W.Y., et al., *Tight junction in blood-brain barrier: an overview of structure, regulation, and regulator substances.* CNS Neurosci Ther, 2012. 18(8): p. 609-15.

4. Gebel, J.M., Jr., et al., *Relative edema volume is a predictor of outcome in patients with hyperacute spontaneous intracerebral hemorrhage.* Stroke, 2002. 33(11): p. 2636-41.

5. Krafft, P.R., et al., *PHA-543613 preserves blood-brain barrier integrity after intracerebral hemorrhage in mice.* Stroke, 2013. 44(6): p. 1743-7.

6. Bake, S., et al., *Insulin-Like Growth Factor (IGF)-I Modulates Endothelial Blood-Brain Barrier Function in Ischemic Middle-Aged Female Rats.* Endocrinology, 2016. 157(1): p. 61-9.

7. Liu, X., et al., *Astrocytes express insulin-like growth factor-I (IGF-I) and its binding protein, IGFBP-2, during demyelination induced by experimental autoimmune encephalomyelitis.* Mol Cell Neurosci, 1994. 5(5): p. 418-30.

8. Shemer, J., et al., *Insulin-like growth factor I receptors in neuronal and glial cells. Characterization and biological effects in primary culture.* J Biol Chem, 1987. 262(16): p. 7693-9.

9. Hetman, M., et al., *Role of glycogen synthase kinase-3beta in neuronal apoptosis induced by trophic withdrawal.* J Neurosci, 2000. 20(7): p. 2567-74.

10. Allen, R.T., et al., *Sustained Akt/PKB activation and transient attenuation of c-jun N-terminal kinase in the inhibition of apoptosis by IGF-1 in vascular smooth muscle cells.* Apoptosis, 2005. 10(3): p. 525-35.

11. Kim, J.W., et al., *Glycogen synthase kinase 3 beta is a natural activator of mitogen-activated protein kinase/extracellular signal-regulated kinase kinase kinase 1 (MEKK1).* J Biol Chem, 2003. 278(16): p. 13995-4001.

12. Feiler, S., et al., *Contribution of matrix metalloproteinase-9 to cerebral edema and functional outcome following experimental subarachnoid hemorrhage.* Cerebrovasc Dis, 2011. 32(3): p. 289-95.

13. Nitta, T., et al., *Size-selective loosening of the blood-brain barrier in claudin-5-deficient mice.* J Cell Biol, 2003. 161(3): p. 653-60.

14. Rolland, W.B., et al., *Fingolimod reduces cerebral lymphocyte infiltration in experimental models of rodent intracerebral hemorrhage.* Exp Neurol, 2013. 241: p. 45-55.

15. Ma, Q., et al., *Vascular adhesion protein-1 inhibition provides antiinflammatory protection after an intracerebral hemorrhagic stroke in mice.* J Cereb Blood Flow Metab, 2011. 31(3): p. 881-93.

16. Yu, L., et al., *Adropin preserves the blood-brain barrier through a Notch1/Hes1 pathway after intracerebral hemorrhage in mice.* J Neurochem, 2017. 143(6): p. 750-760.

17. Zhao, L., et al., *Recombinant CTRP9 administration attenuates neuroinflammation via activating adiponectin receptor 1 after intracerebral hemorrhage in mice.* J Neuroinflammation, 2018. 15.

18. Fletcher, L., et al., *Intranasal delivery of erythropoietin plus insulin-like growth factor-I for acute neuroprotection in stroke. Laboratory investigation.* J Neurosurg, 2009. 111(1): p. 164-70.

19. Cai, Z., et al., *Intranasal administration of insulin-like growth factor-1 protects against lipopolysaccharide-induced injury in the developing rat brain.* Neuroscience, 2011. 194: p. 195-207.

20. Chang, H.C., et al., *Effects of insulin-like growth factor 1 on muscle atrophy and motor function in rats with brain ischemia.* Chin J Physiol, 2010. 53(5): p. 337-48.

21. Chang, H.C., et al., *Insulin-like growth factor I signaling for brain recovery and exercise ability in brain ischemic rats.* Med Sci Sports Exerc, 2011. 43(12): p. 2274-80.

22. Hua, Y., et al., *Behavioral tests after intracerebral hemorrhage in the rat.* Stroke, 2002. 33(10): p. 2478-84.

23. Garcia, J.H., et al., *Neurological deficit and extent of neuronal necrosis attributable to middle cerebral artery occlusion in rats. Statistical validation.* Stroke, 1995. 26(4): p. 627-34; discussion 635.

24. Manaenko, A., et al., *Comparison Evans Blue injection routes: Intravenous versus intraperitoneal, for measurement of blood-brain barrier in a mice hemorrhage model.* J Neurosci Methods, 2011. 195(2): p. 206-10.

25. Nys, G.M., et al., *Cognitive disorders in acute stroke: prevalence and clinical determinants.* Cerebrovasc Dis, 2007. 23(5-6): p. 408-16.

26. Fouque, D., S.C. Peng, and J.D. Kopple, *Pharmacokinetics of recombinant human insulin-like growth factor-1 in dialysis patients.* Kidney Int, 1995. 47(3): p. 869-75.

27. Endres, M., et al., *Serum insulin-like growth factor I and ischemic brain injury.* Brain Res, 2007. 1185: p. 328-35.

28. Lin, S., et al., *Intranasal administration of IGF-1 attenuates hypoxic-ischemic brain injury in neonatal rats.* Exp Neurol, 2009. 217(2): p. 361-70.

29. Liu, X.F., et al., *Intranasal administration of insulin-like growth factor-I bypasses the blood-brain barrier and protects against focal cerebral ischemic damage.* J Neurol Sci, 2001. 187(1-2): p. 91-7.

30. Sharma, H.S. and C.E. Johanson, *Intracerebroventricularly administered neurotrophins attenuate blood cerebrospinal fluid barrier breakdown and brain pathology following whole-body hyperthermia: an experimental study in the rat using biochemical and morphological approaches.* Ann N Y Acad Sci, 2007. 1122: p. 112-29.

31. Li, W., et al., *Chronic relapsing experimental autoimmune encephalomyelitis: effects of insulin-like growth factor-I treatment on clinical deficits, lesion severity, glial responses, and blood brain barrier defects.* J Neuropathol Exp Neurol, 1998. 57(5): p. 426-38.

32. Lekic, T., et al., *Intranasal IGF-1 Reduced Rat Pup Germinal Matrix Hemorrhage.* Acta Neurochir Suppl, 2016. 121: p. 209-12.

33. Chisalita, S.I. and H.J. Arnqvist, *Insulin-like growth factor I receptors are more abundant than insulin receptors in human micro- and macrovascular endothelial cells.* Am J Physiol Endocrinol Metab, 2004. 286(6): p. E896-901.

34. Torres-Aleman, I., F. Naftolin, and R.J. Robbins, *Trophic effects of insulin-like growth factor-I on fetal rat hypothalamic cells in culture.* Neuroscience, 1990. 35(3): p. 601-8.

35. Bondy, C.A. and C.M. Cheng, *Signaling by insulin-like growth factor 1 in brain.* Eur J Pharmacol, 2004. 490(1-3): p. 25-31.

36. Krafft, P.R., et al., *alpha7 nicotinic acetylcholine receptor agonism confers neuroprotection through GSK-3beta inhibition in a mouse model of intracerebral hemorrhage.* Stroke, 2012. 43(3): p. 844-50.

37. Han, Y.H., et al., *Regulation of Nur77 nuclear export by c-Jun N-terminal kinase and Akt.* Oncogene, 2006. 25(21): p. 2974-86.

38. Ramirez, S.H., et al., *Inhibition of glycogen synthase kinase 3beta promotes tight junction stability in brain endothelial cells by half-life extension of occludin and claudin-5.* PLoS One, 2013. 8(2): p. e55972.

39. Parrizas, M., et al., *Specific inhibition of insulin-like growth factor-1 and insulin receptor tyrosine kinase activity and biological function by tyrphostins.* Endocrinology, 1997. 138(4): p. 1427-33.

40. Luey, B.C. and F.E. May, *Insulin-like growth factors are essential to prevent anoikis in oestrogen-responsive breast cancer cells: importance of the type I IGF receptor and PI3-kinase/Akt pathway.* Mol Cancer, 2016. 15: p. 8.

41. Lin, C.H., et al., *MEKK1, JNK, and SMAD3 mediate CXCL12-stimulated connective tissue growth factor expression in human lung fibroblasts.* J Biomed Sci, 2018. 25(1): p. 19.

42. Morita, K., et al., *BAALC potentiates oncogenic ERK pathway through interactions with MEKK1 and KLF4.* Leukemia, 2015. 29(11): p. 2248-56.

43. Xiao, H., et al., *Role of glycogen synthase kinase 3 in ischemia-induced blood-brain barrier disruption in aged female rats.* J Neurochem, 2017. 142(2): p. 194-203.

44. Zhang, X., et al., *Nobiletin inhibits invasion via inhibiting AKT/GSK3beta/beta-catenin signaling pathway in Slug-expressing glioma cells.* Oncol Rep, 2017. 37(5): p. 2847-2856.

45. Severson, E.A., et al., *Glycogen Synthase Kinase 3 (GSK-3) influences epithelial barrier function by regulating occludin, claudin-1 and E-cadherin expression.* Biochem Biophys Res Commun, 2010. 397(3): p. 592-7.

46. Hwang, S.M., et al., *Inhibition of Wnt3a/FOXM1/beta-Catenin Axis and Activation of GSK3beta and Caspases are Critically Involved in Apoptotic Effect of Moracin D in Breast Cancers.* Int J Mol Sci, 2018. 19(9).

47. Johnston, B.M., et al., *Insulin-like growth factor-1 is a potent neuronal rescue agent after hypoxic-ischemic injury in fetal lambs.* J Clin Invest, 1996. 97(2): p. 300-8.

48. Carrozzino, F., et al., *Inhibition of basal p38 or JNK activity enhances epithelial barrier function through differential modulation of claudin expression.* Am J Physiol Cell Physiol, 2009. 297(3): p. C775-87.

49. Radu, M. and J. Chernoff, *An in vivo assay to test blood vessel permeability.* J Vis Exp, 2013(73): p. e50062.

50. Yang, G.Y., et al., *Experimental intracerebral hemorrhage: relationship between brain edema, blood flow, and blood-brain barrier permeability in rats.* J Neurosurg, 1994. 81(1): p. 93-102.

51. MacLellan, C.L., et al., *Intracerebral hemorrhage models in rat: comparing collagenase to blood infusion.* J Cereb Blood Flow Metab, 2008. 28(3): p. 516-25.

52. Mracsko, E. and R. Veltkamp, *Neuroinflammation after intracerebral hemorrhage.* Front Cell Neurosci, 2014. 8.

53. Siaw-Debrah, F., et al., *Preclinical Studies and Translational Applications of Intracerebral Hemorrhage.* Biomed Res Int, 2017. 2017.

54. Spies, M., et al., *Liposomal IGF-1 gene transfer modulates pro- and anti-inflammatory cytokine mRNA expression in the burn wound.* Gene Ther, 2001. 8(18): p. 1409-15.

55. Wang, C.Y., et al., *Insulin-like growth factor-1 improves diabetic cardiomyopathy through antioxidative and anti-inflammatory processes along with modulation of Akt/GSK-3beta signaling in rats.* Korean J Physiol Pharmacol, 2016. 20(6): p. 613-619.

56. Hou, X., et al., *IGF-1 protects against Abeta25-35-induced neuronal cell death via inhibition of PUMA expression and Bax activation.* Neurosci Lett, 2017. 637: p. 188-194.

57. Saunders, N.R., et al., *Markers for blood-brain barrier integrity: how appropriate is Evans blue in the twenty-first century and what are the alternatives?* Front Neurosci, 2015. 9: p. 385.

58. Kassner, A. and Z. Merali, *Assessment of Blood-Brain Barrier Disruption in Stroke.* Stroke, 2015. 46(11): p. 3310-5.

CHAPTER THREE

ADROPIN PRESERVES THE BBB THROUGH A NOTCH1/HES1 PATHWAY AFTER INTRACEREBRAL HEMORRHAGE IN MICE

Lingyan Yu, Zhangyang Lu, Sherrefa Burchell, Derek Nowrangi, Anatol. Manaenko, Xue Li, Yang Xu, Ningbo Xu, Jiping Tang, Haibin Dai, John H. Zhang

Department of Pharmacy, Second Affiliated Hospital, Zhejiang University School of Medicine, Hangzhou, Zhejiang, China

Departments of Neurosurgery & Brain and Nerve Research Laboratory, The First Affiliated Hospital, Soochow University, Suzhou, China

Departments of Anesthesiology and Basic Sciences, School of Medicine, Loma Linda University, Loma Linda, CA, USA

Corresponding Author: John H. Zhang, M.D./PhD

Department of Physiology & Pharmacology

Loma Linda University School of Medicine Risley Hall, Room 223

Loma Linda, CA 92354, USA

Phone: 909-558-4723

Fax: 909-558-0119

Email: johnzhang3910@yahoo.com

The work presented in this chapter has been published

J Neurochem 2017 Dec;143(6):750-760

Abstract

Adropin is expressed in the central nervous system (CNS) and plays a crucial role in the development of stroke. However, little is currently known about the effects of Adropin on the blood-brain barrier (BBB) function after intracerebral hemorrhage (ICH). In this study, the role of Adropin in collagenase-induced ICH was investigated in mice. At 1-h post ICH, mice were administered with recombinant human Adropin by intranasal. Brain water content, BBB permeability, and neurological function were measured at different time intervals. Proteins were quantified using Western blot analysis, and the localizations of Adropin and Notch1 were visualized via immunofluorescence staining. It is shown that Adropin reduced brain water content and improved neurological functions. Adropin preserved the functionality of BBB by increasing N-cadherin expression and reducing extravasation of albumin. Moreover, in vivo knockdown of Notch1 and Hes1 both abolished the protective effects of Adropin. Taken together, our data demonstrate that Adropin constitutes a potential treatment value for ICH by preserving BBB and improving functional outcomes through the Notch1 signaling pathway.

Introduction

Intracerebral hemorrhage (ICH) constitutes a severe public health issue that leads to high mortality and morbidity [1] and its global incidence is increasing annually. Blood-brain barrier (BBB) disruption is the hallmark of ICH-induced brain injury. From both animal models and human studies, it has been shown that BBB disruption occurs in the acute phase after ICH [2, 3]. The development of vasogenic brain edema from increased BBB permeability has been regarded as an important contributor to high mortality after ICH [4, 5]. Thus, elucidating the mechanisms underlying BBB dysfunction in ICH is critical for developing methods to prevent and treat this major form of stroke [6].

Adropin is encoded by the Energy Homeostasis Associated gene, which is expressed in the liver and brain [7, 8]. In the brain, the immunoreactivity of Adropin showed that it is expressed in the vascular area, pia matter, neuroglial cells, Purkinje cells, granular layer, and neurons [9, 10]. An in vitro study also found that Adropin reduced endothelial monolayer permeability and greater cell proliferation in Adropin-treated human umbilical vein and coronary artery endothelial cells [11]. In addition, pretreatment with Adropin has been demonstrated to attenuate hypoxia/low glucose-induced endothelial barrier damage in a concentration-dependent manner [12]. However, the precise effects of Adropin on BBB after ICH have not yet been evaluated.

In Adropin knockout mice, it is found that Adropin regulates locomotor activity and motor coordination by the NB3/Notch signaling pathway and plays an important role in cerebellum development [13]. Treatment with Adropin achieves

the effect on glucose tolerance and substrate utilization with Notch1 signaling pathways in diet-induced obese mice [14]. Notch1 signaling performs an essential function in CNS development, which was conserved as an evolutionarily pathway [15]. It has been recently reported that the Notch1 signaling pathway regulates neurogenesis, neuronal networks, synaptic plasticity, learning, and memory in adult brains [16]. In a neonatal ICH study, it was shown that smad4 stabilized cerebrovascular EC-pericyte interactions by regulating the transcription of N-cadherin through associating with the Notch intracellular complex at the RBP-J binding site of the N-cadherin promoter [17]. The activation of Notch results in the sequential proteolytic cleavage of the Notch receptor, which releases Notch intracellular domain (NICD) into the nucleus, which in turn activates downstream transcription of several genes, including Hes and Hey [18, 19].

In the present study, our aim was first to test whether Adropin treatment can counteract the effects of ICH-induced BBB disruption, and then determine whether it is dependent on Notch1 signaling activation, thus presenting a potential therapy for ICH.

Materials and Methods

Animals

A total of 170 CD1 mice (male, eight-weeks-old, weight 30±5 g, Charles River, Wilmington, MA) were used. All of the procedures applied to animals complied with the Guide for the Care and Use of Laboratory Animals and were

approved by the Institutional Animal Care and Use Committee at Loma Linda University. All mice were housed in filter-top cages under controlled temperature and humidity with a 12-h light/dark cycle. Free access to food and water were supplied. The mice were arbitrary divided into different experiment groups. Animals died before endpoint were excluded and replaced with new animals. A total of 2 mice died because of anesthesia.

ICH Models

The time-line of the study design was shown in Fig. 8. A collagenase-induced ICH model in mouse was established as previously reported [20]. Briefly, ketamine (100 mg/kg) and xylazine (10 mg/kg, intraperitoneal, ip injection) were used for anesthesia for the mice. Bacterial collagenase (0.075 units, Type VII-S, Sigma-Aldrich, St. Louis, MO, U.S.A.) was dissolved in 0.5 μL saline, and infused into the right basal ganglia at a rate of 0.1667 μL/min, using an infusion pump (Stoelting, Wood Dale, IL, USA). The needle was left for an additional 10 min to prevent possible leakage of the collagenase solution, and withdrawn slowly at a rate of 1 mm/min. The cranial burr hole was sealed with bone wax, the skin was sutured, and 0.4 mL of normal saline was injected subcutaneously. Animals were allowed to recover fully under observation. The sham operation was performed with needle insertion only.

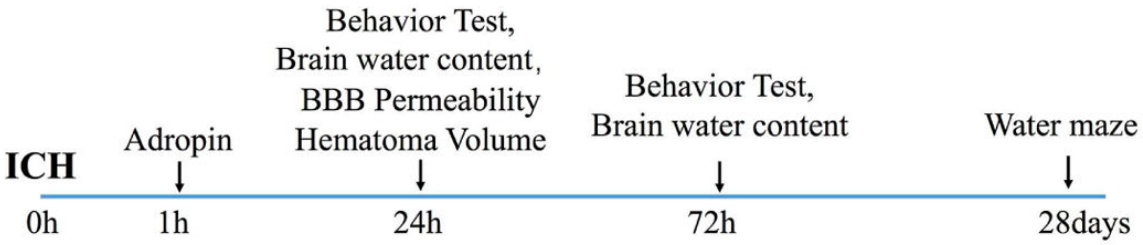

Figure 8. Time-line of study design. ICH: Intracerebral Hemorrhage. BBB: blood-brain barrier.

Drugs and RNA Administration

Adropin was dissolved in saline and tested at three different doses (0.5 μg, 1.5 μg, and 5.0 μg per mouse), which were administered by intranasal 1 h after ICH. Both Notch1 and Hes1 small interfering RNA (siRNA), as well as scrambled RNA (scRNA), were dissolved in sterile RNAse free resuspension buffer according to the manufacturer's instructions (OriGene, Rockville, MD, U.S.A.). They were administered via intracerebroventricular injection (i.c.v.) 48 h prior to ICH-induction [21]. SiRNA or scRNA (100 pmol) was delivered into the ipsilateral ventricle (1.0 mm lateral of the bregma, 2.3 mm deep) at a rate of 0.67 μL/min. After waiting for 8 min, the needle was removed over a 3 min period. The burr hole was sealed with bone wax.

Brain Water Content

Brain water content was measured at 24 h and 72 h after ICH, according to previous literature [22]. Mice were decapitated under deep anesthesia, and the brains were removed immediately. Then, the brains were divided into five parts (ipsilateral and contralateral cortex, ipsilateral and contralateral basal ganglia, and cerebellum). All brain samples were weighed on an analytical microbalance (APX-60 Denver Instrument, Bohemia, NY, U.S.A.) to obtain the wet weight (WW). Samples were dried at 100 °C for 48 h to obtain the dry weight (DW). Brain water content was calculated using the following formula: (WW-DW)/WW × 100%.

Neurobehavioral Function Assessment

Neurobehavioral functions were assessed by an independent investigator who was blinded to the treatment groups. Modified Garcia, Forelimb placement, and Corner turn tests were used to evaluate neuro-deficits at 24 and 72 h after ICH. For long-term evaluation of spatial learning, a Morris Water Maze test was employed.

Evaluation of BBB Permeability and Hematoma Volume

BBB permeability evaluation involves the staining of serum albumin, known as the Evans Blue assay. Evans Blue dye extravasation assay was conducted by I.P. injection of a 4% solution of Evans Blue dye in PBS 24 h after ICH [23, 24]. The dye was allowed to circulate for 3 h, and then the mice were transcardially perfused with cold PBS. The brains were then removed and divided into left and right hemispheres. The samples were homogenized in 1,100 μL of PBS, sonicated and centrifuged separately. Trichloroacetic acid (500 μL) was added to 500 μL of the supernatant layer and incubated overnight at 4 °C. Evans Blue dye absorbance was determined by spectrophotometry (Thermo Fischer Scientific Inc., Waltham, MA, U.S.A.) with wavelengths at 610 nm. Results are presented as μg of Evans Blue dye per g of brain tissue.

The hemoglobin assay was performed as previously described [24]. The supernatant was collected as above, and Drabkin's reagent (800 μL, Sigma) was added to 200 μL of the supernatant and allowed to stand for 15 min at room temperature. Absorbance of hemoglobin was measured at 540 nm.

Western blot

Brain samples were collected at 24 h after ICH. Mice were perfused transcardially with 40 mL PBS, and proteins of the ipsilateral hemispheres were extracted by homogenizing in RIPA buffer (Santa Cruz Biotechnology). Western blotting was performed as previously described [25] using primary antibodies, such as Adropin (ProSci Inc., RRID: AB_2316252), Notch1 (Santa Cruz Biotechnology, RRID: AB_650336), NICD (Abcam, RRID:AB_306863), Hes1 (Santa Cruz Biotechnology, RRID: AB_647992), p-Akt, Akt (Cell Signaling Technology, RRID AB_329825, RRID: AB_329827), ZO-1(Santa Cruz Biotechnology, RRID: AB_628459), Claudin-5(Santa Cruz Biotechnology, RRID: AB_2260866), N-cadherin (Santa Cruz Biotechnology, RRID: AB_647794), and Albumin (Cell Signaling Technology, RRID: AB_2225785).

Immunofluorescence Staining

Immunofluorescence was performed using a previously described method [4]. Coronal slices (10 μm) were sectioned using a cryostat (CM3050S; Leica Microsystems) and permeabilized with 0.3% Triton X-100 in PBS for 10∼30 min. Sections were blocked with 5% donkey serum for 2 h, and incubated overnight at 4 °C with primary antibodies: Adropin (ProSci Inc.), Notch1 (Santa Cruz Biotechnology, RRID: AB_650336), CD13 (Abcam, AB_726095), GFAP (Abcam, RRID: AB_880202), and vWF (Abcam, RRID: AB_298501). Afterwards, sections were washed with PBS and incubated with appropriate secondary antibodies for

2 h at room temperature. Photographs were then taken using LASX software with a Leica DMi8 fluorescence microscope (Leica Microsystems, Germany).

Statistics

In this exploratory study, all tests were done two-sided. Normal distribution and similar variation between experimental groups were inspected for appropriateness before statistical tests. Parametric data was analyzed using one-way ANOVA with Tukey's post-hoc test and is expressed as mean (standard deviation, SD). Non-parametric data was analyzed with Kruskall-Wallis with Dunn's post-hoc tests and are presented as the median and the interquartile range (25th percentile, 75th percentile). This longitudinal data was also analyzed using repeated measures two-way ANOVA with Tukey post-hoc test. P values of less than 0.05 were considered statistically significant. On the basis of the results of the pilot preliminary study for brain water content, neurobehavioral function, Evans Blue Dye extravasation and hemoglobin assay, 6 animals were required to achieve 80% power to detect a difference, with a probability of $p < 0.05$. GraphPad Prism 6 and SPSS18.0 were used for graphing and analyze all data.

Results

ICH Transiently Changed the Level of Adropin and Notch1 expression

The protein expression of Adropin was transiently decreased at 3 h, 6 h and 12 h, and increased at 24 h, after ICH. However, the protein expression of Notch1, NICD, and Hes1 all increased at 24 h after ICH (Fig. 9). Double immunostaining of Adropin and Notch1 with CD13 (pericytes), vWF (endothelial cells), and GFAP (astrocytes) showed that Adropin and Notch1 are intensely expressed and co-localized with pericytes, endothelial cells, and astrocytes at 24 h after ICH (Fig. 10A and 10B).

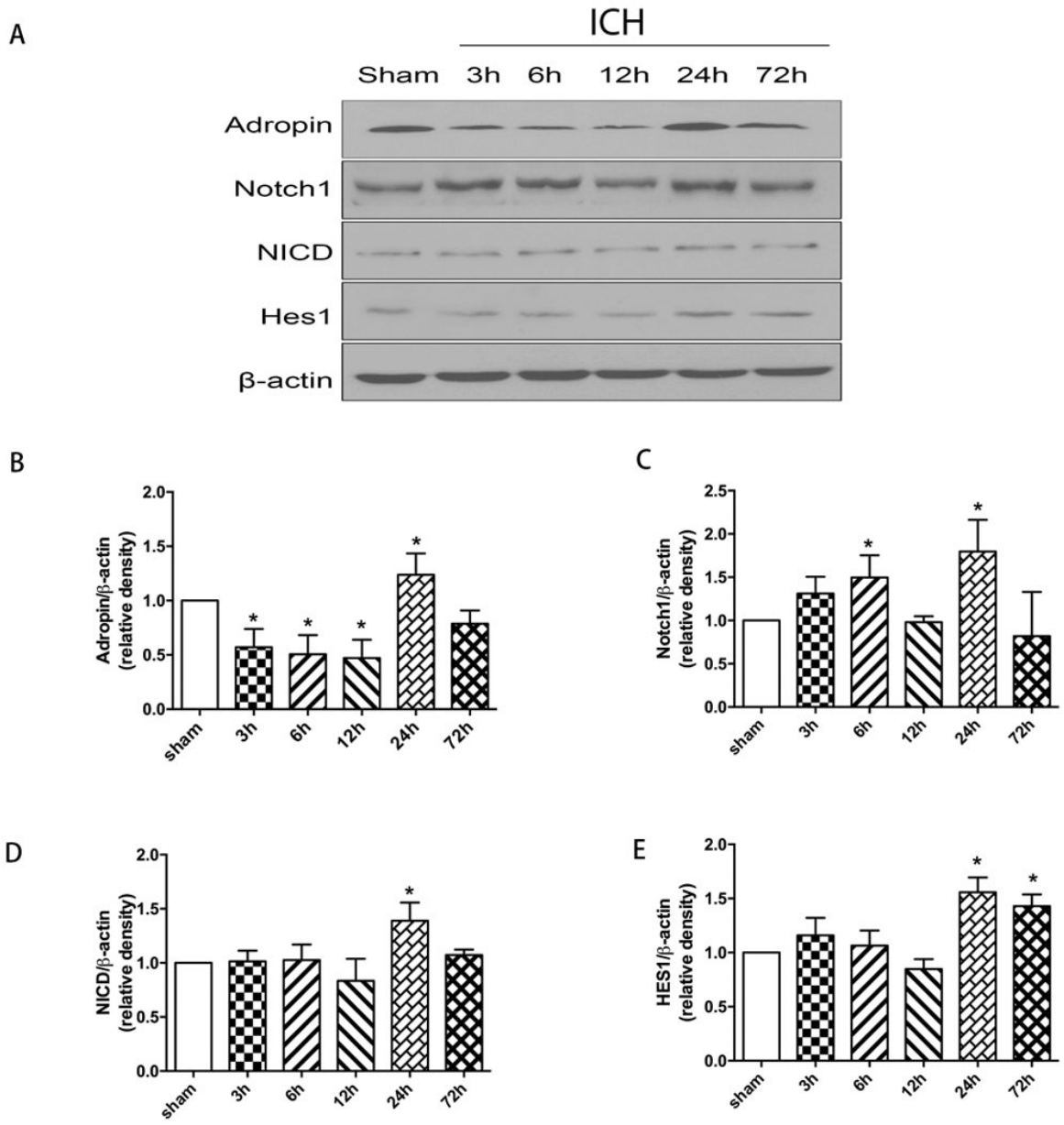

Figure 9. Time course expression of Adropin, Notch1, NICD, and Hes1 (A) by Western blot. N = 4-6 mice/group. *p<0.05 vs. sham.

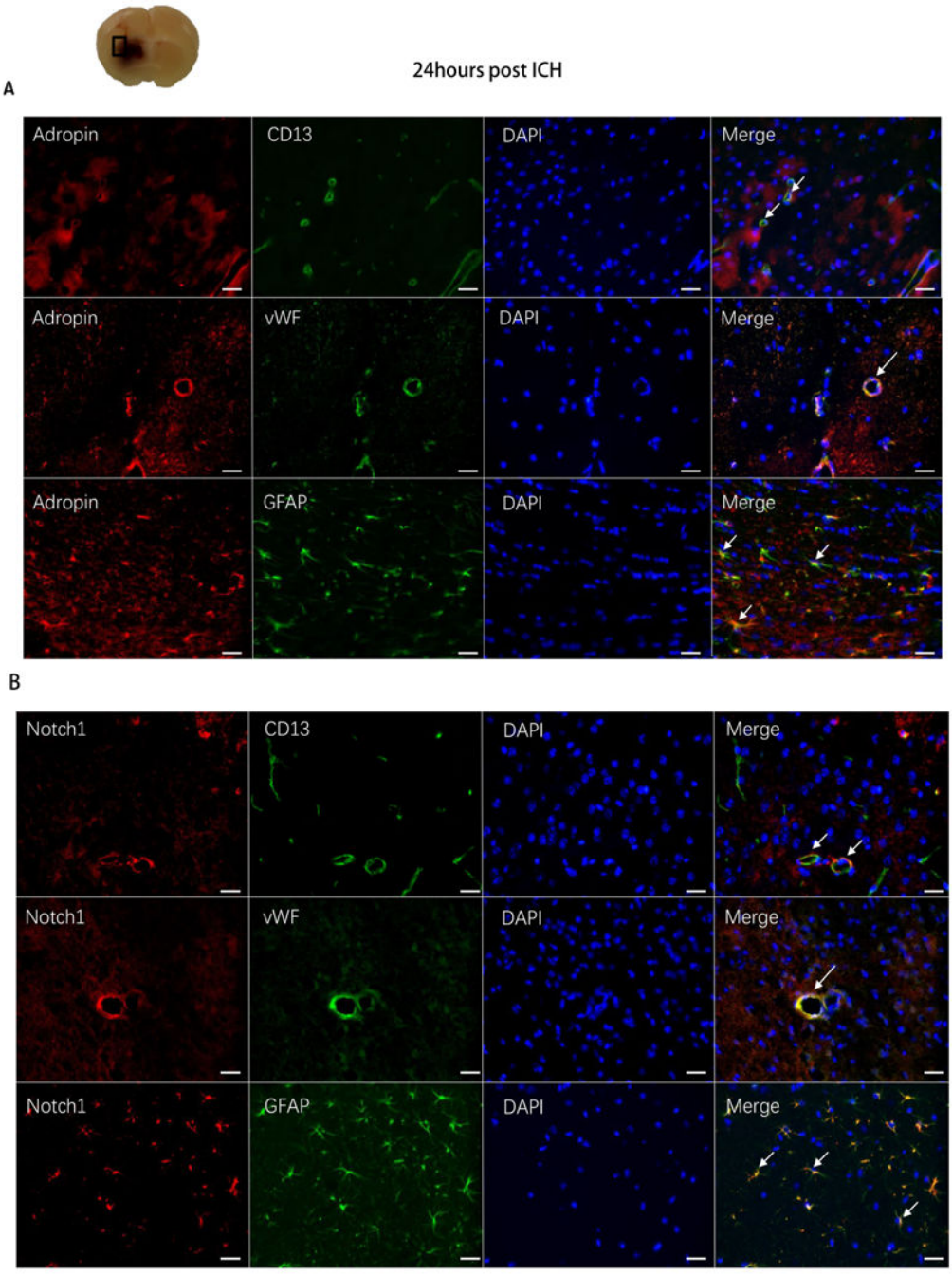

Figure 10. Immunostaining of Adropin (B) and Notch1 (C) with CD13 (pericytes), vWF (endothelial cell), and GFAP (astrocytes) at 24 hours after ICH. Scale bar = 50 μm.

Intranasal Administration of Adropin Decreased Brain Edema and Improved Neurological Functions at 24 h and 72h After ICH

Three different dosages of Adropin (0.5, 1.5, and 5.0 μg) were administered by intranasal 1 h after ICH. Brain water content and neurological scores were measured at 24 h after ICH. It was found that Adropin at 1.5 μg decreased brain water content (Fig. 11A; $p< 0.05$, vs. ICH +vehicle), and improved Modified Garcia scores and Limb placements (Fig. 11B and 4C; $p<0.05$ vs. ICH+vehicle) at 24 h after ICH; however, there was no change in the Corner turn test. The results indicated that the middle dosage of Adropin was more effective as a treatment for early brain injury. Thus, this dosage was selected to further determine the effects at 72 h and to elucidate Adropin's mechanism of action.

Adropin treatment significantly improved performance on Modified Garcia, Forelimb placement, and Corner turn tests at 72 h after ICH, as compared to the vehicle group ($p<0.05$, Fig. 12B, C, and D). In the ipsilateral basal ganglia, brain water content was significantly higher in the vehicle group than the sham animals ($p<0.05$ vs. sham, Fig. 12A), and Adropin treatment reduced brain edema significantly ($p<0.05$, compared to ICH+vehicle, Fig. 12A).

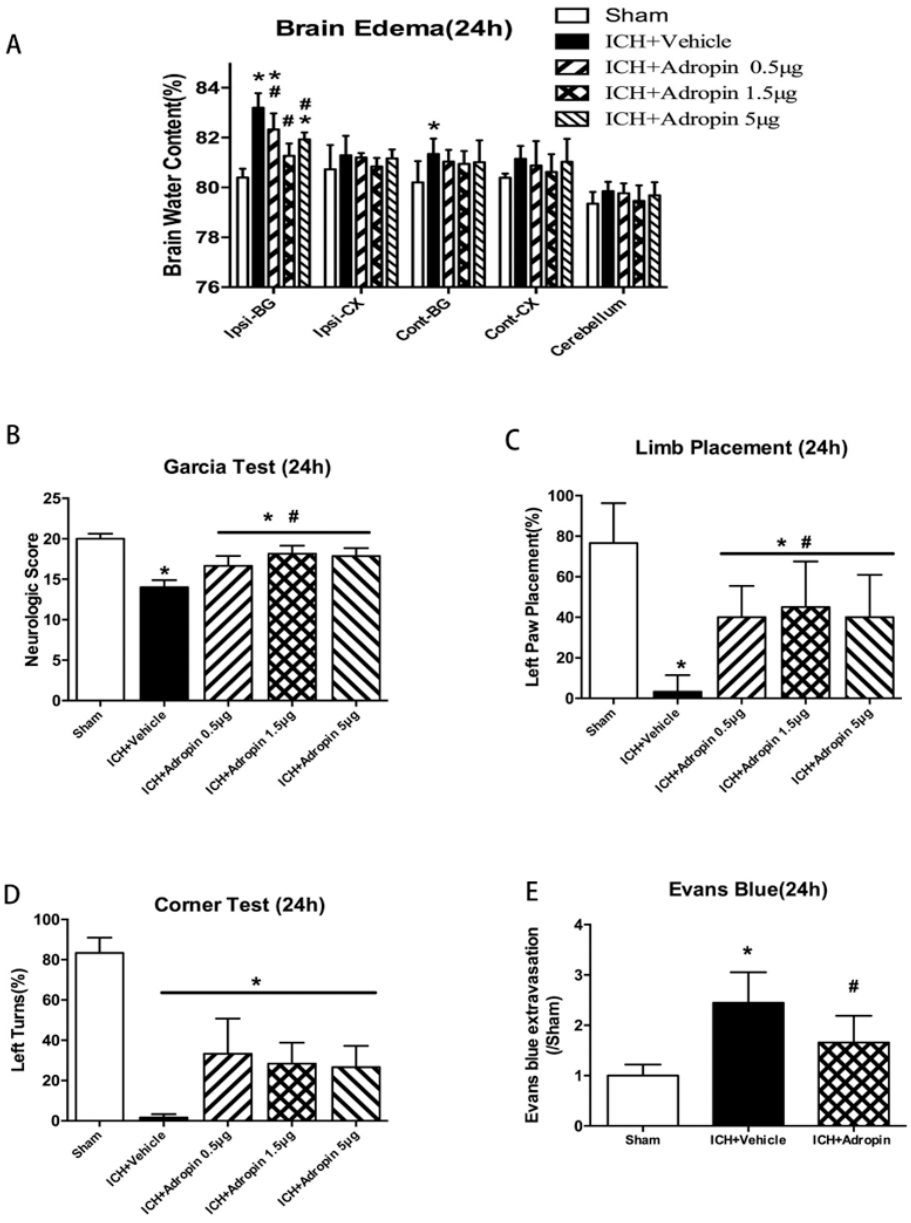

Figure 11. Administration of Adropin decreased brain water content and improved neurobehavioral performance at 24 h after intracerebral hemorrhage (ICH). (A) Brain water content; (B) Modified Garcia test; (C) Limb placement test, and (D) Corner turn test. Administration of Adropin decreased blood-brain barrier permeability (E). N = 6 mice/group. *p<0.05 vs. sham, #p<0.05 vs ICH+vehicle. Values are expressed as mean ± SD.

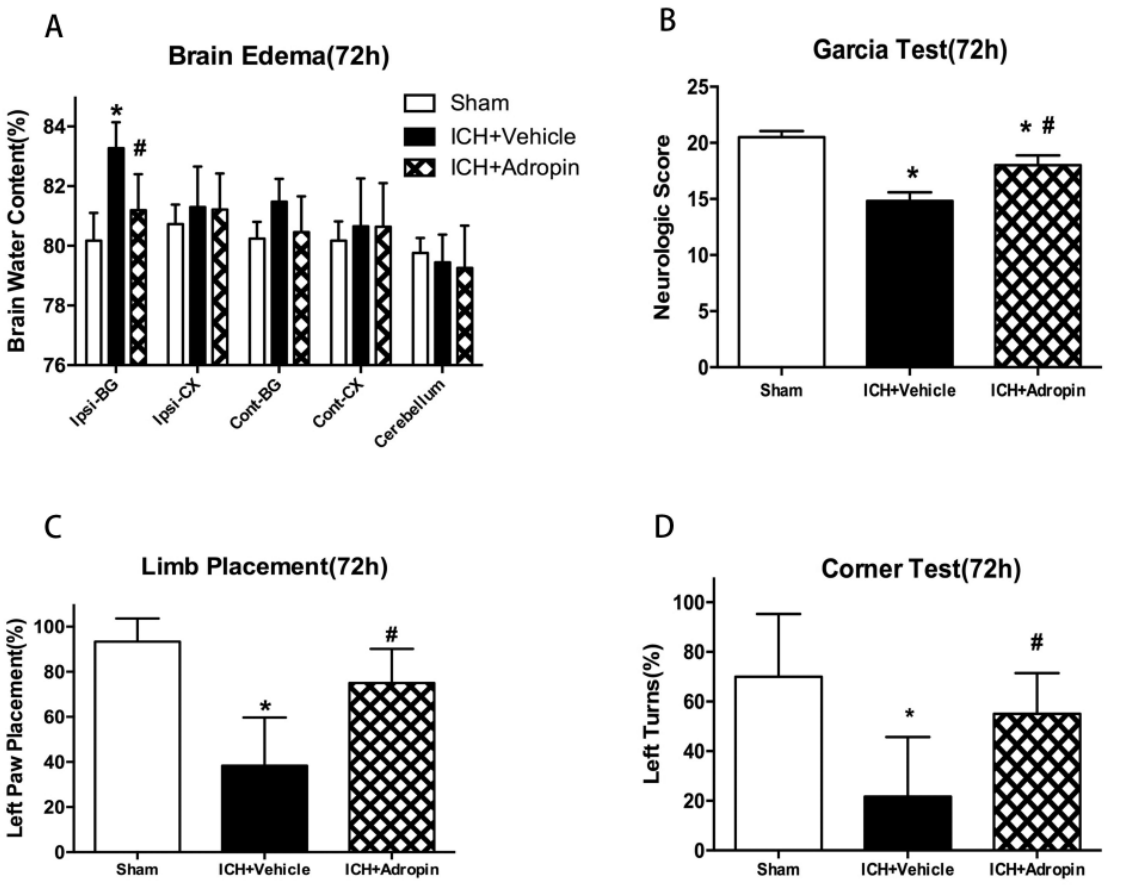

Figure 12. Administration of Adropin decreased brain water content and improved neurobehavioral performance at 72 h after intracerebral hemorrhage (ICH). (A) Brain water content; (B) Modified Garcia test; (C) Limb placement test; and (D) Corner turn test. N = 6 mice/group. *p<0.05 vs. sham, #p<0.05 vs ICH+vehicle. Values are expressed as mean ± SD.

Adropin Improved Long-Term Neurological Function at Four Weeks Post ICH

To test the effects of Adropin treatment on the long-term neurological impairments neurological function was assessed by water maze at four weeks post ICH. It was found that vehicle group performed significantly worse compared to sham group on water maze test. Adropin treatment showed significant memory function recovery compared to vehicle group in reduced swimming distance to platform (Fig. 13A), reduced escape latency (Fig. 13B), and spent more time during target quadrant. (Fig. 13C).

Adropin Treatment Attenuated ICH-induced Disruption of BBB Without Having an Effect on the Hematoma Volume

The Evans Blue assay revealed significant BBB disruption at 24 h after ICH. A significant accumulation of Evans Blue dye in the ipsilateral hemisphere of vehicle-treated animals compared to sham animals was observed at 24 h after ICH (Fig. 11E, $p<0.05$ vs. sham). Adropin significantly decreased ICH-induced dye accumulation (Fig. 11E, $p<0.05$ vs. ICH +vehicle), but there was no effect on hematoma volume (Fig. S1).

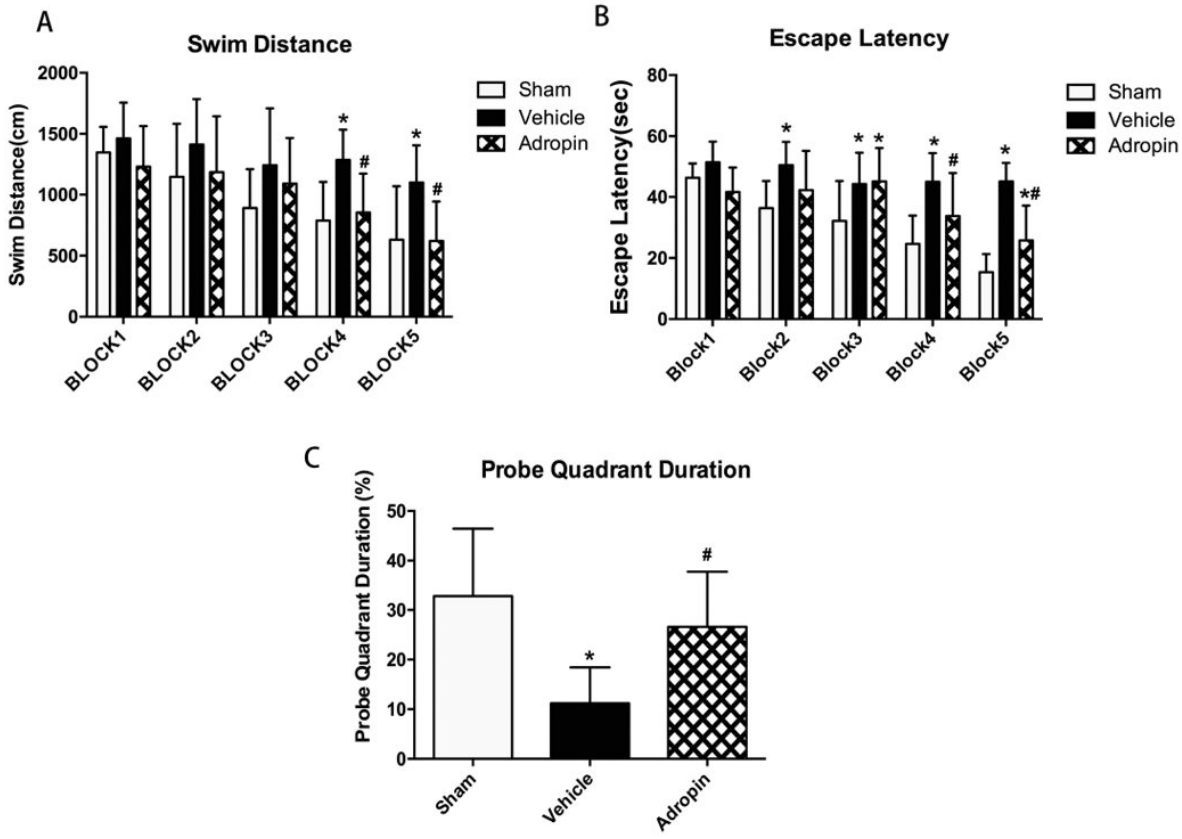

Figure 13. Administration of Adropin improved long-term neurological function at four weeks post ICH. Adropin treatment group showed significant memory function recovery compared to vehicle group in reduced swimming distance to platform (A), reduced escape latency (B), and spent more time during target quadrant (C). N = 8-10 mice/group. *p<0.05 vs. ICH+vehicle. Values are expressed as mean ± SD.

Knockdown of Notch1 or Hes1 Increased Brain Edema and Brain Levels of Albumin, and Decreased Neurological Scores

To investigate the potential mechanisms of Adropin, Notch1 siRNA, Hes1 siRNA, or scramble siRNA were administered along with Adropin treatment in ICH mice. Administrations of Notch1 siRNA and Hes1 siRNA significantly increased brain water content (Fig. 14A; $p<0.05$ vs. ICH + Adropin + Scramble siRNA) and decreased neurological scores when compared with ICH + Adropin + Scramble siRNA group at 24 h after ICH (Fig. 14B and 25C; $p<0.05$ vs. ICH + Adropin + Scramble siRNA). The level of albumin was measured by Western blot at 24 h after ICH. Results from Western blot indicated that Adropin treatment significantly reduced the expression of albumin compared with the vehicle group after ICH (Fig. 14E; $p<0.05$ vs. vehicle). Knockdown Notch1 or Hes1 reversed these effects of Adropin (Fig. 14; $p<0.05$ vs. ICH + Adropin + Scramble siRNA).

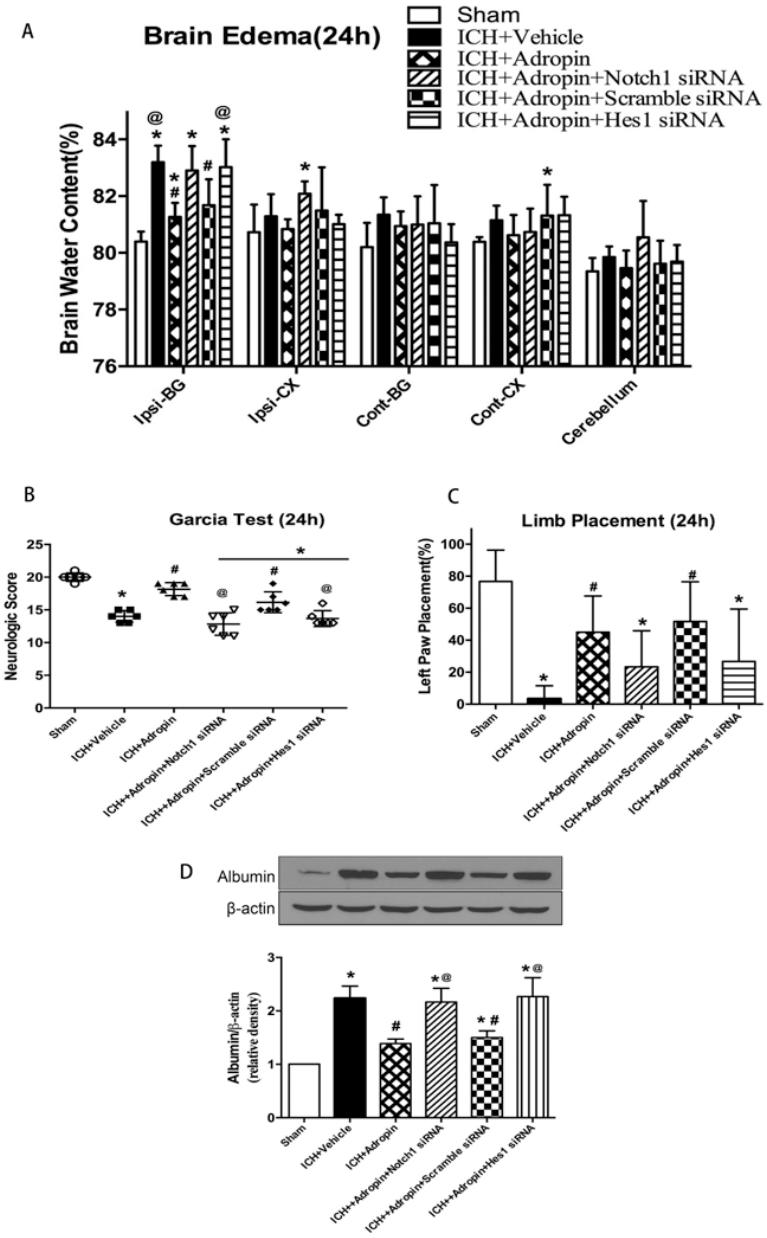

Figure 14. Administration of Notch1 siRNA and Hes1 siRNA increased brain edema (A), reduced Modified Garcia scores (B), Limb placements (C) and Corner turn test (D), and increased the expression of albumin (E) in the ICH brain. N = 6/group in A, B, C, and D; N = 4 for each group in E. *p<0.05 vs sham, #p<0.05 vs ICH+vehicle, @p<0.05 vs. ICH+Adropin+Scramble siRNA. Values are expressed as mean ± SD.

Adropin Treatment Increased the Expression of BBB Integrity Through a Notch1/Hes1- Dependent Mechanism

Administration of Adropin increased the protein levels of Notch1, NICD, Hes1, phosphorylated Akt, and BBB Integrity at 24 h after ICH, compared with the vehicle group (Fig. 15B, C, D, E, F, G and H; $p<0.05$ vs. vehicle). Knockdown of Notch1 with Notch1 siRNA remarkably decreased the expression of Notch1, NICD, Hes1, and p-Akt in Adropin- treated animals (Fig. 15; $p<0.05$ vs. ICH + Adropin + Scramble siRNA). Notch1 knockdown also abolished the effect of Adropin on BBB Integrity. Knockdown of Hes1 produced similar effects, reversing the Adropin-induced increase of BBB Integrity, and reducing the expression of Hes1 (Fig. 15; $p<0.05$ vs. ICH + Adropin + Scramble siRNA).

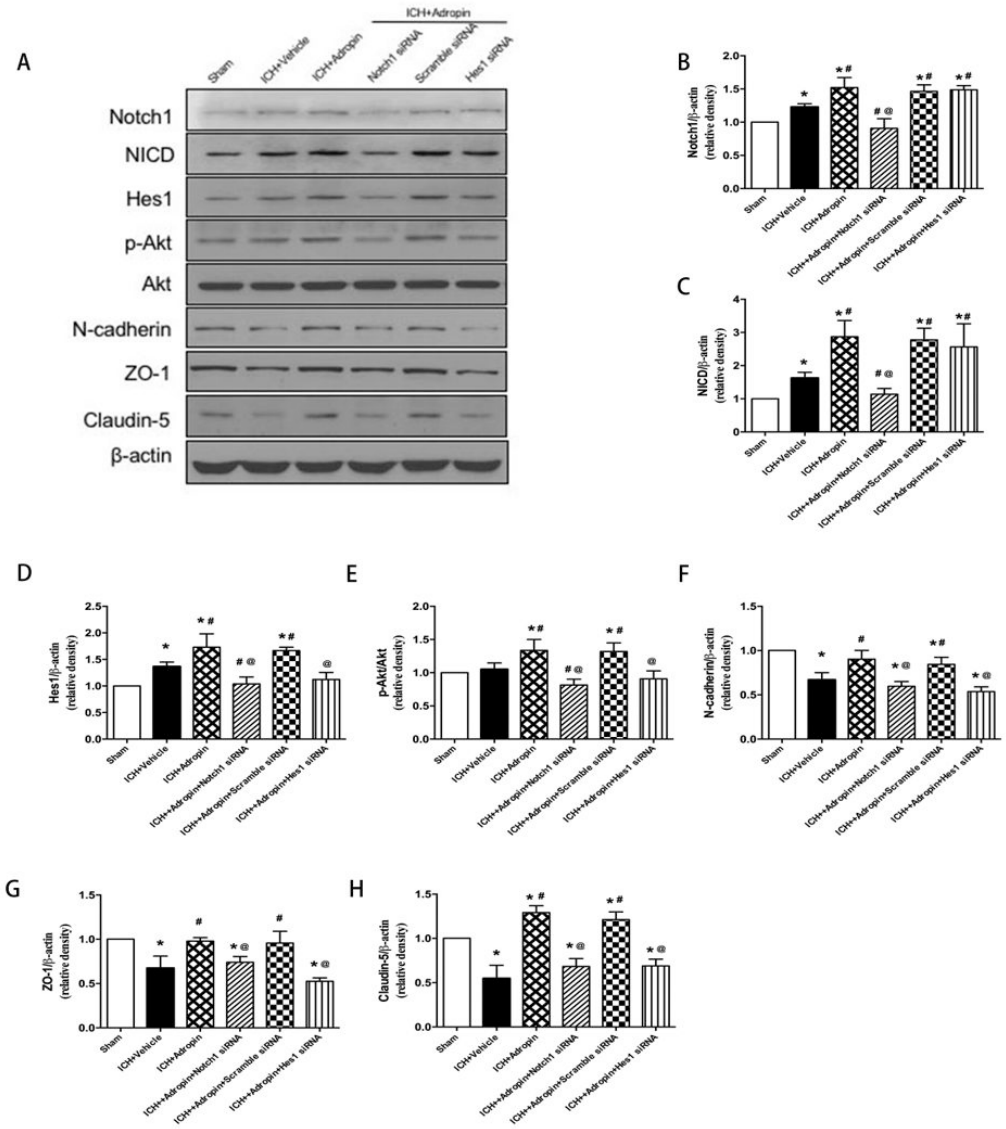

Figure 15. Effects of Adropin, Notch1 siRNA, and Hes1 siRNA on the expression of Notch1, NICD, Hes1, p-Akt, and BBB Integrity after ICH. Administration of Adropin increased protein level of Notch1 (B), NICD (C), Hes1 (D), p-Akt (E), and BBB integrity (F,G, and H). Silencing Notch1 by siRNA reduced the expression of Notch1 (B), and abolished the effect of Adropin on N-cadherin (F). Silencing Hes1 by siRNA reduced the expression of Hes1 (D), and also abolished the effect of Adropin on BBB integrity (F,G, and H). N = 4 mice/group. *p<0.05 vs sham, $^{\#}$p<0.05 vs. ICH+vehicle, $^{@}$p<0.05 vs. ICH+Adropin+Scramble siRNA. Values are expressed as mean ± SD.

Discussion

ICH is a fatal stroke subtype characterized by extensive blood-brain barrier disruption [26]. Currently, there is a lack of effective treatment options for ICH. In the present study, we demonstrated that administration of exogenous Adropin reduced brain edema, minimized BBB disruption, and improved neurological function in mice after ICH at 24 h and 72 h, also improved long- term neurological function as assessed by water maze. Adropin, with a molecular weight of 4.5 kDa, is critical for the maintenance of metabolic and non-metabolic homeostasis. However, little is currently known about its ability to cross the BBB. In the extant literature, utilizing intranasal administration has enabled many drugs to bypass the BBB, and reach the CSF and olfactory bulb via olfactory sensory neurons [27]. Thus, in the present study, we administered Adropin intranasally. We found that Adropin expression in the brains of treated animals was increased after treatment, compared to Vehicle animals (Fig. S2).

BBB disruption is correlated with poor outcomes after ICH [28, 29]. The interaction between pericytes and endothelial cells with other cells is vital for BBB maintenance [30]. In this study, Adropin and Notch1 co-localized with pericytes, endothelial cells and astrocytes after ICH, indicating that Adropin may play a significant role in maintaining BBB permeability and stability after ICH, as it interacts with its receptor on these cell types known to function in BBB preservation.

Prospective treatments that stabilize adherens junctions may reduce vasogenic brain edema, and therefore attenuate brain injury after ICH [4]. In the

present study, treatment with Adropin resulted in a significant reduction of brain water content, with concomitant improvements in neurological functions. We found that Adropin treatment also decreased BBB permeability, as Evans Blue dye extravasation and albumin levels in the brain of Adropin-treated animals were reduced in comparison to vehicle. This reduction coincided with the improvement in neurobehavioral scores.

The Notch1 signaling pathway has been established as one of the downstream effectors of Adropin [13, 14]. In the pathogenesis of CNS disorders, the role of Notch1 signaling remains controversial. However, modulation of Notch1 signaling may restore neurogenesis and cognitive functioning in animal models of Alzheimer's Disease [31]. In addition, the Notch1/Hes1 signaling pathway participates in melatonin-mediated cardioprotective effects in both in vivo and in vitro models of myocardial ischemia–reperfusion injury [32, 33]. Notch1 is cleaved by γ-secretase to release the NICD, which translocates to the nucleus and binds to a transcription factor [34]. Previous studies have demonstrated that administration of a Notch1 activator reduced infarct volumes and improved neurological deficits in aged rats after focal cerebral ischemia [35]. Yet, whether Notch1 signaling is involved in the protective effects of Adropin in ICH remains undetermined. We found that, after Adropin treatment in ICH mice, the expression of Notch1 and NICD was significantly increased, while administering Notch1 siRNA and Hes1 siRNA reversed these effects of Adropin, suggesting that the neuroprotection of Adropin is mediated by the Notch1/Hes1 signaling pathway. Furthermore, Notch1 signaling is dynamically regulated during

brain development and disease processes via crosstalk with numerous signaling pathways [15, 16]. Therefore, additional studies are needed to elucidate the precise mechanism of Adropin in Notch1 signaling modulation after ICH.

Adropin treatment also induced phosphorylation and activation of Notch1 and Akt, leading to increased BBB Integrity. N-cadherin is a candidate molecule which could be involved in endothelial commitment to blood–retina and blood–brain barrier phenotype [36]. Moreover, N-cadherin is required for pericyte recruitment and vessel stabilization [37]. Previous studies have shown that knockdown of N-cadherin by siRNA resulted in increased permeability and influenced capillary tube formation in EC-pericyte co-culture systems [17]. Notch1 signaling in ECs promotes adhesion by upregulating N-cadherin expression [38]. Our findings corroborate these previous studies, further verifying Adropin's role in BBB maintenance following ICH.

However, there are some limitations in the current study. Since we only focus on BBB function, we cannot exclude the possibility that antiapoptosis, anti-inflammatory, preservation of axonal integrity, or other effects of Adropin also play neuroprotective roles after ICH. Thus future studies are needed to investigate the other protective functions, as well as signaling mechanisms.

In conclusion, our study demonstrated that Adropin was protective in the early injury stages after ICH, maintained BBB integrity, and improved functional outcomes via the Notch1/ Hes1 signaling pathway. These findings indicate that Adropin may constitute a particularly promising treatment for ICH.

References

1. Qureshi, A.I., A.D. Mendelow, and D.F. Hanley, *Intracerebral haemorrhage.* Lancet, 2009. 373(9675): p. 1632-44.

2. Lee, K.R., et al., *Mechanisms of edema formation after intracerebral hemorrhage: effects of thrombin on cerebral blood flow, blood-brain barrier permeability, and cell survival in a rat model.* J Neurosurg, 1997. 86(2): p. 272-8.

3. Thiex, R. and S.E. Tsirka, *Brain edema after intracerebral hemorrhage: mechanisms, treatment options, management strategies, and operative indications.* Neurosurg Focus, 2007. 22(5): p. E6.

4. Chen, S., et al., *An update on inflammation in the acute phase of intracerebral hemorrhage.* Transl Stroke Res, 2015. 6(1): p. 4-8.

5. Selim, M. and K.N. Sheth, *Perihematoma edema: a potential translational target in intracerebral hemorrhage?* Transl Stroke Res, 2015. 6(2): p. 104-6.

6. Keep, R.F., et al., *Vascular disruption and blood-brain barrier dysfunction in intracerebral hemorrhage.* Fluids Barriers CNS, 2014. 11: p. 18.

7. Ganesh Kumar, K., et al., *Adropin deficiency is associated with increased adiposity and insulin resistance.* Obesity (Silver Spring), 2012. 20(7): p. 1394-402.

8. Kumar, K.G., et al., *Identification of adropin as a secreted factor linking dietary macronutrient intake with energy homeostasis and lipid metabolism.* Cell Metab, 2008. 8(6): p. 468-81.

9. Aydin, S., et al., *Expression of adropin in rat brain, cerebellum, kidneys, heart, liver, and pancreas in streptozotocin-induced diabetes.* Mol Cell Biochem, 2013. 380(1-2): p. 73-81.

10. Yolbas, S., et al., *Serum adropin level and ENHO gene expression in systemic sclerosis.* Clin Rheumatol, 2016. 35(6): p. 1535-40.

11. Lovren, F., et al., *Adropin is a novel regulator of endothelial function.* Circulation, 2010. 122(11 Suppl): p. S185-92.

12. Yang, C., et al., *Adropin reduces paracellular permeability of rat brain endothelial cells exposed to ischemia-like conditions.* Peptides, 2016. 81: p. 29-37.

13. Wong, C.M., et al., *Adropin is a brain membrane-bound protein regulating physical activity via the NB-3/Notch signaling pathway in mice.* J Biol Chem, 2014. 289(37): p. 25976-86.

14. Gao, S., et al., *Therapeutic effects of adropin on glucose tolerance and substrate utilization in diet-induced obese mice with insulin resistance.* Mol Metab, 2015. 4(4): p. 310-24.

15. Ables, J.L., et al., *Not(ch) just development: Notch signalling in the adult brain.* Nat Rev Neurosci, 2011. 12(5): p. 269-83.

16. Alberi, L., et al., *Notch signaling in the brain: in good and bad times.* Ageing Res Rev, 2013. 12(3): p. 801-14.

17. Li, F., et al., *Endothelial Smad4 maintains cerebrovascular integrity by activating N-cadherin through cooperation with Notch.* Dev Cell, 2011. 20(3): p. 291-302.

18. Hayward, P., T. Kalmar, and A.M. Arias, *Wnt/Notch signalling and information processing during development.* Development, 2008. 135(3): p. 411-24.

19. McCright, B., *Notch signaling in kidney development.* Curr Opin Nephrol Hypertens, 2003. 12(1): p. 5-10.

20. Krafft, P.R., et al., *Modeling intracerebral hemorrhage in mice: injection of autologous blood or bacterial collagenase.* J Vis Exp, 2012(67): p. e4289.

21. Huang, L., et al., *Phosphoinositide 3-Kinase Gamma Contributes to Neuroinflammation in a Rat Model of Surgical Brain Injury.* J Neurosci, 2015. 35(29): p. 10390-401.

22. Tang, J., et al., *Mmp-9 deficiency enhances collagenase-induced intracerebral hemorrhage and brain injury in mutant mice.* J Cereb Blood Flow Metab, 2004. 24(10): p. 1133-45.

23. Ma, Q., et al., *PDGFR-α inhibition preserves blood-brain barrier after intracerebral hemorrhage.* Ann Neurol, 2011. 70(6): p. 920-31.

24. Manaenko, A., et al., *Comparison Evans Blue injection routes: Intravenous versus intraperitoneal, for measurement of blood-brain barrier in a mice hemorrhage model.* J Neurosci Methods, 2011. 195(2): p. 206-10.

25. Zhang, Y., et al., *Activation of Dopamine D2 Receptor Suppresses Neuroinflammation Through αB-Crystalline by Inhibition of NF-κB Nuclear*

Translocation in Experimental ICH Mice Model. Stroke, 2015. 46(9): p. 2637-46.

26. Schlunk, F. and S.M. Greenberg, *The Pathophysiology of Intracerebral Hemorrhage Formation and Expansion.* Transl Stroke Res, 2015. 6(4): p. 257-63.

27. Patel, M.M., et al., *Getting into the brain: approaches to enhance brain drug delivery.* CNS Drugs, 2009. 23(1): p. 35-58.

28. Li, L., et al., *A Cannabinoid Receptor 2 Agonist Prevents Thrombin-Induced Blood-Brain Barrier Damage via the Inhibition of Microglial Activation and Matrix Metalloproteinase Expression in Rats.* Transl Stroke Res, 2015. 6(6): p. 467-77.

29. Shi, Y., et al., *Translational Stroke Research on Blood-Brain Barrier Damage: Challenges, Perspectives, and Goals.* Transl Stroke Res, 2016. 7(2): p. 89-92.

30. Zhao, Z., et al., *Establishment and Dysfunction of the Blood-Brain Barrier.* Cell, 2015. 163(5): p. 1064-1078.

31. Tanveer, R., et al., *The endocannabinoid, anandamide, augments Notch-1 signaling in cultured cortical neurons exposed to amyloid-β and in the cortex of aged rats.* J Biol Chem, 2012. 287(41): p. 34709-21.

32. Pazar, A., et al., *The neuroprotective and anti-apoptotic effects of melatonin on hemolytic hyperbilirubinemia-induced oxidative brain damage.* J Pineal Res, 2016. 60(1): p. 74-83.

33. Yu, L., et al., *Melatonin rescues cardiac thioredoxin system during ischemia-reperfusion injury in acute hyperglycemic state by restoring Notch1/Hes1/Akt signaling in a membrane receptor-dependent manner.* J Pineal Res, 2017. 62(1).

34. Gridley, T., *Notch signaling in vascular development and physiology.* Development, 2007. 134(15): p. 2709-18.

35. Sun, F., et al., *Notch1 signaling modulates neuronal progenitor activity in the subventricular zone in response to aging and focal ischemia.* Aging Cell, 2013. 12(6): p. 978-87.

36. Gerhardt, H., et al., *N-cadherin expression in endothelial cells during early angiogenesis in the eye and brain of the chicken: relation to blood-retina and blood-brain barrier development.* Eur J Neurosci, 1999. 11(4): p. 1191-201.

37. Paik, J.H., et al., *Sphingosine 1-phosphate receptor regulation of N-cadherin mediates vascular stabilization.* Genes Dev, 2004. 18(19): p. 2392-403.

38. Winkler, E.A., R.D. Bell, and B.V. Zlokovic, *Central nervous system pericytes in health and disease.* Nat Neurosci, 2011. 14(11): p. 1398-1405.

CHAPTER 4

INHIBITION OF STRESS FIBER FORMATION PRESERVES BLOOD-BRAIN BARRIER AFTER INTRACEREBRAL HEMORRHAGE IN MICE

Anatol Manaenko [a *], Peng Yang [a,f *], Derek Nowrangi, Enkhjargal Budbazar [a], Richard E. Hartman [b], Andre Obenaus [c], William J. Pearce [a], John H. Zhang [a,d,e], Jiping Tang [a**]

Departments of [a] Physiology and Pharmacology, [b] Psychology, [c] Pediatrics [d] Anesthesiology, [e] Neurosurgery, Loma Linda University, Loma Linda, CA, USA; [f] Department of Emergency Surgery, the First Affiliated Hospital of Soochow University, Suzhou, Jiangsu, China

Correspondence to: Jiping Tang MD, Department of Physiology & Pharmacology, Loma Linda University School of Medicine, 11041 Campus St, Loma Linda, CA, USA, 92350. Phone 909-558-7693, Fax 909-558-0119, E-mail: jtang@llu.edu

The work presented in this chapter has been published.

J Cereb Blood Flow Metab. 2018 Jan;38(1):87-102.

Abstract

Intracerebral hemorrhage (ICH) represents the deadliest subtype of all strokes. The development of brain edema, a consequence of blood–brain barrier (BBB) disruption, is the most life-threatening event after ICH. Pathophysiological conditions activate the endothelium, one of the components of BBB, inducing rearrangement of the actin cytoskeleton. Upon activation, globular actin assembles into a filamentous actin resulting in the formation of contractile actin bundles, stress fibers. The contraction of stress fibers leads to the formation of intercellular gaps between endothelial cells increasing the permeability of BBB. In the present study, we investigated the effect of ICH on stress fiber formation in CD1 mice. We hypothesized that ICH-induced formation of stress fiber is triggered by the activation of PDGFR-β and mediated by the cortactin/RhoA/LIMK pathway. We demonstrated that ICH induces formation of stress fibers. Furthermore, we demonstrated that the inhibition of PDGFR-β and its downstream reduced the number of stress fibers, preserving BBB and resulting in the amelioration of brain edema and improvement of neurological functions in mice after ICH.

Introduction

Intracerebral hemorrhage (ICH) represents the deadliest subtype of all strokes. Brain edema, a life- threatening consequence of ICH, significantly contributes to a high mortality after ICH. The most common type of brain edema, vasogenic edema, results from increased blood-brain barrier (BBB) permeability [1-4]. The BBB permeability is regulated by adherens and tight junctions. While the function of adherens junctions is to hold neighboring primary epithelial cells together, the tight junctions mediate the gate functions of the BBB and prevent solutes from paracellular diffusion [5, 6]. Under pathophysiological conditions, the endothelium, one of the components of BBB, is activated, inducing re-arrangement of the actin cytoskeleton. Actin in resting endothelium is present as a monomeric globular actin (G-actin). Upon activation, G-actin assembles into a filamentous actin (F-actin) and the shift from G-actin to F-actin results in the formation of contractile actin bundles called stress fibers [7]. Stress fibers anchor to adherens junctions on the membranes of neighboring endothelial cells [8]. Under stress, the contraction of stress fibers results in the formation of intercellular gaps between endothelial cells, increasing the permeability of the BBB [8].

The platelet-derived growth factor receptors (PDGFRs) are a possible trigger of the BBB disintegrity. PDGFRs exist in two isoforms (α and β) and are expressed in all cells of the neurovascular unit, including endothelial cells [9]. While the detrimental role of the α-isoform in the development of secondary brain injury after stroke has been established [10, 11], the role of the β-isoform is

controversial. Some studies suggest that PDGFR-β signaling is crucial for maintaining BBB integrity and tissue repair [12], and others demonstrate that PDGFR-β activation causes fibrosis after brain injury [13] and stress fiber formation [14, 15].

One of the possible mechanisms that PDGFR-β activation contributes to BBB disruption is formation of stress fibers via activation of the cortactin/RhoA/LIMK pathway. Cortactin is a regulator of cytoskeleton and is downstream of PDGFR-β [16]. Upon activation, cortactin transmits a signal from PDGFR to RhoA and re-arranges the cytoskeleton [17, 18]. RhoA is able to interact directly with LIM kinase (LIMK), another potent regulator of actin dynamics that is abundantly expressed in the CNS [19-21]. There are clear indications that F-actin accumulation and stress fiber formation are critically dependent on the LIMK activation [22].

After brain injury, the activation of RhoA is accompanied by BBB disruption, and inhibition of RhoA preserves BBB after ICH [23, 24]. Even without stroke, activation of RhoA in animals increases BBB permeability [25]. However, the effects of stroke on the activation of cortactin or LIMK and the consequences of this activation have not been evaluated yet. In this study, we tested the hypothesis that ICH induces formation of stress fibers triggered by activation of PDGFR-β that is mediated via the cortactin-RhoA-LIMK pathway. We postulated that stress fiber formation causes degradation of adherens/tight junction and consequently disruption of BBB. Most importantly, we tested whether PDGFR-β

inhibition counteracts the effects of BBB disruption by ICH thus presenting itself as a potential therapy for ICH patients.

Materials and Methods

Animals

A total of 166 male CD1 mice (eight-week-old, weight 30g±5g; Charles River, Wilmington, MA) were housed in a vivarium for a minimum of 3 d before surgery with a 12 h light/dark cycle and ad libitum access to food and water. All procedures in this study were approved by the Institutional Animal Care and Use Committee at Loma Linda University and comply with the National Institutes of Health's Guide for the Care and Use of Laboratory Animals, and the manuscript adheres to the ARRIVE (Animal Research: Reporting of In Vivo Experiments) guidelines for reporting animal experiments. Animals were randomly divided into different experimental groups. Animals, which died before final assessment, were replaced. There were no significant differences in the mortality rate between the different experimental groups.

Intracerebral Hemorrhage Mouse Model

Experimental ICH was induced by intrastriatal injection of bacterial collagenase. We adopted the collagenase-induced intracerebral hemorrhage model in mice as previously described [10]. Briefly, mice were anesthetized with ketamine (100 mg/kg) and xylazine (10 mg/kg, intraperitoneal (I.P.) injection) and positioned prone in a stereotaxic head frame. An electronic thermostat-controlled

warming blanket was used to maintain the core temperature at 37° C. The calvarium was exposed by a midline scalp incision from the nasion to the superior nuchal line, and the skin was retracted laterally. With a variable speed drill (Fine Scientific Tools, Foster City, CA, USA) a 1 mm burr hole was made 0.9 mm posterior to bregma and 1.4 mm to the right of the midline. A 26-G needle on a Hamilton syringe was inserted with stereotaxic guidance 4 mm into the right deep cortex/basal ganglia at a rate 1 mm/min. The collagenase (0.075 units in 0.5 µl saline, VII-S; Sigma, St Louis, MO, USA) was infused into the brain at a rate of 0.25 µl/min over 2 minutes with an infusion pump (Stoelting, Wood Dale, IL, USA). The needle was left in place for an additional 10 minutes after injection to prevent the possible leakage of the collagenase solution. After removal of the needle, the incision was closed, and the mice were allowed to recover. The sham operation was performed with needle insertion only.

Drugs and RNAs Administration

The PDGFR-β antagonist CP-673451 (Selleckchem, Inc.) was dissolved in 0.1% DMSO and tested at two different concentrations: 15 and 50 mg/kg of body weight. The LIMK inhibitor, LIMKi 3 (Tocris Bioscience), was dissolved in 0.1% DMSO and tested at two different concentrations: 0.3 and 1 mg/kg of body weight. Both drugs were administered via I.P. injection in 500 µl. Vehicle treated animals received equal amounts of 0.1% DMSO. Both PDGFR-β and LIMKi antagonists were administrated one hour after ICH induction

Both the PDGFR-β and cortactin small interfering RNA (si-RNA), as well as scrambled RNA (sc-RNA), were dissolved in sterile RNAse free resuspension buffer according to the manufacturer's instructions (OriGene). They were administrated via intraventricular injection (i.c.v.) to the right hemisphere twice (24 hrs prior to and 24 hrs after ICH) at 0.9 mm and 3.3 mm lateral from bregma. Si-RNA or sc-RNA (100 pmol) was delivered in 2 μl with a Hamilton syringe over 2 minutes. The needle was left in place for an additional 5 minutes after injection to prevent possible leakage and then slowly withdrawn over 4 minutes. After the needle was removed, the burr hole was sealed with bone wax, the incision was closed with sutures, and the mice were allowed to recover. Vehicle treated animals received an injection of suspension buffer. Recombinant PDGF-D (Abcam) was injected into the right basal ganglia of naïve mice (200 ng/2ul PBS per mouse) using the same coordinates as the collagenase injections.

Evaluation of BBB Permeability and Hematoma Volume

Evaluation of BBB permeability

BBB permeability was evaluated by brain water content measurement and the Evans Blue assay. For brain water content measurement, the dry/wet method was used. Briefly, mice were euthanized under deep anesthesia. Brains were removed immediately and divided into five parts: ipsilateral and contralateral basal ganglia, ipsilateral and contralateral cortex, and cerebellum. The cerebellum was used as an internal control for brain water content. Tissue samples were weighed on an electronic analytical balance (model AE 100;

Mettler Instrument Co., Columbus, OH, USA) to the nearest 0.1 mg to obtain the wet weight. The tissue was then dried at 100^0C for 24 hours to determine the dry weight. Brain water content (%) was calculated as [(wet weight - dry weight)/wet weight] x 100.

The Evans Blue assay was conducted by injecting I.P. a 2% solution of Evans Blue in normal saline (4 ml/kg of body weight), and the stain was then allowed to circulate for three hours[26, 27]. Afterwards, the mice were transcardially perfused with 100 ml of ice-cold PBS, the brain tissue was removed and divided into right and left hemispheres, frozen in liquid nitrogen, and stored at −80°C until analysis. The samples were homogenized in 1100 µl of PBS, sonicated and centrifuged (30 minutes, 15,000 rcf, 4° C). The supernatant was collected in aliquots. To each 500 µl aliquot, an equal amount of 50% trichloroacetic acid was added, incubated over night at 4° C, and then centrifuged (30 min, 15,000 rcf, 4 °C). Evans Blue stain was measured by spectrophotometer (Thermo Spectronic Genesys 10 UV, Thermo Fischer Scientific Inc., Waltham, MA, USA) at 610 nm and quantified according to a standard curve. The results are presented as (µg of Evans Blue stain)/(g of tissue).

Evaluation of hematoma value (hemoglobin assay)

Initially, a standard curve was obtained using a “virtual” model of hemorrhage. Brain tissue was obtained from naive mice subjected to complete transcardial perfusion to remove intravascular blood. Incremental volumes of homologous blood (0, 2, 4, 8, 16, and 32µl) were added to each brain tissue

sample with PBS to reach a total volume of 1100 µl, followed by homogenization for 30 seconds, sonication on ice for 1 minute, and centrifugation at 15,000 rpm for 30 minutes (4° C). Drabkin's reagent (0.4 ml, Sigma) was added to 0.1 ml supernatant aliquots and allowed to stand for 15 minutes at room temperature. Optical density was measured and recorded at 540 nm with a spectrophotometer (Thermo Spectronic Genesys 10 UV, Thermo Fischer Scientific Inc., Waltham,MA, USA). These procedures yielded a linear relationship between measured hemoglobin concentrations in perfused brain and the volume of added blood.

For hematoma evaluation, supernatant was collected as described above (see evaluation of BBB permeability). For standard curve generation, Drabkin's reagent (0.4 ml, Sigma) was added to 0.1 ml supernatant aliquots and allowed to stand for 15 minutes at room temperature. Optical density was measured and recorded at 540 nm with a spectrophotometer (Thermo Spectronic Genesys 10 UV, Thermo Fischer Scientific Inc., Waltham, MA, USA)

Neurobehavioral Function Test

Neurological scores were assessed by an independent researcher blinded to the procedure 23 and 71 hours after ICH as previously described [24]. Two tests were used to evaluate neurological deficits: 1) The modified Garcia test, in which mice were given a score ranging from 0 to 21. The scoring system consists of 7 tests (spontaneous activity, axial sensation, vibrissae proprioception, limb outstretching, lateral turning forelimb walking and climbing), with possible scores

of 0–3 (0=worst; 3=best) for each. 2) The limb placement test, in which the animals were held by their trunk positioned parallel to a table top and slowly moved up and down, allowing the vibrissae on one side of the head to brush along the table surface. Refractory placements of the impaired (left) forelimb were evaluated, and a score was calculated as the number of successful forelimb placements out of 10 consecutive trials.

For long-term evaluation of spatial learning, a Morris Water Maze test was employed as described in our previous publication.[26]

Sample Preparation, Western blot and RhoA activity evaluation

Mice were perfused transcardially with 40 ml of cold PBS. Hemispheres were isolated and stored at (-80° C) until analysis.

Western blot analysis

Protein extraction and Western blots were performed according to the manufacturer's recommendation, as previously reported [28]. Whole-cell lysates were obtained by gently homogenizing in RIPA lysis buffer (Santa Cruz Biotechnology, Inc., sc-24948) and centrifuging (14,000 g at 4° C for 30 minutes). The supernatant of the extract was collected, and the protein concentration was determined using a detergent compatible assay (Bio-Rad, Dc protein assay). Equal amounts of protein (50 µg) were loaded and subjected to electrophoresis on an SDS-PAGE gel. After being electrophoresed and transferred to a nitrocellulose membrane, the membrane was blocked and incubated with the

primary antibody overnight at 4° C. Following antibody were used: For an internal control, the same membrane was probed with an antibody against β-actin (Santa Cruz, 1:1000) after being stripped. Secondary antibodies (Santa Cruz Biotechnology) were incubated for one hour at room temperature. Immunoblots were then probed with an ECL Plus chemiluminescence reagent kit (Amersham Biosciences, Arlington Heights, IL) and visualized with an imaging system (Bio-Rad, Versa Doc, model 4000). Data was analyzed using Image J software.

Evaluation of RhoA activity

RhoA activity was evaluated using a commercially available kit (Cytoskeleton Inc., Denver Co.). Two equal aliquots of each sample were taken. One aliquot was processed according to the manufacturer's recommendations and used for RhoA activity evaluation. The second aliquot was probed with an antibody against β-actin for the loading control.

Immunofluorescence Study

Seventy-two hours after ICH, the mice were perfused under deep anesthesia with cold phosphate-buffered saline (PBS, pH 7.4), followed by infusion of 10% paraformaldehyde. Brains were then removed and fixed in formalin at 4 °C overnight. Samples were then dehydrated with 30% sucrose in phosphate-buffered saline (PBS, pH 7.4), and the frozen coronal slices (10 μm thick) were then sectioned using a cryostat (CM3050S; Leica Microsystems). Immunofluorescence was performed as previously described[2]. Briefly, samples

were incubated with phospho-LIMK antibody (1:50, Abcam) at room temperature for one hour. Afterward samples were washed three times with PBS and incubated with the secondary antibody (1:1000) in a cocktail with Alexa Fluor-phalloidin (100 nM, Cytoskeleton, Inc.). The slides were viewed and images were taken using LAS X software with a Leica DMi 8 fluorescence microscope (Leica Microsystems, Germany).

Statistics

Analysis was performed using SigmaStat software, and data are expressed as mean ± standard error of the mean. Statistical differences were analyzed with one-way analysis of variance (ANOVA) followed by Fisher LSD Method. Statistical significance was defined as $p < 0.05$.

,

Results

Mortality

A total of 16 animals died before the end point as listed in the following:

24-h study: sham (N 1⁄4 0), vehicle (N 1⁄4 2), CP 673,451 (15 mg/kg) (N 1⁄4 1), LIMKi (0.3 mg/kg) (N 1⁄4 1), CP 673,451 (50 mg/kg) (N 1⁄4 1).

72-h study: sham (N 1⁄4 0), vehicle (N 1⁄4 3), CP 673,451 (15 mg/kg) (N 1⁄4 2), LIMKi (0.3 mg/kg) (N 1⁄4 1), CP 673,451 (50 mg/kg) (N 1⁄4 1), LIMKi (1.0 mg/kg) (N1⁄41).

28-day study: sham (N 1⁄4 0), vehicle (N 1⁄4 2), CP 673,451 (50 mg/kg) (N 1⁄4 1).

The mortality (7.7%) of ICH animals was calculated and no statistical difference was obtained between experimental groups in this study.

ICH activated cortactin-LIMK pathway

ICH did not affect the expression of total cortactin or LIMK, induced, however, phosphorylation forms of these proteins at 24 and 72 hours after ICH (Fig. 16A-B). At the same time points, activation of RhoA (Fig. 16C) was observed.

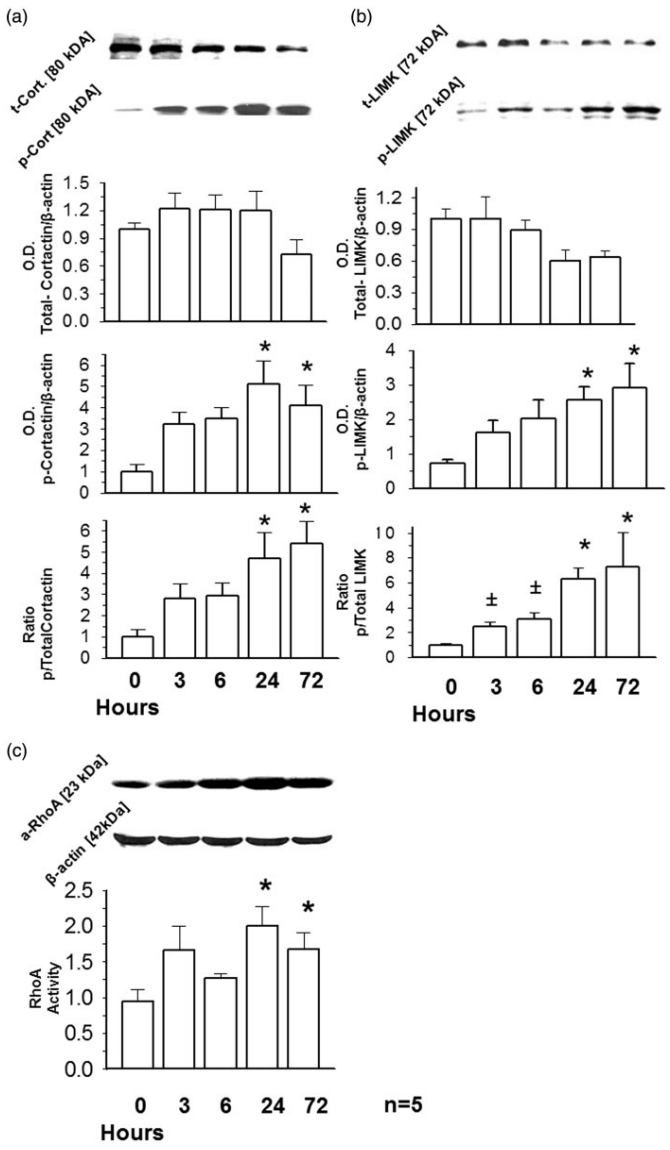

Figure 16. Time-dependent effects of ICH on cortactin-RhoA-LIMK pathway activation**.** Although ICH had no effect on expression of total cortactin (Fig. 16A), ICH significantly activated the cortactin and induced its phophorylation as early as three hours after ICH. The difference to time point 0 became statistically significant 24 and 72 hours after ICH. ICH had no effect on the expression of the total LIMK (Fig. 16B) but activated it, via phosphorylation of the protein, at 24 and 72 hours after ICH. ICH activated RhoA 24 and 72 hours after ICH (Fig. 16C). n=5 per time point; * $p<0.05$ *vs.* time point 0, ± $p<0.05$ *vs.* time point 72 hours. Values are expressed as mean± SEM.

ICH caused degradation of adherens/tight junction proteins

ICH caused degradation of the adherens junction protein VE-cadherin at 3, 24 and 72 hours (Supplemental Fig. 2A). Significant degradation of tight junction proteins, occludin and claudin-3 were observed 72 hours after ICH (Supplemental Fig. 2B-C).

PDGFR-β inhibition attenuated ICH-induced disruption of BBB and improved neurological function, without having an effect on the hematoma volume

No toxic effect of the PDGFR-β inhibition was observed in this study.

A collagenase injection at 24 hours resulted in a significant elevation of brain water content in the ipsilateral basal ganglia of ICH (collagenase injected) animals compared to sham operated (needle trauma) animals (79.26±0.25% vs. 83.55±0.49% respectively, $p<0.01$ Fig. 17A). While low concentrations (15 mg/kg) of the PDGFR-β inhibitor CP-673451 showed only a tendency to decrease ICH-induced increases of brain water content, the high concentration (50 mg/kg) significantly reduced post-ICH brain edema (83.55±0.79 vs. 81.55±0.5; $p=0.012$ Fig. 17A). Seventy-two hours after ICH, we observed an increase in brain water content in both the ipsilateral and contralateral basal ganglia of ICH compared to the sham animals (ipsilateral 83.69±0.47 *vs* 79.26±0.25 $p<0.001$; contralateral 80.73±0.33 *vs* 78.92±0.3 respectively $p=0.005$, Fig. 17B). High concentrations of CP-673,451 decreased brain edema in the ipsilateral (81.53±0.24, $p<0.001$) and showed a

none significant tendency to decrease brain water content in the contralateral basal ganglia (p=0.546) (Fig. 2B).

In agreement with that, PDGFR-β inhibition improved ICH-impaired neurological function as evaluated by the modified Garcia test (Fig. 17C left panel vehicle *vs* CP-673,451 (50 mg/kg), p=0.004) and limb placement tests (Fig. 17D left panel, vehicle *vs* CP-673,451 (50 mg/kg), p=0.006). Amelioration of ICH-induced brain edema was accompanied with improvement of neurological function evaluated 72 hours after ICH (Fig. 17C-D right panel, vehicle *vs* CP-673,451 (50 mg/kg): modified Garcia, p=0,002: Limp Placement test p=0.004).

In long-term study, we observed significant impairment of spatial learning of ICH compared to vehicle animals evaluated on Morris Water Maze Test (Figure 17(E)). CP-673,451 (50 mg/kg) ameliorated ICH-induced impairment of spatial learning (Figure 2(e)).

The Evans Blue assay revealed significant BBB disruption after ICH. The accumulation of Evans Blue stain in the ipsilateral hemisphere of ICH compared to the sham animals was observed both at 24 and 72 hours after ICH induction (Fig. 17E). PDGFR-β inhibition significantly decreased ICH-induced stain accumulation at 72 hours and showed a tendency to decrease stain accumulation at 24 hours after ICH (Fig. 17E).

PDGFR-β inhibition did not affect hematoma volume (data not shown).

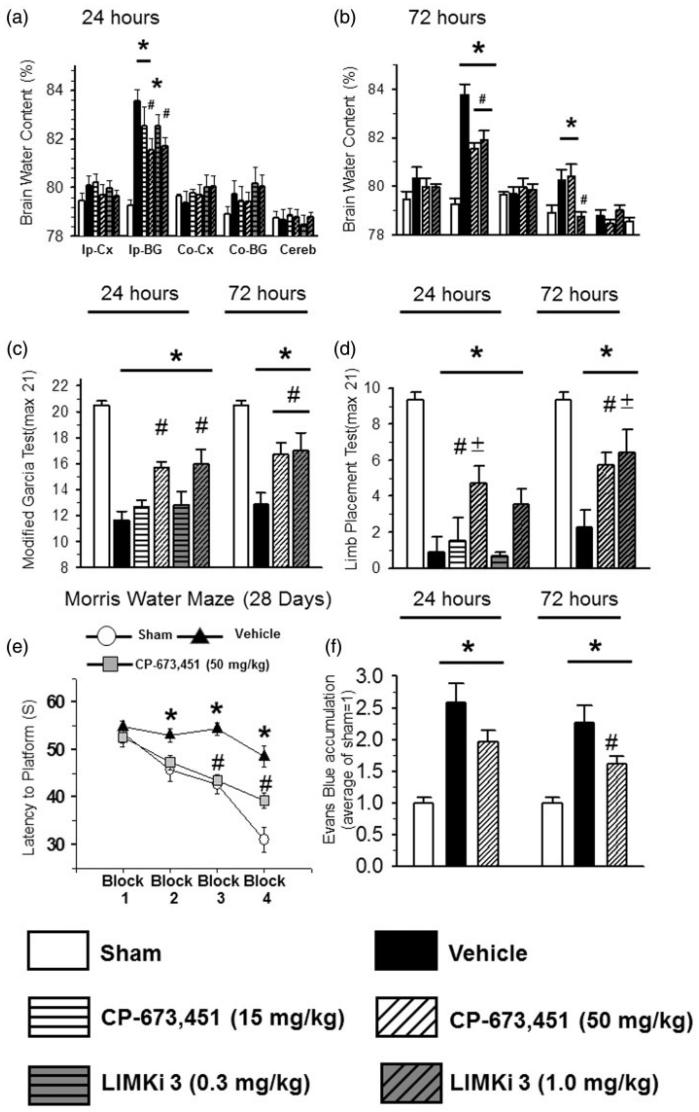

Figure 17. PDGFR-β inhibition preserved BBB integrity and improved neurological functions after ICH**.** Collagenase injection caused significant increase of brain water content in the ipsilateral basal ganglia of ICH-animals (n=7) compared to sham-operated animals (n=6) at both 24 and 72 hours after ICH (Fig. 17A and B). Although a low concentration of the inhibitor (n=6) showed only tendency to attenuate the ICH induced brain edema, a high concentration (n=7), administrated one hour after ICH, significantly reduced this parameter both at 24 (A) and at 72 (B) hours after ICH. PDGFR-β inhibition improved neurological function according to performance on the modified Garcia (Fig. 17C) and limb

placement (Fig. 17D) tests. Compared to sham animals (n=6), ICH-induced disruption of BBB resulted in significant accumulation of Evans Blues stain in the ipsilateral hemisphere of ICH animals (24 hours n=6, 72 hours n=7) (Fig. 17E). A high concentration of PDGFR-β inhibitor attenuated this effect without effecting of hematoma volume (24 hours n=6, 72 hours n=7) (Fig. 17F). Ip=ipsilateral; Cont=contralateral; Cx=Cortex; BG=Basal Ganglia; Cerebel=Cerebellum* $p<0.05$ *vs.* sham, # $p<0.05$ *vs.* vehicle, ± $p<0.05$ *vs.* low concentration. Values are expressed as mean± SEM.

PDGFR-β knock-down attenuated both ICH-induced activation of cortactin-RhoA-LIMK pathway and degradation of adherens/tight junction proteins

To rule out non-specific effects of the PDGFR-β inhibitor, we used si-RNA for the receptor to investigate the molecular mechanisms that underlie the protective effects of the receptor inhibition. Administration (I.c.v).of si-RNA decreased the expression of the receptor (Fig. 18A, vehicle vs si-RNA $p<0.001$). This was accompanied by attenuating activation of the cortactin-RhoA-LIMK pathway (Fig. 18B vehicle vs si-RNA pCort $P=0.039$, aRhoA=0.02, pLIMK $p<0,001$) and by decreased degradation of adherens/tight junction proteins (Fig. 18C, vehicle vs si-RNA, Ve-Cadherin $p=0.017$, Occludin $p=0.002$, Claudin 3 $p=0.002$)). Administration of sc-RNA did not affect these parameters.

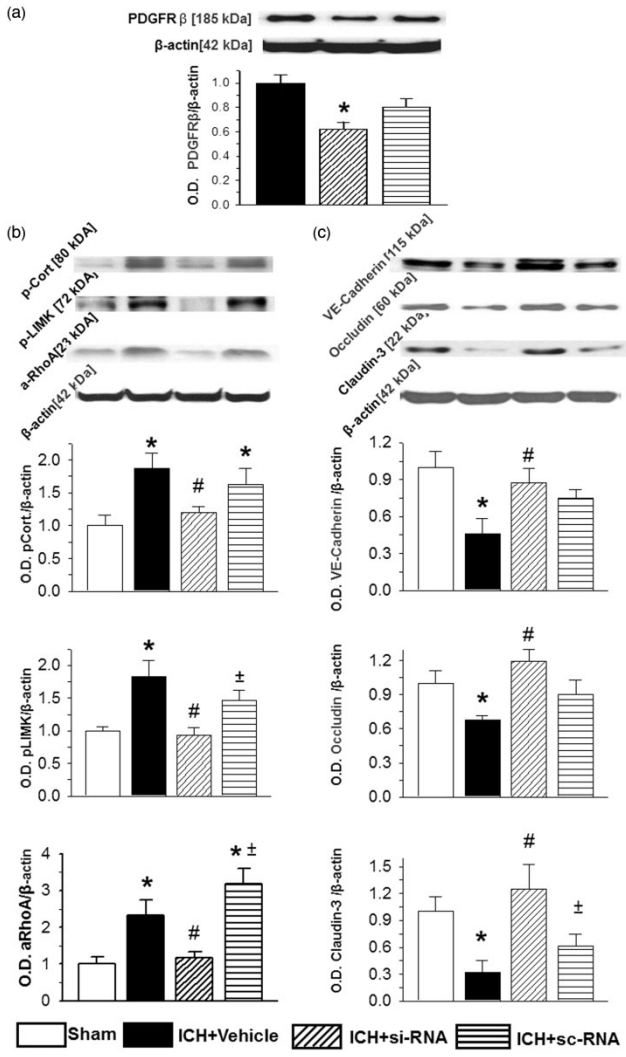

Figure 18. Knockdown of PDGFR-β attenuated ICH induced activation of the cortactin-RhoA-LIMK pathway and preserved BBB. I.c.v. administration of si-RNA for PDGFR-β (si-RNA) significantly decreased expression of the receptor when evaluated 72 hours after ICH. Sc-RNA administration did affect the receptor expression (sc-RNA) (Fig. 18A). Decrease of the PDGFR-β expression was accompanied with significant attenuation of ICH induced activation of the cortactin-RhoA-LIMK pathway (Fig. 3B) and resulted in preservation of adherens/tight junction proteins (Fig. 18C) 72 hours after ICH. (n=6 per group, * $p<0.05$ *vs.* sham, # $p<0.05$ *vs.* vehicle, ± $p<0.05$ *vs.* scrambled RNA). Values are expressed as mean± SEM.

Knock-down of PDGFR-β downstream, cortactin attenuated both ICH-induced activation of RhoA-LIMK pathway and degradation of adherens/tight junction proteins

Administration (I.c.v.) of cortactin si-RNA decreased the expression of this protein (Fig. 19A, vehicle vs si-RNA $p=0.021$). Decreased expression of the cortactin corresponded both with diminished activation of the RhoA-LIMK pathway (Fig. 19B, vehicle vs si-RNA: pLIMK p=0,031, RhoA $p<0.001$) and with decreased degradation of adherens/tight junction proteins (Fig. 19C, vehicle vs si-RNA: Occludin $p<0.001$). Administration of sc-RNA did not affect these parameters.

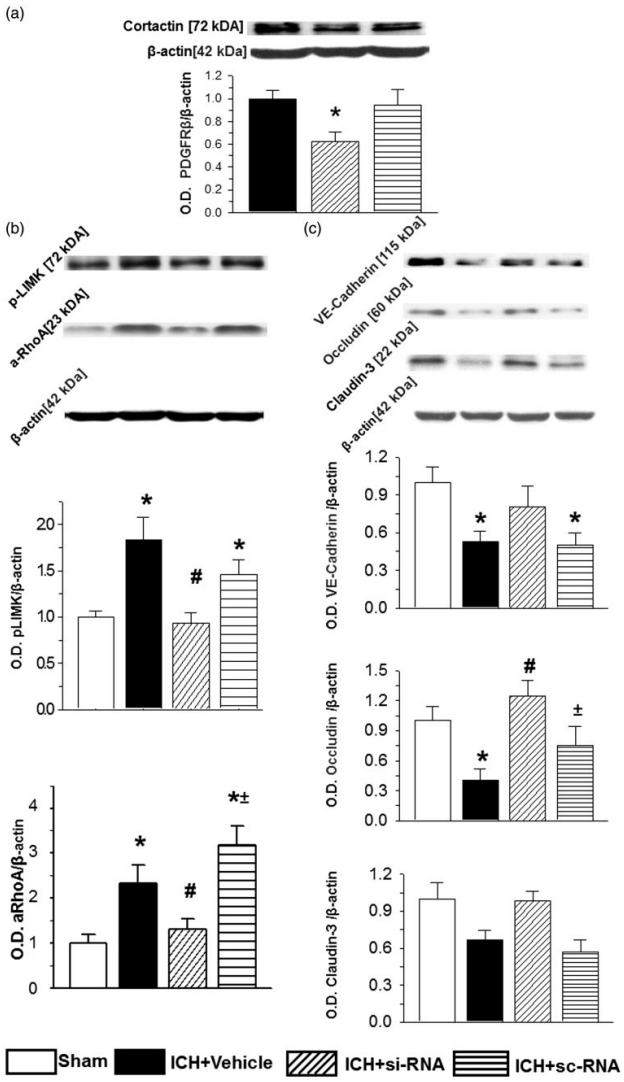

Figure 19. Knockdown of PDGFR-β downstream, cortactin, attenuated ICH induced activation of the RhoA-LIMK pathway and preserved BBB. I.c.v. administrations of si-RNA for cortactin (si-RNA) significantly decreased expression of the protein 72 hours after ICH. Scrambled RNA administration did affect the receptor expression (sc-RNA) (Fig. 19A). At 72 hours the decrease of the cortactin was accompanied with significant attenuation of ICH induced activation of RhoA-LIMK pathway (Fig. 19B) and resulted in preservation of adherens/tight junction proteins (Fig. 19C). n=6 per group, * $p<0.05$ *vs.* sham, # $p<0.05$ *vs.* vehicle, ± $p<0.05$ *vs.* scrambled RNA. Values are expressed as mean± SEM.

LIMK inhibition preserved BBB and attenuated neurological deficits after ICH

Compared to vehicle treated animals, animals treated with high concentrations of the LIMK inhibitor LIMKi 3 (1 mg/kg) had significantly decreased brain water content at both 24 and 72 hours after ICH (24 hours: 83.271±0.412 vs. 81.730±0.34, p=0.007; 72 hours: 83.77±0.44 vs. 81.92±0.37, p=0.003; vehicle vs. treatment respectively (Fig. 20A1-A2)). Correspondingly, high concentrations of LIMKi 3 significantly improved post-ICH neurological functions as evaluated by the modified Garcia(vehicle *vs* treatment 24 hours p=0.002, 72 hours p=0.02) and Limb placement tests (vehicle *vs* treatment 24 hours p=0.011, 72 hours p=0.003) (Fig. 20B1-B2).

Seventy-two hours after ICH, a high concentration of LIMKi 3 decreased ICH-induced phosphorylation of LIMK in treated compared to untreated animals (Fig. 20C, p=0.008). This was accompanied by attenuation of adherens/tight junction protein degradation (Fig. 20D vehicle *vs* treatment occludin p=0.021).

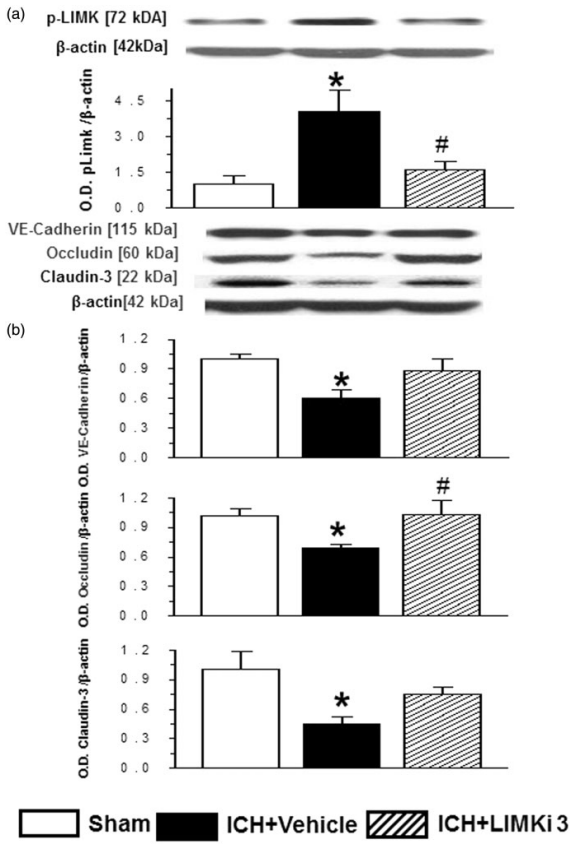

Figure 20. LIMK inhibitor, LIMKi 3, both reduced ICH-induced phosphorylation of LIMK and preserved BBB as well as improved post ICH neurological function**.** Fig. 20A1 24 hours after ICH, LIMK inhibition (one hour after ICH) decreased ICH-induced brain edema dose dependently (sham n=6, ICH n=6; LIMKi 3 low concentration n=6, LIMKi3 high concentration n=7). Fig. 20A2 72 hours after ICH, LIMK inhibition decreased ICH induced brain edema (sham n=6, ICH n=9; LIMKi3 high concentration n=7). Fig. 20B In agreement with brain water content evaluation, LIMK inhibition improved neurological functions at both 24 (Fig. 20B1) and 72 hours (Fig. 20B2) after ICH. Fig. 7C: LIMKi 3 (1 mg/kg n=6) attenuated ICH-induced LIMK activation (ICH n=6) evaluated 72 hours after ICH. Fig. 20D A high dose of LIMK inhibitor attenuated ICH degradation of adherens/tight junction proteins (n=6 per group) evaluated 72 hours after ICH. * $p<0.05$ *vs.* sham, # $p<0.05$ *vs.* vehicle, ± $p<0.05$ *vs.* scrambled RNA. Values are expressed as mean± SEM.

The endogenous PDGFR-β agonist PDGF-D induced activation of cortactin-RhoA-LIMK pathway and degradation of adherens/tight junction proteins in naïve animals

Seventy-two hours after injection of the recombinant PDGF-D into the brains of naïve animals, we observed significant activation of the RhoA-LIMK pathway (sham vs PDGF D: pCortactin p=0.002, pLIMK p=0.008) and a tendency to activate cortactin (p=0.071; Fig. 21A). The activation of the pathway resulted in degradation of VE-cadherin (p=0.012) and occludin (p=0.041= (Fig. 21B).

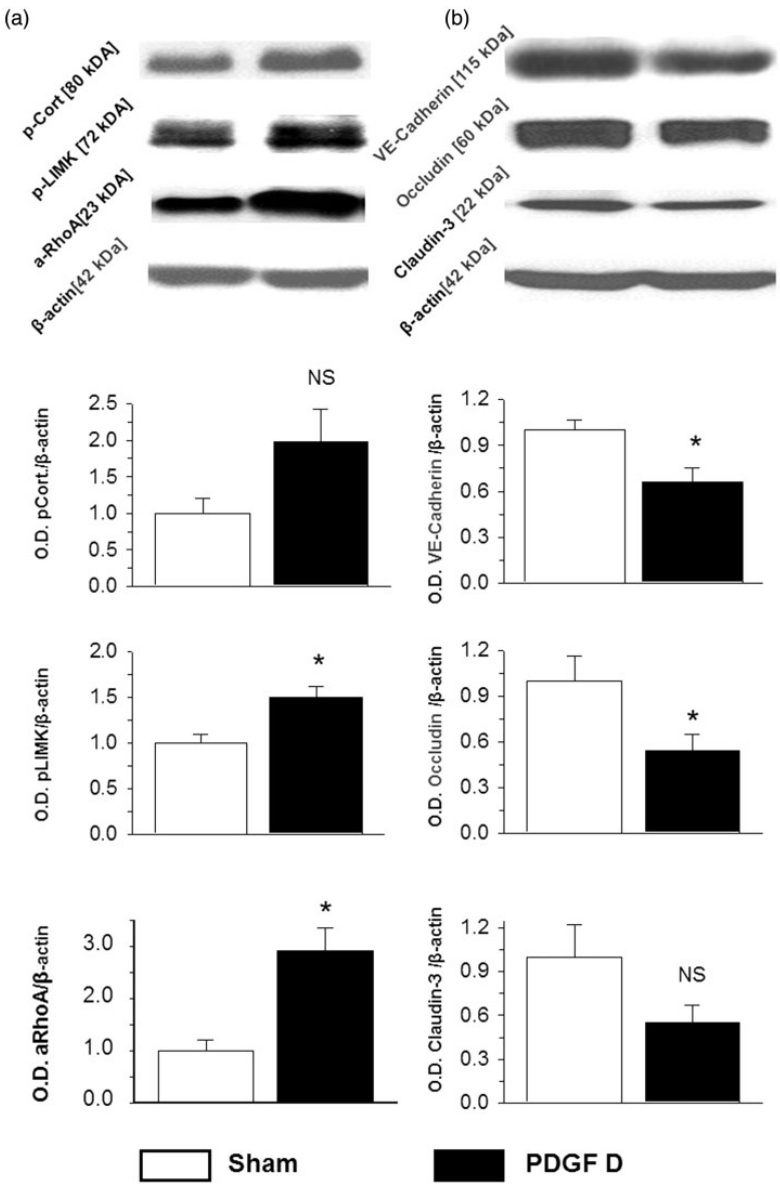

Figure 21. The endogenous agonist of PDGFR-β, PDGF-D, partly induced activation of the RhoA-LIMK pathway and degradation of adherens/tight junction proteins**.** 72 hours after administration of PDGF-D into the basal ganglia of naïve animals, partial activation of the cortactin-RhoA-LIMK pathway was observed (Fig. 21A). That was accompanied with degradation of adherens/tight junction proteins (Fig. 21B). n=6 per group, * $p<0.05$ *vs.* sham, # $p<0.05$ *vs.* vehicle, ± $p<0.05$ *vs.* scrabble RNA. Values are expressed as mean± SEM.

ICH and PDGF-D induced formation of stress fibers, inhibition of PDGFR-β, cortactin or LIMK resulted in decreased stress fiber formation after ICH

Immunostaining revealed that ICH caused a dramatic increase of phalloidin-positive cells (Figure 22) in ICH versus sham-operated animals, indicating stress fiber formation. Most of the stress fibers were posi- tive for phosphorylated LIMK (pLIMK), demon- strating the importance of pLIMK in the formation of stress fibers. Inhibition of the proposed pathway considerably decreased the amount of both stress fiber and pLIMK-positive cells. Sc-RNA did not affect this parameter. Recombinant PDGF-D increased the number of stress fibers compared to sham animals.

Morphology of F-actin stress fiber and their colocalization with phosphorylated LIMK in the higher magnification is demonstrated in Supplemental Figure 3.

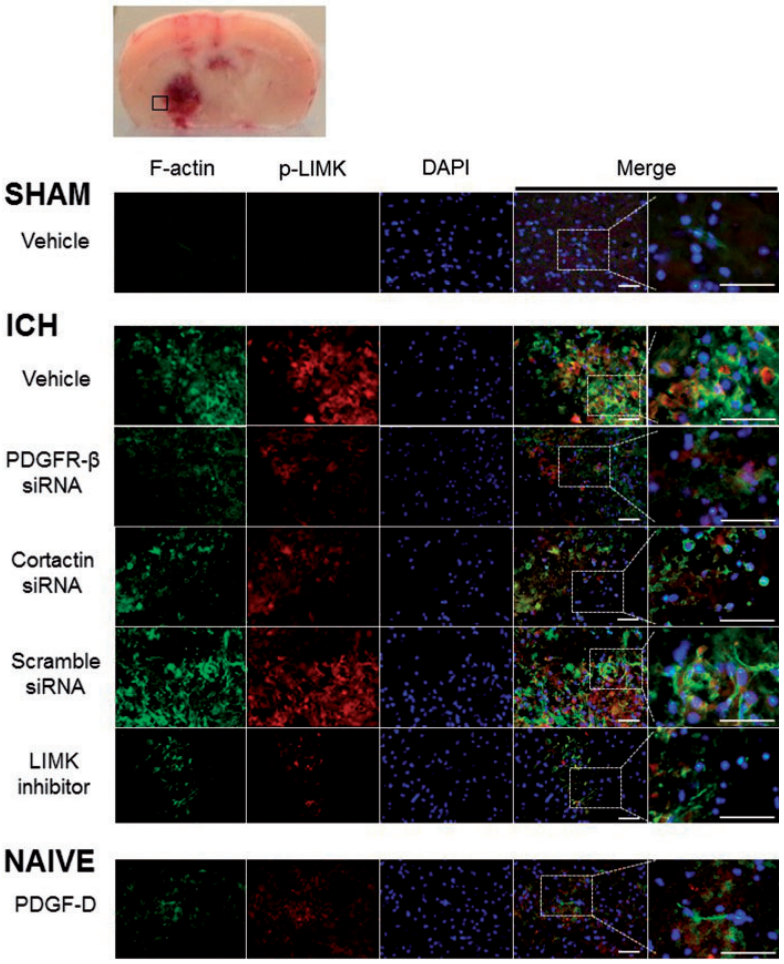

Figure 22. ICH induced activation of LIMK and intensive formation of F-actin stress fibers. Stress fibers were visualized with Alexa Fluor-phalloidin kit. Phalloidin has a high affinity to the F-actin and stress fibers appear green (column “F-actin”). Cells positive for the activated LIMK appear red (column “p-LIMK”). The ICH significantly increased the number of both activated LIMK-positive (red) and phalloidin-positive (green) cells as well as double-positive phalloidin/pLIMK stress fibers (first column “Merge”). While treatment with siRNA for both PDGFR-β and cortactin as well as LIMK inhibition resulted in fewer LIMK positive stress fibers, scrambled RNA did not have such effect. Injection of PDGF-D into the brain of naïve animals resulted in activation of LIMK and formation of stress fiber compared to sham-operated animals. The second “Merge” column show the detailed morphology of pLIMK positive stress fiber in more details.

Discussion

In the present study, we investigated for the first time the effects of ICH on stress fiber formation. We demonstrated that (1) ICH induced formation of stress fibers that were associated with degradation of BBB components, BBB disruption, and the consequent development of brain edema, and (2) these post-ICH events were mediated, at least partly, by PDGFR-β activation via the cortactin/RhoA/LIMK pathway. Furthermore, we established that inhibition of the PDGFR-β pathway is beneficial and protects BBB integrity after ICH.

We demonstrated previously that ICH induced a time-dependent increase of both PDGF production and PDGFR expression [10]. The expression of PDGFR-β increased at 6 h, peaked at 12 h, remained upregulated at 24 h, and returned to the baseline 72 h after ICH. In the present study, we demonstrated that ICH caused rapid activation of cortactin/RhoA/LIMK, in a manner similar to PDGF-β activation. Compared to baseline, these proteins became activated six hours after ICH. The difference from baseline became statistically significant at 24 hrs and remained upregulated 72 hrs after ICH. RhoA activation was observed at the same time points, consistent with the previous study [24].

Next we investigated whether activation of cortactin/RhoA/LIMK would be accompanied with degradation of BBB components as a consequence of stress fiber formation. The BBB's permeability is regulated by adherens junctions, which in turn, play an important role in stabilizing tight junctions [29]. There are indications that pathophysiological conditions activate endothelia, changing

endothelial cytoskeletons in the BBB. This process forms stress fibers that create gaps between intact endothelial cells and promote tissue edema [7, 30].

We confirmed that activation of the proposed pathway leads to time-dependent degradation of adherens/tight junction proteins. We investigated the effects of ICH on VE-cadherin, occludin and claudin-3. VE-cadherin is an endothelial-specific cell-to-cell adhesion protein in the adherens junction that is essential for endothelial cell permeability [31]. Genetic or pharmacologic inactivation of the VE-cadherin decreases vascular integrity and facilitates transmigration of leukocytes [32]. Moreover, decreased VE-cadherin expression was accompanied by increased permeability of the BBB to Evans Blue stain in different models of brain injury [33]. VE-cadherin directly controls expression of the tight junction protein claudin-5 [34]. The degradation of claudin-5 after ICH has been demonstrated previously [35, 36]. Claudin-3, another protein of the claudin family, is expressed in brain endothelia [37] and its degradation compromises BBB under pathological conditions [38]. Additionally, we investigated the time-dependent effects of ICH on occludin, another tight junction protein playing a key role in BBB integrity[39]. In our study, VE-cadherin degradation was detectable 24 and 72 hours after ICH, and degradation of claudin-3 and occludin was detected 72 hours after ICH.

The degradation of BBB proteins corresponded to the activation of the cortactin-RhoA-LIMK pathway after ICH. Importantly, we were able to demonstrate that ICH-induced degradation of the BBB components was accompanied by formation of stress fibers. We investigated this parameter 72

hours after ICH, the time point of maximal degradation of adherent-tight junction proteins. For visualization of stress fibers, we used phalloidin staining. Phalloidin, a bicyclic peptide with high affinity for F-actin, is commonly used to visualize F-actin stress fibers [40, 41]. We observed a significant increase in phalloidin-positive cells in the brain after ICH, indicating endothelial activation and stress fiber formation.

Furthermore, we investigated whether inhibition of PDGFR-β would decrease ICH-induced stress fiber formation and BBB disruption, leading to improved neurological functions. For the PDGFR-β inhibition, we used a commercially available receptor antagonist, CP-673,451 that is a selective inhibitor of PDGFRs, having 10 fold more selectivity for the β-isoform as compared to its selectivity for the α-isoform of the receptor [42]. The drug concentrations used in this study were chosen according to previous publications. In agreement with prior reports, no toxic effect of the drug was observed [42-44]. We demonstrated that the inhibition of the receptor attenuated ICH-induced brain edema and improved ICH-impaired neurologic functions at both 24 and 72 hours post-ICH. These findings agree with our previous study, demonstrating that a selective, si-RNA-induced, *in-vivo* knock-down of PDGFRβ, decreased brain water content and improved neurological functions 24 and 72 hours after ICH [45]. Additionally, we investigated the effect of PDGFR-β inhibition on BBB integrity using the Evans Blue assay. Although PDGFR-β inhibition only slightly decreased the amount of Evans Blue stain in the brain at 24 hours, PDGFR-β inhibition significantly decreased ICH-induced accumulation

of the stain after 72 hours. That differed from the results on none-selective PDGFR inhibition [10]. We demonstrated previously that none-selective inhibition of both α and β isoform of the PDGFR by Gleevec was able to decrease Evan Blue stain accumulation both at 24 and at 72 hours after ICH significantly [10]. Both brain water content and the Evans Blue assays are used to evaluate BBB integrity, the two approaches revealed different outcomes. While brain water content accounts for both cytotoxic and vasogenic brain edema, the Evans Blue assay evaluates permeability of BBB to high molecular weight proteins, which is a sign of vasogenic brain edema. The mechanism of edema formation after ICH is not completely understood. Most of the investigators, however, postulate that both cytotoxic and vasogenic brain edema is present after ICH [46].

Whereas cytotoxic edema is prominent in the early stages of ICH, vasogenic edema follows later with the disruption of BBB. Twenty-four hours after ICH, both cytotoxic and vasogenic edema are simultaneously present.

We previously demonstrated that ICH induced a quick activation of the PRGFRα isoform as early as 3 hours after ICH. The activation peaked (6-fold compared to sham operated animals) 6 hours after ICH. Although PRGFRα remained activated 12 hours after ICH, the activation declined rapidly (2.5-fold) [10]. The β-isoform became activated more slowly. The activation of β-isoform peaked at 12 hours and remained on the same level 24 hours after ICH [45]. None-selective inhibition of both PDGFR isoforms via Gleevec decreased ICH induced increase of brain water content and Evan Blue stain accumulation 24 and 72 hours after ICH and obviously attenuated the development of both

cytotoxic and vasogenic form of brain edema at this time points [10]. 24 hours after ICH the treatment, inhibiting mostly the β-isoform of the receptor, was also able to attenuate the development of cytotoxic edema, evaluated be brain water content calculation (the molecular pathways underlying the receptor inhibition on cytotoxic brain edema remain to be investigated). That was, however, not sufficient for attenuation of vasogenic edema. We are postulating that at this time point (due to low affinity of our drug to the α-isoform of the receptor and only minor activation of β-isoform) CP-673,451 was unable to inhibit the receptor completely. The partly inhibition of the PDGRs did not lead to the amelioration of the vasogenic edema in the early stage of ICH. However in the time point of the maximal PDGFR-β activation (72 hours post ICH), the inhibition of the PDGFR via a β-isoform inhibitor (CP-673,451), resulted in amelioration of BBB disruption, and attenuation of vasogenic edema, as evaluated by Evans Blue. These facts let us to the conclusion that a further, a head-to-head, investigation of the advantages of none-selective vs selective inhibition of the different PDGFR isoform need to be done.

There are the indications in the literature that PDGFR-β is a positive regulator of tissue repair and angiogenesis after ischemic stroke [47, 48]. The inhibition of the receptor might have undesirable effects and affect the post-ICH recovery process negatively. In order to investigate this option we conducted a long-term study. Our results demonstrated that the receptor inhibition significantly improved neurological functions after ICH. We believe therefore that the drug,

used in the study did not have adverts effects on angiogenesis und recovery after ICH.

Although CP-673451, the PDGFR-β inhibitor used in this study, is 10-fold more selective for the β-isoform as compared to the α-isoform of the PDGFR, it is challenging to rule out effects of the drug on the α-isoform in an *in vivo* study. To determine the effects of the β-isoform, we used si-RNA for the PDGFR-β. I.c.v administration of the si-RNA decreased expression of PDGFR-β and diminished the amount of phalloidin positive F-actin stress fibers. Furthermore, si-RNA for PDGFR-β significantly reduced ICH-induced activation of cortactin-RhoA-LIMK pathway and attenuated degradation of adherens/tight junction proteins.

To investigate the role of cortactin on the induction of stress fibers after ICH, we used si-RNA for cortactin. Similar to PDGFR-β, si-RNA for cortactin significantly decreased expression of the protein. This reduction was accompanied by deactivation of RhoA and LIMK, decreased number of stress fibers, and the stabilization of adherens/tight junction proteins.

To investigate of the effects of LIMK inhibition, we used a commercially available inhibitor, LIMKi 3 [49]. First, we established a dose dependent response of the drug on ICH- induced elevation of brain water content and neurological deficits in the short time study. The drug, at a dose of 1 mg/kg, decreased brain edema and improved neurological function 72 hours after ICH. At 72 hours, this dose of LIMKi 3 significantly attenuated of ICH-induced LIMK phosphorylation in brain tissue, indicating that LIMKi 3 can penetrate the BBB after ICH and has effects on the CNS. The results of the Western blot study were confirmed by

immunostaining, which also revealed a decrease of pLIMK positive cells in ICH animals treated with LIMKi 3- compared to vehicle-treated animals. The effects of LIMKi 3 on post-ICH LIMK phosphorylation were associated with fewer stress fibers and preservation of adherens-tight junction proteins.

Finally, we investigated whether the injection of recombinant PDGF-D into the brain of naïve animals would result in activation of the proposed pathway and in the degradation of BBB proteins. PDGF-D is the endogenous agonist of the PDGFRs. Although there are some indications that PDGF-D has some affinity for the α-isoform of the receptor [50], most investigators consider PDGF-D as a selective agonist for the PDGFR-β isoform [51-55]. Accordingly, PDGF-D administration should primarily activate PDGFR-β. We demonstrated that PDGF-D administration increased the amount of stress fibers, which was accompanied by RhoA-LIMK activation and degradation of VE-cadherin/occludin.

The current study has limitations. The drug used in the study has not been approved for patients. Intraperitoneal administration of the drug is untypical for patient. It is, however, worth to mention that intra- peritoneal administration is very common for in small animals [56]. The pharmacokinetic partially mimics oral administration in human patients [57].

In conclusion, our findings suggest that PDGFR-β contributes, at least partly, to ICH-induced stress fiber formation, BBB impairment, and impairment of neurological functions via the cortactin-RhoA-LIMK pathway. PDGFR-β inhibition had no toxic side effects and did not increase mortality after ICH. Although the PDGFR-β inhibition was not able to completely pre- vent brain injury after ICH, it

attenuated significantly ICH-induced brain injury and improved neurological function after ICH. Our results, however, demonstrated that targeting PDGFR-β signaling may pave the way for a new therapeutic strategy for ICH patients.

References

1. Balami, J.S. and A.M. Buchan, *Complications of intracerebral haemorrhage.* Lancet Neurol, 2012. 11(1): p. 101-18.

2. Chen, S., et al., *An update on inflammation in the acute phase of intracerebral hemorrhage.* Transl Stroke Res, 2015. 6(1): p. 4-8.

3. Merali, Z., et al., *Longitudinal assessment of imatinib's effect on the blood-brain barrier after ischemia/reperfusion injury with permeability MRI.* Transl Stroke Res, 2015. 6(1): p. 39-49.

4. Selim, M. and K.N. Sheth, *Perihematoma edema: a potential translational target in intracerebral hemorrhage?* Transl Stroke Res, 2015. 6(2): p. 104-6.

5. Liu, W.Y., et al., *Tight junction in blood-brain barrier: an overview of structure, regulation, and regulator substances.* CNS Neurosci Ther, 2012. 18(8): p. 609-15.

6. Schlunk, F. and S.M. Greenberg, *The Pathophysiology of Intracerebral Hemorrhage Formation and Expansion.* Transl Stroke Res, 2015. 6(4): p. 257-63.

7. Adyshev, D.M., et al., *Ezrin/radixin/moesin proteins differentially regulate endothelial hyperpermeability after thrombin.* Am J Physiol Lung Cell Mol Physiol, 2013. 305(3): p. L240-55.

8. Millan, J., et al., *Adherens junctions connect stress fibres between adjacent endothelial cells.* BMC Biol, 2010. 8: p. 11.

9. Shih, R.H., et al., *Cigarette smoke extract upregulates heme oxygenase-1 via PKC/NADPH oxidase/ROS/PDGFR/PI3K/Akt pathway in mouse brain endothelial cells.* J Neuroinflammation, 2011. 8: p. 104.

10. Ma, Q., et al., *PDGFR-alpha inhibition preserves blood-brain barrier after intracerebral hemorrhage.* Ann Neurol, 2011. 70(6): p. 920-31.

11. Su, E.J., et al., *Activation of PDGF-CC by tissue plasminogen activator impairs blood-brain barrier integrity during ischemic stroke.* Nat Med, 2008. 14(7): p. 731-7.

12. Bell, R.D., et al., *Pericytes control key neurovascular functions and neuronal phenotype in the adult brain and during brain aging.* Neuron, 2010. 68(3): p. 409-27.

13. Papke, C.L., et al., *Smooth muscle hyperplasia due to loss of smooth muscle alpha-actin is driven by activation of focal adhesion kinase, altered p53 localization and increased levels of platelet-derived growth factor receptor-beta.* Hum Mol Genet, 2013. 22(15): p. 3123-37.

14. Stice, L.L., et al., *Desensitization of the PDGFbeta receptor by modulation of the cytoskeleton: the role of p21(Ras) and Rho family GTPases.* Exp Cell Res, 2002. 275(1): p. 17-30.

15. Theisen, C.S., et al., *NHERF links the N-cadherin/catenin complex to the platelet-derived growth factor receptor to modulate the actin cytoskeleton and regulate cell motility.* Mol Biol Cell, 2007. 18(4): p. 1220-32.

16. Gunning, P.W., et al., *Tropomyosin - master regulator of actin filament function in the cytoskeleton.* J Cell Sci, 2015. 128(16): p. 2965-74.

17. Boyle, S.N., et al., *A critical role for cortactin phosphorylation by Abl-family kinases in PDGF-induced dorsal-wave formation.* Curr Biol, 2007. 17(5): p. 445-51.

18. Lai, F.P., et al., *Cortactin promotes migration and platelet-derived growth factor-induced actin reorganization by signaling to Rho-GTPases.* Mol Biol Cell, 2009. 20(14): p. 3209-23.

19. Park, J.B., et al., *Transcriptional profiling of GBM invasion genes identifies effective inhibitors of the LIM kinase-Cofilin pathway.* Oncotarget, 2014. 5(19): p. 9382-95.

20. Yi, R., G. Xiao-Ping, and L. Hui, *Atorvastatin prevents angiotensin II-induced high permeability of human arterial endothelial cell monolayers via ROCK signaling pathway.* Biochem Biophys Res Commun, 2015. 459(1): p. 94-9.

21. Gong, C., K.V. Stoletov, and B.I. Terman, *VEGF treatment induces signaling pathways that regulate both actin polymerization and depolymerization.* Angiogenesis, 2004. 7(4): p. 313-21.

22. Thirone, A.C., et al., *Hyperosmotic stress induces Rho/Rho kinase/LIM kinase-mediated cofilin phosphorylation in tubular cells: key role in the osmotically triggered F-actin response.* Am J Physiol Cell Physiol, 2009. 296(3): p. C463-75.

23. Fu, Z., et al., *Increased activity of Rho kinase contributes to hemoglobin-induced early disruption of the blood-brain barrier in vivo after the occurrence of intracerebral hemorrhage.* Int J Clin Exp Pathol, 2014. 7(11): p. 7844-53.

24. Huang, B., et al., *Fibroblast growth factors preserve blood-brain barrier integrity through RhoA inhibition after intracerebral hemorrhage in mice.* Neurobiol Dis, 2012. 46(1): p. 204-14.

25. Yu, Y., et al., *Role of Rho kinase in lysophosphatidic acid-induced altering of blood-brain barrier permeability.* Int J Mol Med, 2014. 33(3): p. 661-9.

26. Chen, Q., et al., *Chronic hydrocephalus and perihematomal tissue injury developed in a rat model of intracerebral hemorrhage with ventricular extension.* Transl Stroke Res, 2015. 6(2): p. 125-32.

27. Manaenko, A., et al., *Comparison Evans Blue injection routes: Intravenous versus intraperitoneal, for measurement of blood-brain barrier in a mice hemorrhage model.* J Neurosci Methods, 2011. 195(2): p. 206-10.

28. Manaenko, A., et al., *Arginine-vasopressin V1a receptor inhibition improves neurologic outcomes following an intracerebral hemorrhagic brain injury.* Neurochem Int, 2011. 58(4): p. 542-8.

29. Dejana, E., F. Orsenigo, and M.G. Lampugnani, *The role of adherens junctions and VE-cadherin in the control of vascular permeability.* J Cell Sci, 2008. 121(Pt 13): p. 2115-22.

30. Dietrich, A. and T. Gudermann, *TRPC6: physiological function and pathophysiological relevance.* Handb Exp Pharmacol, 2014. 222: p. 157-88.

31. Harris, E.S. and W.J. Nelson, *VE-cadherin: at the front, center, and sides of endothelial cell organization and function.* Curr Opin Cell Biol, 2010. 22(5): p. 651-8.

32. Gotsch, U., et al., *VE-cadherin antibody accelerates neutrophil recruitment in vivo.* J Cell Sci, 1997. 110 (Pt 5): p. 583-8.

33. Liu, W.Y., et al., *Increasing the Permeability of the Blood-brain Barrier in Three Different Models in vivo.* CNS Neurosci Ther, 2015. 21(7): p. 568-74.

34. Gavard, J. and J.S. Gutkind, *VE-cadherin and claudin-5: it takes two to tango.* Nat Cell Biol, 2008. 10(8): p. 883-5.

35. Zhou, W., M. Marinescu, and R. Veltkamp, *Only very early oxygen therapy attenuates posthemorrhagic edema formation and blood-brain barrier disruption in murine intracerebral hemorrhage.* Neurocrit Care, 2015. 22(1): p. 121-32.

36. Sun, H., et al., *Effects of selective hypothermia on blood-brain barrier integrity and tight junction protein expression levels after intracerebral hemorrhage in rats.* Biol Chem, 2013. 394(10): p. 1317-24.

37. Schrade, A., et al., *Expression and localization of claudins-3 and -12 in transformed human brain endothelium.* Fluids Barriers CNS, 2012. 9: p. 6.

38. Wolburg, H., et al., *Localization of claudin-3 in tight junctions of the blood-brain barrier is selectively lost during experimental autoimmune encephalomyelitis and human glioblastoma multiforme.* Acta Neuropathol, 2003. 105(6): p. 586-92.

39. Abbott, N.J., et al., *Structure and function of the blood-brain barrier.* Neurobiol Dis, 2010. 37(1): p. 13-25.

40. Benkoel, L., et al., *Effect of dietary lipid (soybean lecithin and triacylglycerol) on hepatic F-actin microfilaments in cyclosporine A-treated rats: image analysis by confocal laser scanning microscopy.* Dig Dis Sci, 2000. 45(6): p. 1096-102.

41. Liu, H. and W.W. Kao, *A novel protocol of whole mount electro-immunofluorescence staining.* Mol Vis, 2009. 15: p. 505-17.

42. Roberts, W.G., et al., *Antiangiogenic and antitumor activity of a selective PDGFR tyrosine kinase inhibitor, CP-673,451.* Cancer Res, 2005. 65(3): p. 957-66.

43. Xi, Y., et al., *CP-673451, a platelet-derived growth-factor receptor inhibitor, suppresses lung cancer cell proliferation and migration.* Onco Targets Ther, 2014. 7: p. 1215-21.

44. Ehnman, M., et al., *Distinct effects of ligand-induced PDGFRalpha and PDGFRbeta signaling in the human rhabdomyosarcoma tumor cell and stroma cell compartments.* Cancer Res, 2013. 73(7): p. 2139-49.

45. Yang, P., et al., *Platelet-Derived Growth Factor Receptor-beta Regulates Vascular Smooth Muscle Cell Phenotypic Transformation and Neuroinflammation After Intracerebral Hemorrhage in Mice.* Crit Care Med, 2016. 44(6): p. e390-402.

46. Yang, G.Y., et al., *Experimental intracerebral hemorrhage: relationship between brain edema, blood flow, and blood-brain barrier permeability in rats.* J Neurosurg, 1994. 81(1): p. 93-102.

47. Shen, J., et al., *PDGFR-beta as a positive regulator of tissue repair in a mouse model of focal cerebral ischemia.* J Cereb Blood Flow Metab, 2012. 32(2): p. 353-67.

48. Renner, O., et al., *Time- and cell type-specific induction of platelet-derived growth factor receptor-beta during cerebral ischemia.* Brain Res Mol Brain Res, 2003. 113(1-2): p. 44-51.

49. Samuel, M.S., et al., *Actomyosin-mediated cellular tension drives increased tissue stiffness and beta-catenin activation to induce epidermal hyperplasia and tumor growth.* Cancer Cell, 2011. 19(6): p. 776-91.

50. Borkham-Kamphorst, E., et al., *Platelet-derived growth factor-D modulates extracellular matrix homeostasis and remodeling through TIMP-1 induction and attenuation of MMP-2 and MMP-9 gelatinase activities.* Biochem Biophys Res Commun, 2015. 457(3): p. 307-13.

51. Fredriksson, L., H. Li, and U. Eriksson, *The PDGF family: four gene products form five dimeric isoforms.* Cytokine Growth Factor Rev, 2004. 15(4): p. 197-204.

52. Bergsten, E., et al., *PDGF-D is a specific, protease-activated ligand for the PDGF beta-receptor.* Nat Cell Biol, 2001. 3(5): p. 512-6.

53. LaRochelle, W.J., et al., *PDGF-D, a new protease-activated growth factor.* Nat Cell Biol, 2001. 3(5): p. 517-21.

54. Reigstad, L.J., J.E. Varhaug, and J.R. Lillehaug, *Structural and functional specificities of PDGF-C and PDGF-D, the novel members of the platelet-derived growth factors family.* FEBS J, 2005. 272(22): p. 5723-41.

55. Usuki, K., et al., *Production of platelet-derived endothelial cell growth factor by normal and transformed human cells in culture.* Proc Natl Acad Sci U S A, 1989. 86(19): p. 7427-31.

56. Turner, P.V., et al., *Administration of substances to laboratory animals: equipment considerations, vehicle selection, and solute preparation.* J Am Assoc Lab Anim Sci, 2011. 50(5): p. 614-27.

57. Abu-Hijleh, M.F., O.A. Habbal, and S.T. Moqattash, *The role of the diaphragm in lymphatic absorption from the peritoneal cavity.* J Anat, 1995. 186 (Pt 3)(Pt 3): p. 453-67.

CHAPTER FIVE

GENERAL DISCUSSION AND CONCLUSIONS

Summary of Key Findings

In the previous chapters we were able to demonstrate that IGF-1, Adropin, and PDGFR-β inhibition were able to preserve BBB integrity following ICH. We also reviewed and discussed the pathophysiology and models of ICH surgeries including cerebellar hemorrhage.

Our research was designed to determine if there was potential for development of clinical treatments in animal models of ICH. We determined if certain medical interventions were capable of improving outcomes in these animals, if different methods of drug delivery affected treatments, and if there were molecular mechanisms that can be targeted to produce these results.

How Our Findings Advance the Field

Our scientific experiments have been able to significantly contribute to the field of Intracerebral Hemorrhage. In our publications, we were able to effectively show how different treatments may be useful in protecting against BBB injury and edema formation in ICH models. Our research identified targets for treatments, neuroprotective molecules, and potential future translational research directions for clinical settings. We explored the effect of IGF-1 on the BBB in an ICH mouse model and determined its ability to improve outcomes of edema and neurobehavior [1]. Our findings showed that IGF-1 was able to reduce edema

found in both models of collagenase and blood-injection. Additionally, we characterized the treatment mechanism occured through activation of the PI3K/AKT pathway thus inhibiting the pGSK3β/MEKK1 pathway. Our study was the first to discover the effects of IGF-1 treatments after ICH and was also the first to determine if intranasal IGF-1 was effective in treatment of the BBB in a stroke model. Previous studies of IGF-1 suggest it plays a role in the protection of neurons and development in injury models [2-7]. This is the first time to our knowledge that we have studied IGF-1 as a protective against edema formation in a brain injury model.

We were also able to show that Adropin was effective in reducing injury to the BBB in a mouse model of ICH. In our study we discovered that this protection occurs through a mechanism the Notch1 signaling pathway, which has previously been seen to regulate neurogenesis [8]. We find that this suggests that this pathway is important in relation to the integrity of the BBB and a further therapy option. Additionally, this is the first time that Adropin has been given intranasally to our knowledge. Little knowledge was given on the ability of Adropins ability to cross the BBB [9-11]. In this study, we tracked Adropin expression in the brain and found that it was effective in reaching the brain tissues via the intranasal method.

We also observed the impact of PDGFR-β on outcomes in ICH. We demonstrated that stress fiber formation is partially activated by PDGF-Rβ and the cortactin/RhoA/LIMK pathway [12]. The inhibition of the receptor caused reduced edema formation and BBB permeability along with reducing the number

of stress fibers after ICH. We showed that this mechanism is present in both the short- and long-term outcomes following ICH.

Limitations To Neuroprotective Strategies after ICH

Significance of Edema formation in BBB injury following ICH

Edema formation generally occurs via two separate mechanisms. The first is the release of fluids from the cells that are injured. The second is through movement of fluids from the vessels to the parenchymal space via a leaky BBB [13-15]. In both cases, edema formation can be considered the critical factor in determining outcomes following a hemorrhagic stroke. The cranium is a limited space that has little room for growth within a hard barrier of bone. As there is increase in fluid in the parenchyma and swelling of the tissue, the skull serves as an obstacle to limit the expansion of tissue thus increasing the pressure within the space. Besides the area of damaged tissue directly surrounding a hemorrhage, further swelling of the brain tissues results in tissue near the skull to be compressed and damaged further.

Several factors have been suggested to induce BBB damage following ICH. This can occur through mechanisms of mechanical stress, inflammation, or direct toxic injury to the cells that compose the BBB [16]. Because of the BBB injury and its subsequent edema formation is of critical importance to the outcomes following a hemorrhagic stroke, it is a highly researched strategy to reduce edema formation via preventing the injury to the BBB. However, reducing BBB injury within the first few hours after a stroke is difficult to achieve for most

hospitals due to limitations of transportation and diagnosis, early edema formation is difficult to treat. Additionally, besides blood pressure control, the only other effective methods of treatment are considered invasive to relieve pressure or remove the hematoma. By providing treatment options that are non-invasive, the barriers to early protection following a stroke can be improved upon to allow for time for other treatment methods to be explored.

Central Nervous System Drug Delivery

In the case of ICH, clinical translation is difficult when in regards to drug administration. Besides the control of hypertension, no other pharmacological developments have been approved for the treatment of cerebral hemorrhage. The huge variability of patients and their access to stroke treatment centers makes developing strategies difficult. Additionally, medical treatments generally take more time to have an effect. It generally takes a while for patients to arrive at the hospital after their symptoms appear, leaving little room to initiate treatments before cerebral tissues begin to degrade.

The inherent difficulty of delivery of medications to the brain tissues is worsened by the presence of the BBB. The BBB provides an inbuilt protective mechanism to filter out toxins and prevent damage. However, when developing medical treatments it serves as an obstacle that prevents particular treatments from reaching the cerebral tissues. The need for drugs that can either successfully pass the BBB to directly protect the neuronal tissues or affect the BBB directly should be highly prioritized. Additionally, drugs should be developed

that can have an effect within the early stages of ICH when assessments are still being made for the use of surgical treatments. Therefore, the goal of treatments should be to have non-invasive drug therapies that can be administered early in the course of the disease in lieu of invasive methods.

Conclusion and Future Prospects

Although there have been significant strides in basic science research to develop new therapeutic strategies for protecting against ICH, there is still a great deal more research needed to be done in order to understand the impact of the disease and produce effective therapies that can be translated for humans. Several gaps of knowledge exist concerning the pathophysiology and cellular mechanisms involved in the injury. The timing of important endogenous neuroprotective mechanisms are still being explored. Basic science research in the field of stroke research aims towards making a translational approach to clinical relevance. As such, there is a need to further explore cellular mechanisms and studies involving combinational therapies. The study of ICH has many promising prospects in relating science to translational research.

References

1. Nowrangi, D.S., et al., *rhIGF-1 reduces the permeability of the blood-brain barrier following intracerebral hemorrhage in mice.* Exp Neurol, 2019. 312: p. 72-81.

2. Aberg, D., et al., *Serum IGF-I levels correlate to improvement of functional outcome after ischemic stroke.* J Clin Endocrinol Metab, 2011. 96(7): p. E1055-64.

3. Anderson, M.F., et al., *Insulin-like growth factor-I and neurogenesis in the adult mammalian brain.* Brain Res Dev Brain Res, 2002. 134(1-2): p. 115-22.

4. Bake, S., et al., *Insulin-Like Growth Factor (IGF)-I Modulates Endothelial Blood-Brain Barrier Function in Ischemic Middle-Aged Female Rats.* Endocrinology, 2016. 157(1): p. 61-9.

5. De Smedt, A., et al., *Insulin-like growth factor I serum levels influence ischemic stroke outcome.* Stroke, 2011. 42(8): p. 2180-5.

6. Hou, X., et al., *IGF-1 protects against Abeta25-35-induced neuronal cell death via inhibition of PUMA expression and Bax activation.* Neurosci Lett, 2017. 637: p. 188-194.

7. Pang, Y., et al., *IGF-1 can either protect against or increase LPS-induced damage in the developing rat brain.* Pediatr Res, 2010. 67(6): p. 579-84.

8. Yu, L., et al., *Adropin preserves the blood-brain barrier through a Notch1/Hes1 pathway after intracerebral hemorrhage in mice.* J Neurochem, 2017. 143(6): p. 750-760.

9. Alberi, L., et al., *Notch signaling in the brain: in good and bad times.* Ageing Res Rev, 2013. 12(3): p. 801-14.

10. Gerhardt, H., et al., *N-cadherin expression in endothelial cells during early angiogenesis in the eye and brain of the chicken: relation to blood-retina and blood-brain barrier development.* Eur J Neurosci, 1999. 11(4): p. 1191-201.

11. Sun, F., et al., *Notch1 signaling modulates neuronal progenitor activity in the subventricular zone in response to aging and focal ischemia.* Aging Cell, 2013. 12(6): p. 978-87.

12. Manaenko, A., et al., *Inhibition of stress fiber formation preserves blood-brain barrier after intracerebral hemorrhage in mice.* J Cereb Blood Flow Metab, 2018. 38(1): p. 87-102.

13. Sahni, R. and J. Weinberger, *Management of intracerebral hemorrhage.* Vasc Health Risk Manag, 2007. 3(5): p. 701-9.

14. Kuramatsu, J.B., H.B. Huttner, and S. Schwab, *Advances in the management of intracerebral hemorrhage.* J Neural Transm, 2013. 120 Suppl 1: p. S35-41.

15. Qureshi, A.I., A.D. Mendelow, and D.F. Hanley, *Intracerebral haemorrhage.* Lancet, 2009. 373(9675): p. 1632-44.

16. Xi, G., R.F. Keep, and J.T. Hoff, *Mechanisms of brain injury after intracerebral haemorrhage.* Lancet Neurol, 2006. 5(1): p. 53-63.